Documentation for the Inamori-Magellan Areal Camera and Spectrograph (IMACS)

Preliminary Design Review

3 April 1999

Observatories of the Carnegie Institution of Washington,
Pasadena, California

IMACS PDR

Compiled by: Bruce Bigelow

Edited by: Bruce Bigelow and Alan Dressler

Authors and Contributors:

Bruce Bigelow	OCIW	Overview (Ch. 1), Mech. design (Ch. 3) Management (Ch. 8), System spec. (Append. A)
Christoph Birk	OCIW	Instr. control (Ch. 7)
Tim Bond	OCIW	Mech. design (Ch. 3)
Greg Burley	OCIW	Detector systems (Ch. 4), (Ch. 5)
David Carr	OCIW	Motion control (Ch. 6)
Alan Dressler	OCIW	Instr. Control (Ch. 8), System Spec. (Append. A)
Brian Sutin	OCIW	Optical design (Ch. 2 & Append. E)
Ian Thompson	OCIW	Detector systems (Ch. 4), (Ch. 5)
Harland Epps	UCSC / Lick Obs.	Optical design (Append. B-D)
Steve Gunnels	Paragon Engineering	Mech. design (Ch. 3)
Gerry Luppino	GL Scientific	Dewar design (Ch. 5)
Alan Schier	J. Alan Schier Co.	Mech. design (Ch. 3)

IMACS PDR Committee

Dan Fabricant	Chair, Harvard / SAO
Peter Hastings	UK ROE / ATC
Matt Johns	OCIW / Magellan Project
Jerry Nelson	UCSC / Lick Obs.
Matt Radovan	UCSC / Lick Obs.
Scott Roberts	HIA / Dominion Astro. Obs.
Steve Vogt	UCSC / Lick Obs.

Contents

List of Figures

List of Tables

Glossary

IMACS	Inamori-Magellan Areal Camera and Spectrograph
MIKE	Magellan Inamori Kyocera Echelle
ADC	Atmospheric Dispersion Corrector
ART	Advanced Recording Technologies Inc.
CCD	Charge-Coupled Device
CF	Carbon Fiber
CFHT	Canada France Hawaii Telescope
DAC	Digital to Analog Converter
DEIMOS	Deep Extragalactic Imager Multi Object Spectrograph (Keck)
DSP	Digital Signal Processor
DSS	Disperser Server System (IMACS)
EDM	Electronic Discharge Machining
EEV	English Electric Valve (CCDs)
ESI	Echelle Imager and Spectrograph (Keck)
ESO	European Southern Observatory
FEA	Finite Element Analysis
FOSS	Forward Optical Support Structure (IMACS)
FOV	Field of View
FP	Fabry-Perot (etalon)
FSS	Filter Server System (IMACS)
FWHM	Full Width Half Maximum
GMOS	Gemini Multi Object Spectrograph
GUI	Graphical User Interface
HR	High Resolution (encoders)
IFU	Integral Field Unit
IR	Infra Red

LAN	Local Area Network
LCAM	Long Camera (IMACS)
LCO	Las Campanas Observatory (OCIW)
LED	Light Emitting Diode
LL	Lincoln Labs (CCDs)
LRIS	Low Resolution Imaging Spectrograph (Keck)
MCS	Motion Control System (IMACS)
MOSS	Main Optical Support Structure (IMACS)
MSS	Mask Server System (IMACS)
MTBF	Mean Time Between Failure
NIR	Nasmyth Instrument Rotator (Magellan)
NIRI	Near Infra Red Imager (Gemini)
NFS	Network File System
OCIW	Observatories of the Carnegie Institution of Washington
PDR	Preliminary Design Review
RFQ	Request For Quotation
RMS	Root Mean Squared
SCAM	Short Camera (IMACS)
SH	Shack-Hartmann (wavefront sensor)
SITe	Scientific Imaging Technologies (Inc.)
TBD	To Be Determined
TCS	Telescope Control System
TE	Thermo Electric (cooler)
UCO/Lick	University of California Observatories / Lick Observatory
UH	University of Hawaii
ULE	Ultra Low Expansion (Corning Glass)
UV	Ultra Violet
VIMOS	Visible Imaging Multi Object Spectrograph
VLT	Very Large Telescope (ESO)
YAG	Yttrium Aluminum Garnet (laser)

Chapter 1

Overview of the IMACS project

1.1 The Project

The Inamori Magellan Areal Camera and Spectrograph (IMACS) is a multi-mode imaging and wide-field multi-object spectrograph for the Magellan I telescope. The instrument will be mounted on the right Nasmyth instrument rotator, where it will operate with the f/11 Gregorian configuration. IMACS is to provide direct imaging over 15' x 15' and 27' x 27' fields with only slight degradation of the median image quality $FWHM = 0.6$" by the optics. The same size fields are available for spectroscopic observations with low-to-medium dispersions (up to $R \leq 10000$). Although IMACS will cover very large fields for multiobject spectroscopy of galactic and extragalactic targets, its on-axis image quality, relevant for single-object or integral field spectroscopy, is as good as is available on any telescope.

Fed by the f/11 Gregorian configuration, with an integral ADC and field corrector mounted at the tertiary mirror, the transmitting, all-spherical collimator of IMACS produces a well corrected, unvignetted field of 24 arc-min in diameter, and slightly vignetted field of 30 arc-sec in diameter.

Two cameras are used to re-image the 150mm diameter collimator exit pupil at 0.111 and 0.200 arc-sec/pixel. The all-spherical, f/2.7 long camera can directly image a 21.2 arc-min diameter FOV, or spectroscopically image a 15 arc-min long slit with a variety of standard 150 x 200 mm diffraction gratings. Ultimately, an aspheric, f/1.5 short camera will be able to directly image a 30 arc-min diameter FOV, or spectroscopically image a 27 arc-min long slit

with a variety of standard 150mm aperture grisms. Both cameras will use the same 8192 x 8192 CCD array, which will interchange between the two cameras.

1.2 The Project Team

The IMACS project is composed of both OCIW staff members and external consultants. The current participants (as of 3/99) include the following people; consultants are listed with their organizations:

Project Leadership	Alan Dressler	Principal Investigator
	Bruce Bigelow	Instrument Scientist
Conceptual Design	Alan Dressler	
	Steve Schectman	
	Bruce Bigelow	
	Brian Sutin	Optical Scientist
	Harland Epps	UCO/Lick Observatory
Mechanical Engineering	Bruce Bigelow	
	Tim Bond	
	Alan Schier	J. Alan Schier Co.
	Gerry Luppino	GL Scientific Co.
Detector Systems	Ian Thompson	
	Greg Burley	
	Gerry Luppino	
Software Development	Christoph Birk	
Electronics Development	Dave Carr	
Administration	Jeanette Stone	Purchasing
	Georgina Nichols	Accounting
	Bronagh Glaser	Administrative Support
	Karen Gross	Administrative Support

1.3 Specification Summary

A summary of the instrument specifications is given below. Tables 1.1 and 1.2 show the dispersion and resolution of the various grating and grism options.

Fields of view	15 x 15 arc-min (long camera) 27 x 27 arc-min (short camera)
Spectral resolution	$\lambda/\Delta\lambda \leq$ 10,000 (1 arc-sec slit, grating mode) $\lambda/\Delta\lambda \leq$ 1800 (1 arc-sec slit, grism mode)
Wavelength ranges	0.365-1.00 microns (long camera) 0.390-1.05 microns (short camera)
Image scales	0.111 arc-sec/pixel (long camera) 0.200 arc-sec/pixel (short camera)
Detector array	8192 x 8192 x 15 micron pixels (4 x 2 array of 2048 x 4096 CCDs)
Telescope configuration	f/11 Gregorian field corrector and ADC at tertiary mirror field de-rotation at Nasmyth instr. mount
Operating modes	grating dispersed single and multi-object spectroscope y grism dispersed single and multi-object spectroscopy 15 x 15 arc-min FOV direct imaging 27 x 27 arc-min dia. FOV direct imaging

grating l/mm	order	Ang/px	v. disp. km/s/px	Ang. 1" slit	reso. 1" slit	reso. 0.5" slit
158	1	1.17	58.48	10.5	569	1138
300	1	0.66	33.10	6.0	1006	2012
600	1	0.37	18.27	3.3	1823	3646
1200	1	0.19	9.74	1.8	3420	6840
1200	2	0.066	3.31	0.66	10052	20105

Table 1.1: Grating selection performance; based on 641.8 mm focal length long camera, 0.111 arcsec/pixel plate scale, 15 μm pixels, wavelength of 6000 A.

grating l/mm	order	Ang/px	v. disp. km/s/px	Ang. 1" slit	reso. 1" slit	reso. 0.5" slit
158	1	2.7	133	13.3	452	904
300	1	1.4	69	6.9	868	1736
600	1	0.7	33	3.3	1830	3660

Table 1.2: Grism selection performance; based on 355.6 mm focal length short camera, 0.201 arcsec/pixel plate scale, 15 μm pixels, wavelength of 6000 A.

1.4 Performance Goals

The following performance goals are being used to guide the optical, mechanical, electronic, and software designs for the instrument:

- Excellent image quality to match the best atmospheric and telescope images
- High throughput to make maximum use of the 6.5m Magellan aperture
- Excellent image stability for optimal sky subtraction, calibration, and observational efficiency
- Simplicity in all aspects of design to minimize cost and maximize reliability.

1.5 Design Philosophy

The Carnegie Observatories are currently in an unprecedented period of instrumentation development. In addition to the design and construction of the two Magellan telescopes, instrument builders at Carnegie are also building three first-generation instruments for Magellan; the multi-object spectrograph IMACS, the Magellan Inamori Kyocera Echelle (MIKE), and DDI, an infrared multi-object spectrograph.

As the current level of activity will not be sustained, an important feature of the IMACS design philosophy follows the telescope project; by making use of a small core team for developing the conceptual design of the instrument, and by using outside consultants for design and fabrication of major sub-systems, the total number of permanent, local contributors will be kept small.

Detail design and fabrication of instrument components is costly in both time and money. As is often the case in astronomical instrumentation, tight constraints on schedule and budget are balanced against scientific and technical requirements. Consequently, commercial solutions to design requirements are being explored vigorously, with the expectation that purchased components, whenever acceptable in cost and performance, are preferable to design and fabrication from scratch.

Simplicity of design is important in several respects. By minimizing the number of fabricated parts in the instrument, overheads in terms of drafting, documentation, and revision control are minimized as well. Additionally, simple designs are more likely to be reliable and more readily repaired in the minimal-support environment expected at the observatory.

1.6 Baseline Design

IMACS is expected to be the work-horse instrument on Magellan I for many years to come. As such, the baseline instrument will have a variety of imaging and spectrographic operational modes. The baseline instrument consists of the slit area systems (guide cameras, Shack-Hartmann camera, calibration lamps, and slit-mask handler), and the main optical system (field lens, collimator, gratings, imaging mirror, filters, and long camera).

In general, the following capabilities are provided by the baseline design:

- Long Camera Direct Imaging
  - 15 x 15 arc-min FOV
  - 8192 x 8192 pixel detector array
  - 15 micron pixels
  - 0.111 arc-sec/pixel imaging scale
  - 0.365 - 1.00 micron band-pass
  - 15 selectable filters
- Long Camera Grating Spectroscopy
  - Long-slit mode
  - Multi-slit masks
  - 5 selectable masks
  - 300, 600, and 1200 l/mm gratings

1.7 Phase II and Additional Capabilities

1.7.1 Short Camera

Although the design exists for the IMACS short camera, fabrication of the short camera, grisms, and supporting systems are currently unfunded. Glass for the short camera has been procured in order to assure its availability at a later date. The short camera and associated grisms will provide the following capabilities:

- Short Camera Direct Imaging
  - 27 x 27 arc-min FOV
  - 8192 x 8192 pixel detector array (Shared with long camera)
  - 15 micron pixels
  - 0.201 arc-sec/pixel imaging scale

  - 0.390 - 1.05 micron band-pass
  - 15 selectable filters (shared with long camera)

- Short Camera Grism Spectroscopy
  - Long-slit mode
  - Multi-slit masks
  - 5 selectable masks
  - 150, 300, and 600 l/mm grisms

1.7.2 Fabry-Perot

Although a Fabry-Perot (FP) has been identified as a desirable addition to IMACS, no funding for an etalon has been secured as of the PDR. However, one manufacturer (Queensgate Instruments) has supplied drawings of a 150mm aperture FP. The preliminary design of the disperser server system has been completed with the possible future addition of an FP in mind.

1.7.3 Integral Field Units

As with the FP, integral field units (IFU) have been identified for later addition to IMACS. The slit mask handling system preliminary design has been completed with IFU's in mind, and efforts have been made to make their future inclusion straightforward.

Chapter 2

Optical Design

2.1 Introduction

The overall optical design is for IMACS is not part of this PDR. This section is included as an overview and status report. The original optical plan was conceived by Steve Shectman, along with a preliminary optical design for the collimator. Harland Epps tuned up the collimator design and designed the long and short camera, completing the optical design.

The development of the short camera is currently being delayed in favor of the long camera. Therefore development of the grisms, Fabry-Perot, and asphere production are of secondary priority.

2.2 Design Philosophy

The requirements driving the optical design were image quality, throughput, and practicality. The requirement of decent transmission into the near-UV leaves only a small handful of acceptable refractive materials, such as calcium fluoride, fused silica, and a few Ohara i-line glasses.

The image quality requirement is that a 0.6-arc-sec FWHM image not be degraded by more than 10%. This requirement is always met in the long camera, and is met in the short camera whenever the image size is less than about 35 microns; ie, almost everywhere.

The estimated throughput of the design is high enough that the major drivers are the telescope and the CCD chip, so attempting to increase throughput of the optical design over what is currently delivered by the design would not be practical.

2.3 Throughput Estimates

The major source of light loss for IMACS is the telescope, with three aluminum reflective surfaces and an ADC/field corrector with 4 inches of non-UV-optimized optical glass. These contributions, which are not controlled by the IMACS project, are included separately in the table below. The next most important loss is due to the CCD at the blue and red ends of the spectrum. Coating losses are extrapolated from those achieved in ESI with multi-layer dielectric coatings.

Figure 2.1 shows the predicted efficiencies for the telescope, long camera, and short camera, for both imaging and spectroscopy.

2.4 Image Quality

The image quality for all modes of IMACS is in the range of (1.0 to 2.0)-pixels RMS diameter. The axial color of the collimator and both cameras conspire to make the images as large as 3.0-pixels RMS diameter near a wavelength of 0.45 microns at the nominal design focus. Plots showing the spot sizes in the various modes are available in the precontruction optical design reports, which are included in the appendices of this document.

2.5 Descriptions of Optics

Detailed descriptions of the each of the optical sub-systems can be found in the IMACS System Specification, also included in the appendices.

Table 2.1: Predicted Efficiencies (Percent).

Wavelength (μm)	0.36	0.4	0.5	0.6	0.7	0.8	0.9	1.0	1.1
TELESCOPE									
Aluminum (three surfaces)	0.57	0.61	0.66	0.70	0.66	0.61	0.68	0.80	0.80
ADC Glass Losses	0.90	0.96	0.98	0.98	0.99	0.99	0.99	0.99	0.99
ADC Coatings (guess 1%/4 surf)	0.96	0.96	0.96	0.96	0.96	0.96	0.96	0.96	0.96
Telescope Total	0.49	0.56	0.62	0.66	0.63	0.58	0.65	0.76	0.76
IMACS LONG CAMERA									
Coating Losses (0.87%/22 surf)	0.82	0.82	0.82	0.82	0.82	0.82	0.82	0.82	0.82
Grating Aluminum	0.83	0.85	0.87	0.89	0.87	0.85	0.88	0.93	0.93
Grating Peak Efficiency	0.85	0.85	0.85	0.85	0.85	0.85	0.85	0.85	0.85
Glass Losses	0.90	0.97	0.99	0.99	0.99	0.99	0.98	0.97	0.97
Site CCD's	0.35	0.65	0.75	0.85	0.85	0.77	0.54	0.20	0.02
Spectrographic Total	0.18	0.37	0.45	0.52	0.51	0.45	0.32	0.13	0.02
Coating Losses (0.87%/22 surf)	0.82	0.82	0.82	0.82	0.82	0.82	0.82	0.82	0.82
Fold Mirror (Silver Star)	0.86	0.99	0.98	0.97	0.98	0.99	0.99	0.99	0.99
Glass Losses	0.90	0.97	0.99	0.99	0.99	0.99	0.98	0.97	0.97
Site CCD's	0.35	0.65	0.75	0.85	0.85	0.77	0.54	0.20	0.02
Imaging Total	0.22	0.51	0.60	0.67	0.68	0.62	0.43	0.16	0.02
IMACS SHORT CAMERA									
Coating Losses (0.86%/26 surf)	0.80	0.80	0.80	0.80	0.80	0.80	0.80	0.80	0.80
Grism Peak Efficiency	0.85	0.85	0.85	0.85	0.85	0.85	0.85	0.85	0.85
Glass Losses	0.84	0.96	0.98	0.98	0.98	0.99	0.98	0.96	0.96
Site CCD's	0.35	0.65	0.75	0.85	0.85	0.77	0.54	0.20	0.02
Spectrographic Total	0.20	0.42	0.50	0.57	0.57	0.52	0.36	0.13	0.02
Coating Losses (0.86%/24 surf)	0.81	0.81	0.81	0.81	0.81	0.81	0.81	0.81	0.81
Glass Losses	0.84	0.96	0.98	0.98	0.98	0.99	0.98	0.96	0.96
Site CCD's	0.35	0.65	0.75	0.85	0.85	0.77	0.54	0.20	0.02
Imaging Total	0.24	0.51	0.60	0.67	0.67	0.62	0.43	0.16	0.02

2.6 Grisms

The three nominal grisms are 150 lines/mm grism at an 8.6-degree blaze angle, a 300 lines/mm grism at a 17.5-degree blaze angle, and a 600 lines/mm grism at a 28.7-degree blaze angle. The rulings are off-the-shelve items from Spectronics. These grisms were chosen for maximum efficiency, and offer a wide range of scientific capability.

2.7 Fabry-Perot

In order to not vignette the beam significantly, a Fabry-Perot for the short camera must have an entrance diameter of approximately 200mm. This is significantly larger than standard FP's in the Queensgate catalog. Queensgate has provided engineering drawings of a 150mm aperture FP, and inquiries have been made regarding the cost and availability of a still larger FP.

2.8 Sensitivity Analyses

2.8.1 Initial Alignment Sensitivities

This table gives initial alignment sensitivities for the IMACS collimator and long camera. The first column is the multiplet number. The second is the motion: Y for decenter, Z for axial motion, and R for rotation. The next column is the size of the delta in inches, where the rotation is equal to atan(delta / diameter). The next column is the WORST increase in RMS spot diameter (microns) for a large ensemble of spots. The last column is the WORST increase in RMS spot diameter after focus of the chip and tilt of the dewar have been approximately

removed from the ensemble average.

mult.	motion	Δ(in.)	$\Delta D(\mu$m)	$\Delta D(\mu$m)	
1	Y	0.003	0.1973	0.0537	
1	Z	0.003	0.1553	0.0078	Field Lens
1	R	0.003	0.0927	0.0135	
2	Y	0.003	0.3273	0.0336	
2	Z	0.003	2.7083	0.0915	Fused Silica Singlet
2	R	0.003	0.5181	0.1413	
3	Y	0.003	1.1347	0.6230	
3	Z	0.003	3.2631	0.0476	S-FSL5Y Singlet
3	R	0.003	1.5440	0.7768	
4	Y	0.003	0.7474	0.6644	
4	Z	0.003	0.4641	0.1028	BSM51Y/CaF2 Doublet
4	R	0.003	2.0541	0.6399	
5	Y	0.003	3.8351	1.0787	
5	Z	0.003	3.5847	0.2096	S-FPL51Y Singlet
5	R	0.003	4.4815	1.4933	
6	Y	0.003	5.6037	1.7257	
6	Z	0.003	0.2796	0.0893	BAL15Y/CaF2/S-LAL7 Triplet
6	R	0.003	0.8169	0.1575	
7	Y	0.003	4.2310	0.7458	
7	Z	0.003	12.1941	0.3400	CaF2 Singlet
7	R	0.003	4.7928	1.1604	
8	Y	0.003	0.0000	0.0000	
8	Z	0.003	0.0000	0.0000	Filter
8	R	0.003	0.0358	0.0082	
9	Y	0.003	1.7715	0.1376	
9	Z	0.003	2.5655	0.6165	BSM51Y Singlet
9	R	0.003	1.6068	0.3054	
10	Y	0.003	0.5982	0.0121	
10	Z	0.003	0.2991	0.0587	Dewar Window
10	R	0.003	0.2079	0.0544	

The initial alignment analysis for the internal elements of the collimator and long camera shows that the overall alignment tolerance is about +/- 0.003" (+/- 76 μm). At this level, a few elements can add about a micron to the RMS image diameter for some image, worst case. Since the current plan is to align the optics during assembly, rather than relying on accurate machining, this number is non-critical.

Initial alignment of the cameras and dispersers is not critical. The spatial positions are relevant only to getting the light onto the optical surfaces, and an error in angular position results in a static shift of the images on detectors. These items need to be aligned to no better than a few arc-minutes in order to keep the detectors roughly centered on the telescope field.

2.8.2 Optics Flexure Sensitivities

This table gives element sensitivities for the IMACS collimator and long camera. The first column is the multiplet number. The second is the motion: Y for decenter and R for rotation. The next column is the size of the delta in inches, where the rotation is equal to atan(delta / diameter). The next column is the largest image motion in microns for a large ensemble of spots. The last column is the largest image motion after x-y flexure control on the ensemble median.

mult.	motion	Δ(in.)	$\Delta D(\mu$m)	$\Delta D(\mu$m)	
1	Y	0.001	0.6099	0.0954	Field Lens
1	R	0.001	1.3209	0.3139	
2	Y	0.001	6.0275	0.4232	Fused Silica Singlet
2	R	0.001	1.4891	0.3967	
3	Y	0.001	10.6576	0.3902	S-FSL5Y Singlet
3	R	0.001	0.2208	0.0881	
4	Y	0.001	4.9215	0.2070	BSM51Y/CaF2 Doublet
4	R	0.001	0.6786	0.3076	
5	Y	0.001	14.3164	0.8836	S-FPL51Y Singlet
5	R	0.001	2.0471	0.5224	
6	Y	0.001	1.5481	1.3083	BAL15Y/CaF2/S-LAL7 Triplet
6	R	0.001	4.8547	0.2310	
7	Y	0.001	16.1773	1.5824	CaF2 Singlet
7	R	0.001	6.5531	0.9193	
8	Y	0.001	0.0000	0.0000	Filter
8	R	0.001	1.0000	0.0404	
9	Y	0.001	3.0522	1.0072	BSM51Y Singlet
9	R	0.001	2.4004	1.9363	
10	Y	0.001	0.7170	0.1730	Dewar Window
10	R	0.001	0.9969	0.7861	

To summarize, $\pm$ 0.001" ($\pm$ 25 μm) is quite adequate with flexure control, given that these are conservative, worst-case numbers. Without flexure control, some elements would have to be held as tightly as 1.5 microns in order to contribute less than 1.0 micron RMS to the images.

2.8.3 Gravitational Flexure Compensation

In order to reduce gravitationally induced image motions, the structure will be tuned to flex primarily in non-critical modes, rather than attempt to make the structure arbitrarily stiff.

This method starts by computing an adequate ANSYS model of the structure. One by one, the stiffness of each member of the structure, and the position of critical nodes, is perturbed. Each variant of the model is run with X-axis and Y-axis gravity in force, and the differences in the positions of the optical components is recorded. A matrix of differences is created, and multiplied by the matrix of optical sensitivities to component motions. Using this matrix, the pertubations required to reduce the image motions can be computed by Newton-Raphson.

In more mathematical terms, let the optical sensitivities be a matrix $\mathbf{S}$. Let the vector of motions of the optical components under gravity be $\mathbf{m_0}$. For each element e, form a vector of motions after tweaking element e and call it $\mathbf{m_e}$. Let the magnitude of the tweak be de, and define a matrix $\mathbf{M}$ where each column is $(\mathbf{m_e} - \mathbf{m_0})/de$, with one column per element. By Newton-Raphson, the tweaks to the mechanical structure required to minimize image motion, $\mathbf{dm}$, are given by $(\mathbf{S} * \mathbf{M} * \mathbf{dm} = -\mathbf{S} * \mathbf{mo})$. The singular value decomposition of $(\mathbf{S} * \mathbf{M})$ will reveal the smallest tweak required to drive down the image motions. Note that $\mathbf{S}$ does not drop out; $\mathbf{S}$ is not necessarily invertible.

After the structure is built, gravitational image motions may still exist because the ANSYS model is not exact. The derivative matrix $\mathbf{M}$ however should be quite accurate, so last minute tweaks to the existing structure can be computed using measured image motions in place of $\mathbf{m_0}$.

2.9 Thermal Scale and Focus Sensitivities

For the long camera, over a span of 20 degrees, the focus shifts by 1.1 mm and an image motion at the corner of the detector of 0.23 mm. This corresponds to a focus shift of 54 microns/C, and image motion of 12 microns/C. The collimator has similar behavior. A passive thermal compensation system to correct both thermal focus and thermal scale is not practical. Therefore the decision was made to passively correct only the thermal scale change in both the collimator and long camera. The thermal-focus can be corrected actively with the dewar focus. In the case of an FP etalon, the collimator thermal focus can be corrected with the telescope focus. A simple scheme has been chosen for passive thermal correction in both the collimator and long camera, with Delrin spacers controlling the axial position of a singlet element in each.

The thermal analysis of the collimator assumed that the field lens and main collimator body are attached together by aluminum. This will not likely be the case, so the analysis must be rechecked when the final design for the structure exists. If the structure is not sufficiently thermally stable, then the collimator will require an active compensator rather than a passive thermal spacer.

2.10 Alignment Plan

The alignment of the field lens is not critical. The collimator must be aligned relatively well with the telescope, so the collimator bolt-flange will be aligned to the telescope with an alignment telescope attached where the collimator bolts to the structure. The alignment of the other dispersers and cameras is also not critical. These items can be set into the structure to the previously mentioned loose tolerances.

The individual lens elements inside the cells must be aligned. The current plan for the cell design calls for loose tolerances on the cell fabrication, with the individual lens elements potted accurately during assembly. The plan for alignment of the lenses in the cells uses an accurate rotating table and dial gauges. A lens element is placed on top of a stand, on the rotating table. Using dial gauges, the upper and lower surfaces are centered, so that the lens is axial with the table. This is repeated for the item into which the element is to be potted. After the element is potted, the procedure may be repeated with the entire assembly.

2.11 Optics Procurement

2.11.1 Lens Materials

The field lens is currently being figured at Contraves. No difficulties are expected.

The fused silica elements for the collimator, dewar window, and dewar test window are currently being fabricated at TORC. The dewar test window is finished.

The Ohara glass for the collimator is currently being figured at TORC.

Most of the glass for the long and short camera is at Carnegie. Ohara is a few months

late delivering the S-FPL51Y needed for both cameras, so the melt sheet update for both cameras is delayed until that material arrives.

The calcium fluoride blanks for the collimator, long camera, and short camera are on order from Optivac. Optivac has not given us a delivery date, but expectations are currently positive. Schott has given us a reasonable quote on a calcium fluoride boule for the collimator, but not a generated blank. A request for a quote on a generated blank has been made.

2.11.2 Mirror, Gratings, and Grisms

The long camera direct-imaging mirror material is Corning ULE, and is currently being figured at TORC.

The 600 lines/mm grating for the long camera is at Carnegie. We have decided to delay ordering the other two long camera gratings, since they will not be needed during the instrument testing process.

The grism procurement has been delayed until a timeline exists for delivery of the short camera.

2.11.3 Filters

The filters have been sized to match the standard 6.5-inch by 6.5-inch Schott filter glass blanks. Any number of companies provide absorption and interference filters for the various astronomical filter bands in this standard size.

2.11.4 Coatings

An RFQ has been submitted to Coherent (multi-layer coatings) and to Cleveland Crystal (Sol-Gel) for coating designs. Both companies were chosen as sole-source providers due to previous experience with similar large, broadband astronomical optics. Coherent has coated the cameras for ESI and DEIMOS, with a reflection of about 0.86% averaged over the bandpass for ESI. At time of writing, neither company has responded to the RFQ's, but the resulting coating designs will be used to chose coatings on a surface-by-surface basis.

2.12 Baffles

In order to reduce stray light throughout the instrument, baffles and absorbers will be built in during the design stage at all possible locations. Baffles will in general be flat sheets of some thin, shiny material such as carbon fiber sheet, cut to precisely fit around the waist of the light beam. These will be placed approximately every centimeter. This method works as a light dump. When stray light hits the shiny baffle material, it is either absorbed or reflected like a mirror, rather than scattered. If reflected, the light proceeds deeper into the space between two baffles, and is eventually absorbed.

The most critical area for stray light is around the disperser server, where gratings and grisms send stray light into unused orders. The design of the baffles in this area must wait until clearances have been established by the final mechanical design.

2.13 Guiders

The optical designs of all three of the guiders are based upon the Canon EF-series Macro lenses. The principal guider and Shack-Hartman guider use the Canon 50mm f/2.5 EF-Macro lens, while the center-field guider uses the Canon 100mm f/2.8 EF-Macro lens. These lenses have a large aperture which reduces vignetting, and are able to focus adequately at very short distances. For all three cameras, a singlet field lens near the focus will move the pupil onto the front aperture of the Canon lens.

In order to use the Shack-Hartman guider, the Canon 50mm lens and field lens are replaced by a pinhole, simple collimator lens, and a lenslet array. The final design of the Shack-Hartman will be delayed as long as possible in order to take advantage of the possible appearance of new, more appropriate lenslet arrays. The current selection of possible lenslet arrays is limited, but does contain possible choices.

For long-slit viewing, a mechanism carrying a long-slit mask, fold mirror, and relay lens are inserted into the center of the field, while the Canon 100mm lens and camera head are stationary. The long-slit mask is tilted roughly at 45 degrees to the incoming beam. In order to reduce reflection off of the edges of the slit, the slit will be made from a very thin (approximately 10 micron) sheet of electro-formed metal.

Chapter 3

Preliminary Mechanical Design

3.1 Introduction

The following sections describe the preliminary mechanical design of IMACS, with the exception of the mechanical designs for the guide cameras and the science detector systems, which are discussed in their own chapters.

3.2 Design Philosophy

The impact of the IMACS instrument design philosophy will be seen most clearly in the mechanical design. The guiding features of the philosophy are:

- Meet or exceed the science requirements
- Minimize flexure and hysteresis
- Tune flexure for linear displacement and against angular displacement
- Use purchased components whenever possible
- Strive for simplicity in the design of components, assemblies, and mechanisms
- Use existing designs or design concepts whenever possible
- Match automation features to motion requirements (use air-cylinders for in-out motions)

3.3 Sub-system Descriptions

The instrument sub-system names and included components are as follows. Stages include related local electronics and wiring harnesses.

- Hatch

  includes a automated door or screen which seals the instrument at the Nasmyth rotator interface, coated to reflect calibration lamp light back to slit

- Mask Server System (MSS)

  includes slit masks, the mask cassette, the cassette shuttle stage, the mask extractor stage, mask kinematics and lock mechanisms at the focal surface

- Principal Guider Camera

  includes a pick-off mirror, camera lens (commercial), Magellan standard guide camera, theta-motion stage, and filter stage

- Shack-Hartmann Camera

  includes a pick-off mirror, collimator and camera lenses (commercial), Magellan standard guide camera, lenslette array and insertion stage, radial-motion stage, theta-motion stage, pin-hole and light-source calibrator

- Center-Field Guider Camera

  includes pick-off mirror (attached to slit-mask), field lens, Magellan standard guide camera, camera lens (commercial), and filter stage

- Calibration Lamps

  includes a lamp holder and calibration lamps

- Field Lens

  includes the field lens, lens cell, mounting

- Forward Optical Support Structure (FOSS)

  the sub-structure nearest the Nasmyth rotator, which supports the guide cameras, mask server system, field lens, and calibration lamps. Attaches to the mainframe

- Main Optics Support Structure (MOSS)

  the structure farthest from the Nasmyth rotator, which supports the collimator, disperser server system, and the short and long camera assemblies

- Mainframe

  includes the instrument mounting flange, the MOSS mounting flange, and the truss which attaches the mounting flange to the MOSS flange

- Instrument Enclosure

  includes the enclosure around the mainframe, slit area enclosure, short camera assy. enclosure, instrument hatch, access ports to the mask server and the disperser server

- Instrument Carriage

  includes the base which carries the mainframe, the force actuators for the auxiliary support at the MOSS flange, the supports which carry the mainframe when the instrument is removed from the telescope, and local electronics enclosures.

- Collimator

  includes the collimator optics, cells, barrels, and thermal compensation system

- Disperser Server System (DSS)

  includes the disperser wheel and drive assembly, grating cells and tilt stages, grisms and cells, imaging mirror and cell, insertion mechanism, kinematics, and lock mechanisms

- Filter Server System (FSS)

  includes the filters, filter cassette, cassette shuttle stage, filter insertion stage. There will be two filter changing mechanisms, but only one filter set and cassette, which can be interchanged

- Long Camera

  includes the long camera optics, cells, barrel, baffles, and focus mechanism

- Long Camera Assembly

  includes the long camera, shutter, filter-changer mechanism, and mounting truss

- Short Camera

  includes the short camera optics, cells, barrel, baffles, and focus mechanism

- Short Camera Assembly

  includes the short camera, shutter, filter-changer mechanism, and mounting truss

- Dewar

  includes the CCD detector array, X-Y motion stage for flexure control, focus stage, dewar window, vacuum vessel, and cryo-coolers or liquid nitrogen dewar

3.4 Mass Properties

3.4.1 Nasmyth Instrument Requirements

The System Specification for the Magellan Telescope (Document No. 95TM0022, Rev. 1, March 22, 1996) describes the Nasmyth instrument interface, including the space envelope, back focal distance to the Nasmyth instrument rotator (NIR), and maximum instrument mass properties (weight, location of center of gravity, imbalance about optical axis, maximum moment on the NIR). The values are shown in Table 3.1 for reference.

Back focal distance (w/field corr.)	390.8 mm
Weight	1364 Kg
Moment of inertia	396 Kg-m^2
Cantilever moment from mounting surface	16,972 N-m
Imbalance about optical axis	1358 N-m

Table 3.1: Nasmyth Instrument Mounting Properties.

From its conception, IMACS has violated most, if not all of the mass and volume requirements, and efforts have been made to both publicize those violations, and by various design features, to mitigate against the consequences of those violations. A prime example is the use of an auxiliary support at the rear of the instrument, to avoid overloading the NIR in mass, bending moment, and mass moment of inertia. The instrument is being designed to be balanced about the optical axis.

Redesign of the Magellan I Nasmyth platform is currently underway, to raise its load limit, to nearly double its floor space, to add removable panels for long instruments (MIKE), and to lower its floor level. The IMACS team is working closely with the telescope project to insure that the final designs for IMACS and the platform are compatible.

Finally, IMACS is expected to exceed the NIR-axis moment of inertia limit by as much as a factor of 3. Measures for raising the moment of inertia limit of the rotator are being investigated.

3.4.2 Weight Estimate

A preliminary weight estimate for IMACS is shown in Table 3.2. Most of the estimates are based on calculated volumes or masses wherever known, or based on previous experience with similar subsystems. The exceptions are the instrument structure and carriage masses, which are based on unrealistic (in terms of mass) preliminary designs. The FOSS, MOSS, housing, and carriage masses will all be reduced in detail design.

Sub-System	Weight (Kg)
Mask Server Sys.	150
Principal Guider	15
Shack-Hartmann Camera	10
Center-Field Guider	20
Calibration System	10
FOSS	200*
MOSS	670*
Mainframe	770*
Instrument Housing	200
Instrument Carriage	1000*
Field Lens	56
Collimator	115
Disperser Server Sys.	165
Long Camera Assy.	206
Short Camera Assy.	250
Detector Array System	25
Total Mass	3862

Table 3.2: IMACS weight estimate. Items with * are preliminary high estimates which will be reduced substantially.

3.4.3 Centroid and Moment of Inertia

The best estimates of the instrument centroid location and moment of inertia come from the finite element model of the instrument structure. Note that the current estimate does not include the slit area mass or moments of inertia. The FEA model is described later; the centroid and moment of inertia estimates are shown in Table 3.3 for reference.

Centroid location:	(0,0,0) at center of mounting flange
C_X	0 mm
C_Y	1700 mm
C_Z	-42 mm (below opt. axis, Icam down)
Moments of Inertia	
I_{XX}	4419 Kg-m2
I_{YY}	4232 Kg-m2
I_{ZZ}	948 Kg-m2

Table 3.3: Instrument centroid location and moments of inertia.

3.5 Mask Server System

3.5.1 Introduction

The mask server system (MSS) stores and selects masks, and inserts masks or other slit area accessories into the telescope focal surface. The MSS consists of a shuttle mechanism for selecting one of five mask positions, an insertion mechanism which extracts a mask from the shuttle and transports it to the focal plane, and three locking mechanisms, which kinematically locate and fix the mask at the focal surface.

Cutting multi-slit masks with up to 300 slits is one of the more challenging aspects of the IMACS project. Multi-slit masks are being produced at various observatories for various instruments, but no site is cutting masks of the size or complexity required for IMACS. Although the mask cutting system is not strictly part of the MSS, it is discussed later in the MSS sections.

3.5.2 Mask Characteristics

The 30 arc-min focal 'plane' of the Magellan I telescope with the Atmospheric Dispersion Corrector / Field Corrector (ADC) is a spherical surface with a 1231.74 mm radius of curvature and a 620 mm diameter. The sagitta over the diameter is 39.7 mm. For small masks and fields (up to 5 arc-min square), the focal surface can be fit with flat masks. Fields 5 arc-min in width and longer in length can be fit with cylindrical masks. But for both the long and short camera full fields of 15 $\times$ 15 and 27 $\times$ 27 arc-min respectively, the slit masks must follow the radius of curvature. IMACS is thus apparently unique among the current generation of large multi-object spectrographs (Keck DEIMOS, VLT VIMOS, Gemini GMOS) in requiring spherical shell slit masks.

3.5.2.1 Mask Materials

Several materials have been investigated as candidates for the IMACS masks. The general requirements are:

- Maximum thickness
  - 1 mm
- Maximum deflection of mask due to gravity loading
  - ± 0.5 mm for any orientation
- Physical Properties
  - opaque from 300 nm to 2.5 microns (log D $\geq$ 4)
  - reflectivity not to exceed 10% over wavelength range
  - dimensionally stable
  - CTE $\leq$ 6 ppm/C

The specifications intentionally do not include a material, as the final material choice is contingent on the mask fabrication methods. Some of the known options are:

- The Keck/DEIMOS instrument is specified to use flat aluminum masks with slitlettes machined into the mask with a highspeed air spindle. The masks are formed into cylindrical shells after machining.

- The Gemini/GMOS instrument uses unidirectional carbon-fiber composite masks with slitlettes burned through the mask with a YAG laser.

Several multi-object spectrograph projects have investigated mask materials and fabrication methods. See "Fabrication of Narrow-Slit Masks for the Gemini Multi-Object Spectrograph", Proc. SPIE 2871, for an excellent review of materials and fabrication methods.

Some of the materials considered in the GMOS study included:

- aluminum

- stainless steel

- molybdenum

- invar

- carbon fiber

The GMOS team eliminated the metals, except for invar, for thermal reasons, and chose carbon fiber for the mask substrate. They concluded that the only method which provided the desired versatility, speed, and precision was laser cutting. After reviewing the GMOS slit mask specs, and considering the special requirements for IMACS, we concluded that laser cutting carbon fiber masks was the best option as well.

Several carbon-fiber fabricators answered a request for quotation (RFQ) to produce 1000 mask blanks. The prices ranged from $135 to $360 per mask, which is high, but not prohibitively so. It may be possible to revise some of the specifications to reduce the price further. The final dimensions of the masks are expected to be about 650 mm in diameter, with the required 40 mm sag, and a shell thickness of about 0.5 mm.

3.5.3 Mask Frames

Although the 0.5 mm thick masks are relatively stiff on their own, the masks will be held in frames. The frames will provide the features which allow the masks to be held in the cassette, automatically inserted, and locked into position at the focal surface. Approximately 15 frames will be fabricated to allow for a set in the instrument, and another two full sets in various stages of fabrication.

Figure 3.1 shows a mask and frame combination. The frame consists of a main ring, and a secondary ring which clamps the mask to the primary ring with a circle of fasteners. The mask frame carries three hemispherical kinematics which engage V-grooves in the active position at the focal surface. The frames slide on a set of rollers which are attached to brackets on the sides of the frames. The rollers are spring loaded to the brackets, to allow the small axial motion of the mask as it engages the V-groove kinematics. The wheel brackets also provide keyhole features which engage with the mask select stage and the cassette locking stages.

The mask frames may be made of aluminum, or possibly carbon-fiber (CF). Aluminum frames will form a bi-metallic spring with CF, and will tend to distort the masks under temperature variations. CF frames, on the other hand, will match the mask, and will be stiffer, lighter, and more easily handled than aluminum counterparts.

3.5.4 Mask Cassette

The mask cassette is a box which carries a set of five masks. The cassette is permanently attached to the mask shuttle stage - masks can be removed from the cassette one at a time by releasing the individual mask locks in the cassette. Figure 3.2 shows the locking mechanism, which can be released automatically by a single air-cylinder when the mask is in the insertion position, or manually when the mask is not in the insert position. The air-cylinder key engages the keyhole feature on the mask which is in the insert position.

3.5.5 Mask Shuttle Stage

The IMACS specifications call for the ability to carry a set of at least five masks which can be selected automatically by the user. The main features of the shuttle are the commercial

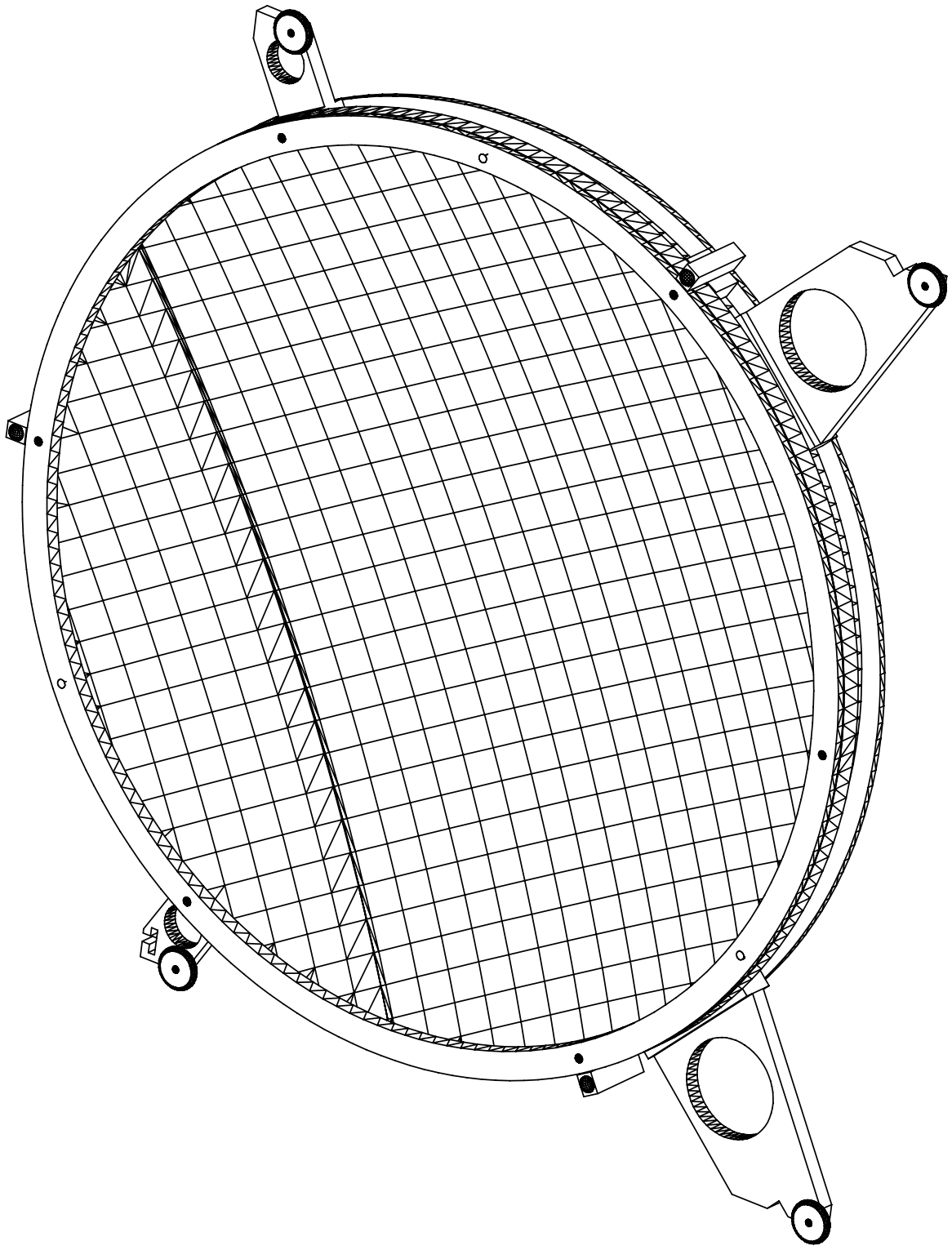

Figure 3.1: Slit mask and frame assembly.

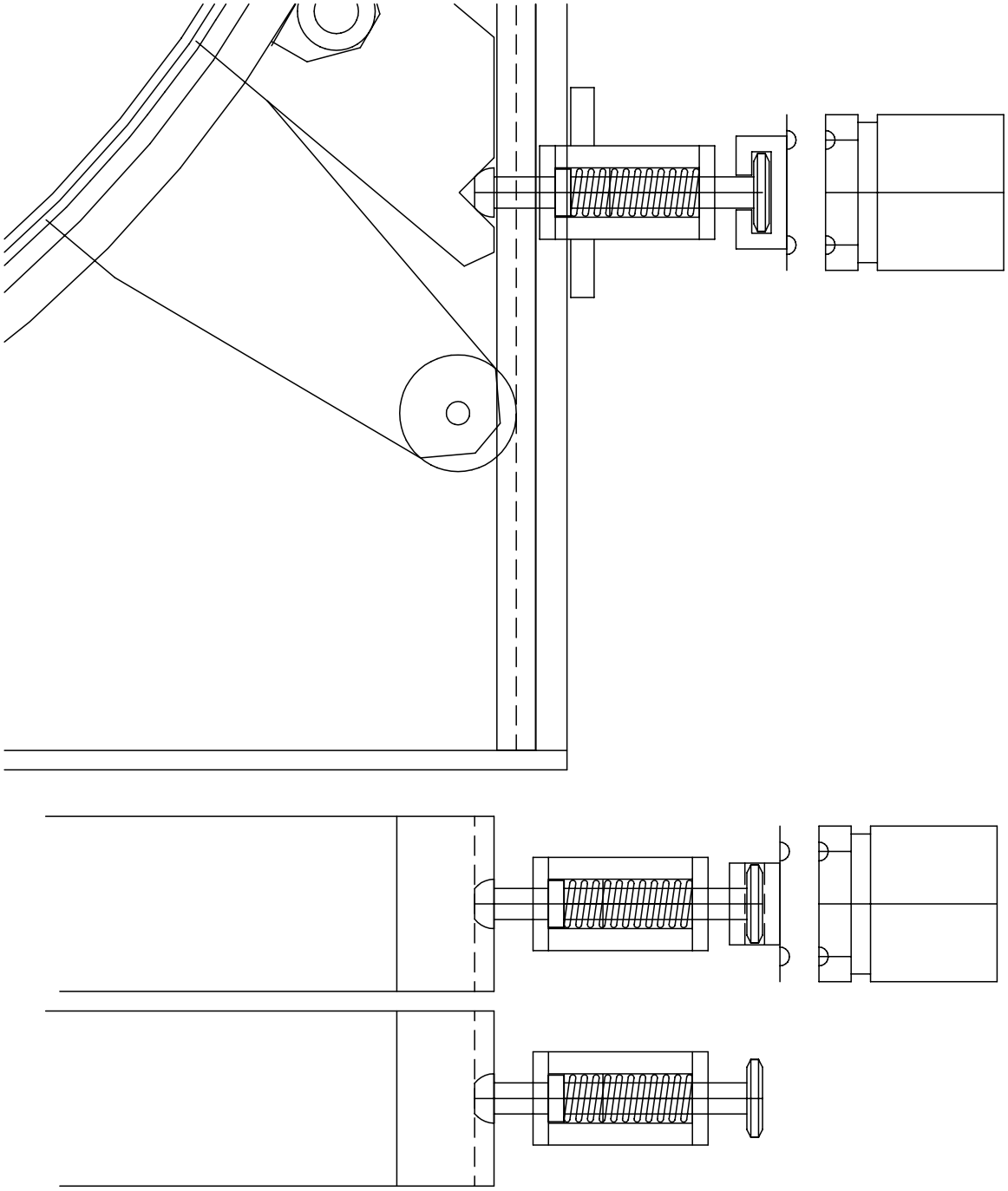

Figure 3.2: Mask cassette locking mechanisms.

motion stage (currently an Aerotech 408121 stepper motor stage with a ground ball-screw), and the cassette which holds the masks on the motion stage.

The cassette carries a set of rails which constrain the masks when not in use. The rails for each mask align with the rails on the FOSS when the mask position is selected for insertion. Figure 3.3 shows an endview of a cassette with five masks installed.

3.5.6 Mask Insertion Stage

The mask insertion stage is fixed to the FOSS bulkhead. The stage is composed of a commercial air-powered linear motion stage and a bracket on the sliding part of the motion stage. The motion stage comes equipped with limit switches which signal its positions at either end of the stroke. A 'key' feature on the mask slider bracket engages a keyhole on whichever mask is located at the insert position. On command from the motion controller, and after checking position sensors on the mask shuttle, kinematic locks, and insertion stage, the insertion stage will install or retract a mask from the focal surface.

3.5.7 Mask Locking Stage

The mask locking stage is composed of a set of three air-powered toggle clamps and the V-groove kinematics which match the three hemispheres on the mask frames. The commercial toggle clamps have limit switches to indicate their state in the locked or unlocked position. The three V-grooves have ramped sides which allow the mask hemispheres to ride slightly up before dropping down into the grooves.

3.5.8 Mask Fabrication

The IMACS specification describes the requirements for the slit mask cutter, and those specifications are summarized here:

- Number of slits
  - 325 nominal (27 arcmin / 5 arcsec), approx. 1000 max.

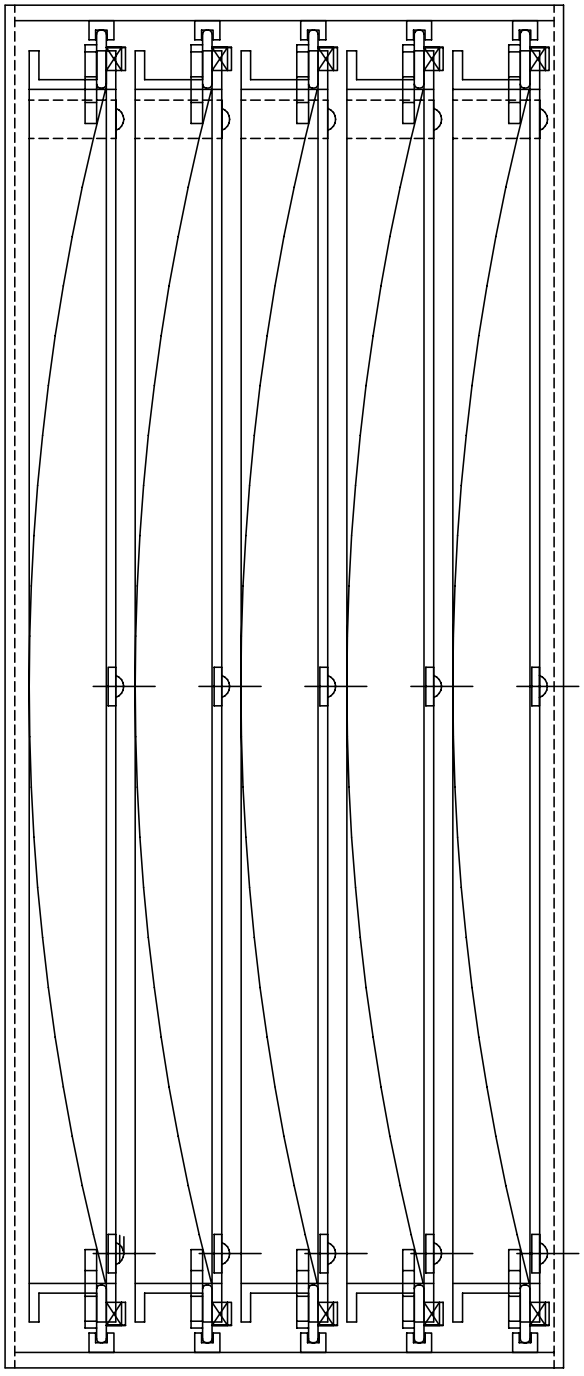

Figure 3.3: Mask cassette.

- Mask sizes
  - 560 mm diameter maximum (27 arcmin square FOV), spherical
  - 312 mm diameter (15 arcmin square FOV), spherical
  - 105 mm square (5 arcmin FOV), single mask, flat
  - 105 mm x 312 mm (5 x 15 arcmin FOV) cylindrical (can be cut flat)
  - 105 mm x 560 mm (5 x 27 arcmin FOV) cylindrical (can be cut flat)
  - 105 mm x 105 mm square, multiple flat masks (up to 3x3 on a 15 arcmin FOV)
- Slit positions
  - $\pm$ 1/10 arcsec, $\pm$ 35 microns, dispersion direction
  - $\pm$ 1 arcsec, $\pm$ 350 microns, perp. to dispersion dir.
  - $\pm$ 1/10 arcsec (f/11), $\pm$ 400 microns normal to surf.
- Fabrication time
  - avg. 30 seconds per slit
  - avg. 1.5 hrs. per 180 slits (1 row, 15 arcmin FOV)
  - avg. 3 hrs for 325 slits (1 row, 27 arcmin FOV)

As mentioned above, we have attempted to make the best possible use of previous research by others into the fabrication of the slit masks. This lead us directly to laser cutters and carbon-fiber masks.

The GMOS team identified the following fabrication methods:

- Conventional machining
- Laser cutting
- Water jet cutting
- Electronic Discharge Machining (EDM)

- Photo-chemical etching.

The only method which could cut the requisite number of slitlettes in a reasonable amount of time was the laser. Commercial laser cutting systems are readily available. The GMOS team received quotes from two companies, and considered fabricating their own cutting machine. Ultimately, they concluded that their own people were busy enough with instrument building, and the potential savings from building a machine from scratch were outweighed by the convenience and security of buying a proven machine from a commercial manufacturer.

The GMOS team has recently installed a laser cutting machine in Hawaii. The machine was manufactured by Advanced Recording Technologies (ART) of Escondido, California. We were able to see the machine in action prior to shipping, and we cut some material samples for testing purposes.

Figures 3.4,3.5, and 3.6 show some of the results of cut testing with the ART laser system. Although they cannot be seen very well in these images, the laser left a fair number of CF whiskers in the straight cuts which ran with the weave in the CF material. On the other hand, the round holes, which were cut across the weave, show excellent edge finishes. It is for this reason that we are confident that by orienting the CF twill at 45 degrees to the slit orientation, clean cuts will be easily achieved.

3.5.9 Integral Field Units

There is no current requirement for integral field units in IMACS. However, as this is a desirable future addition, the mask serving system is being designed with IFU in mind. In particular, the leading position in the mask cassette is oversized to accommodate an IFU. The focal surface area has been left as open as possible for the same reason.

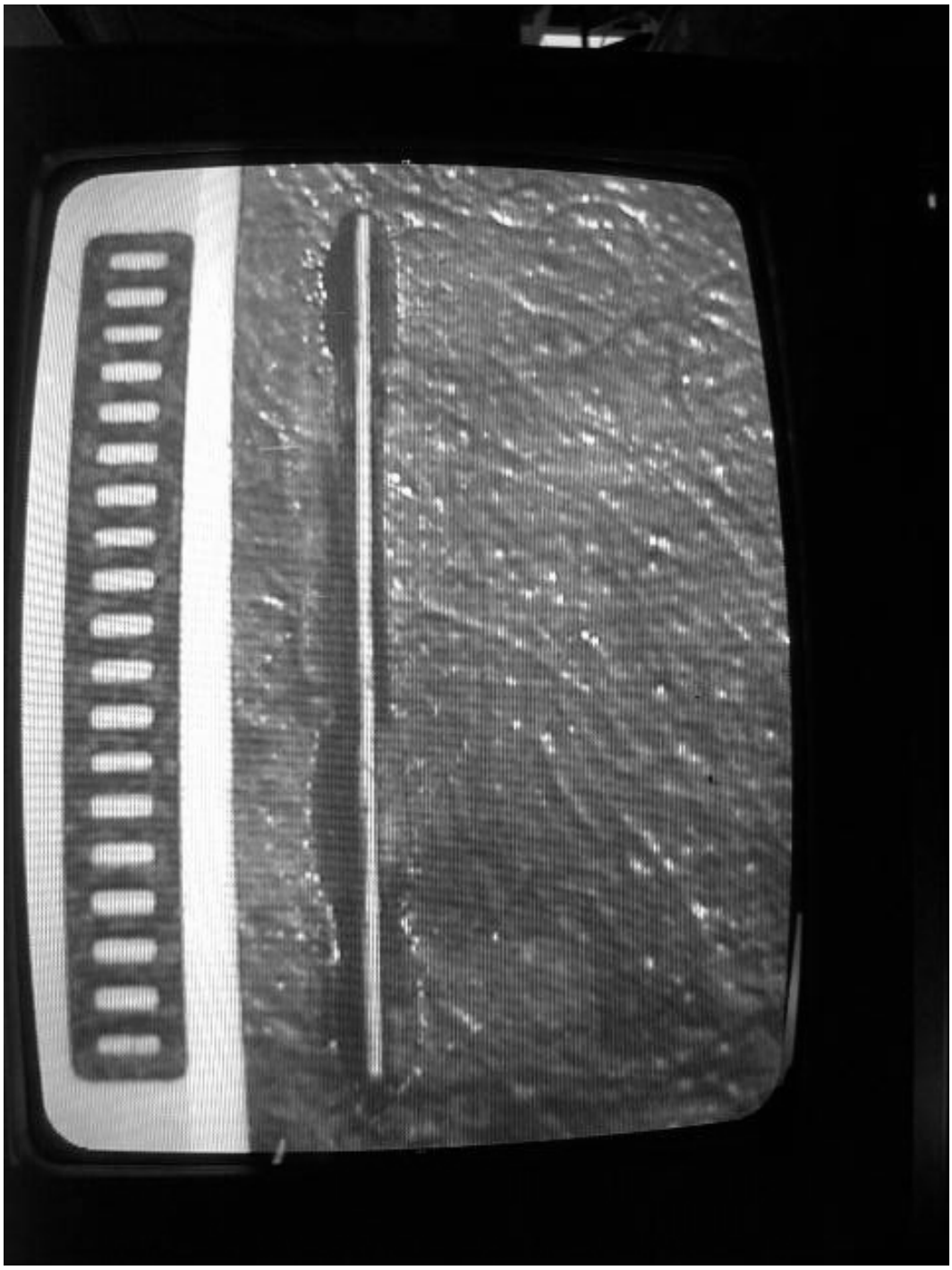

Figure 3.4: Laser-cut slit in carbon-fiber mask material. The material is 0.5 mm thick, made of 2 plys of CF 2x2 twill. The cut is 10mm long by 0.124 mm (29 $\times$ 0.36 arc-sec). The ladder pattern lines are on 0.5 mm centers for scale.

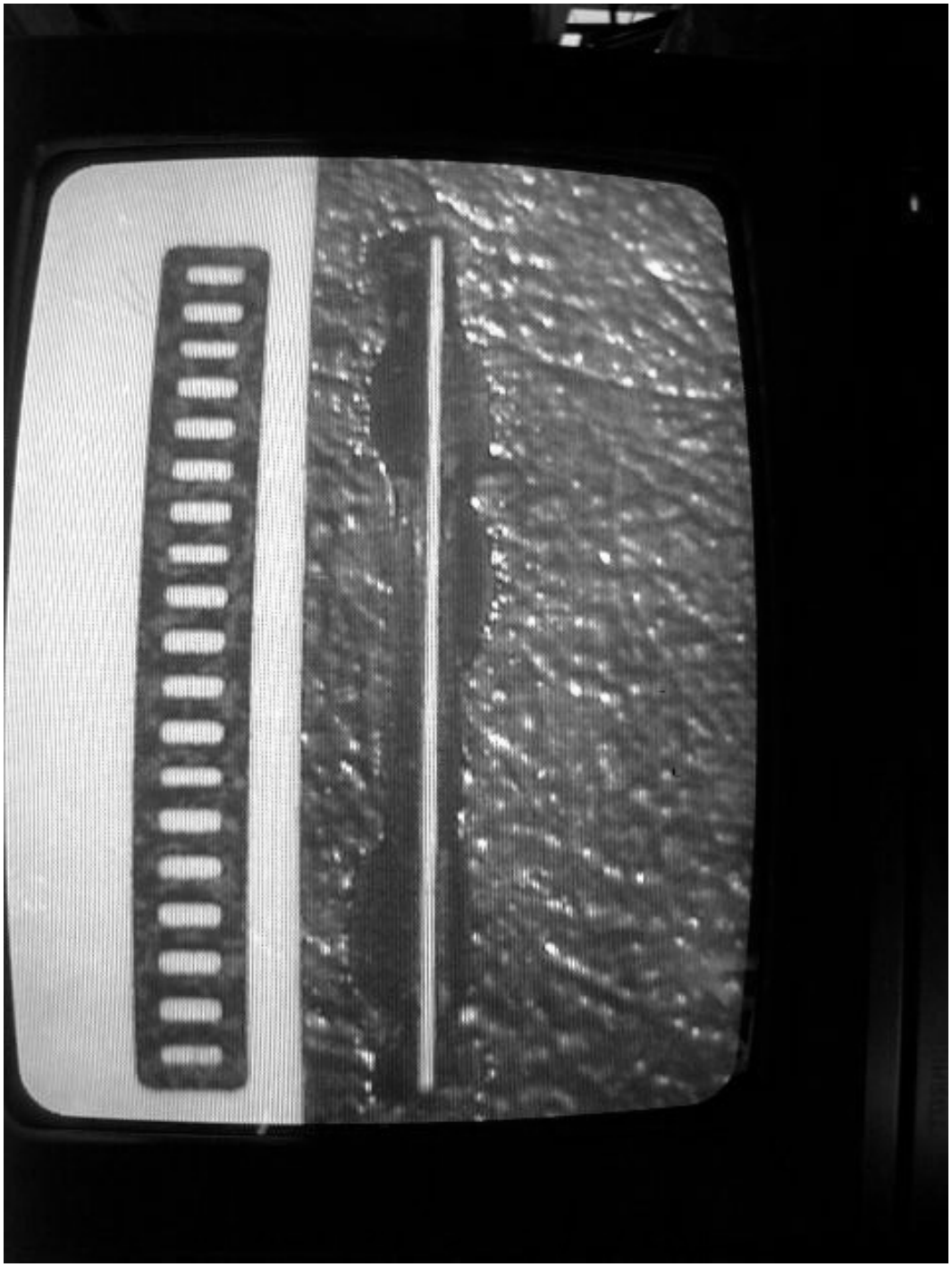

Figure 3.5: A second laser-cut slit in carbon-fiber mask material at a different laser power setting. The material is 0.5 mm thick, made of 2 plys of CF 2x2 twill. The cut is 10mm long by 0.124 mm (29 $\times$ 0.36 arc-sec). The ladder pattern lines are on 0.5 mm centers for scale.

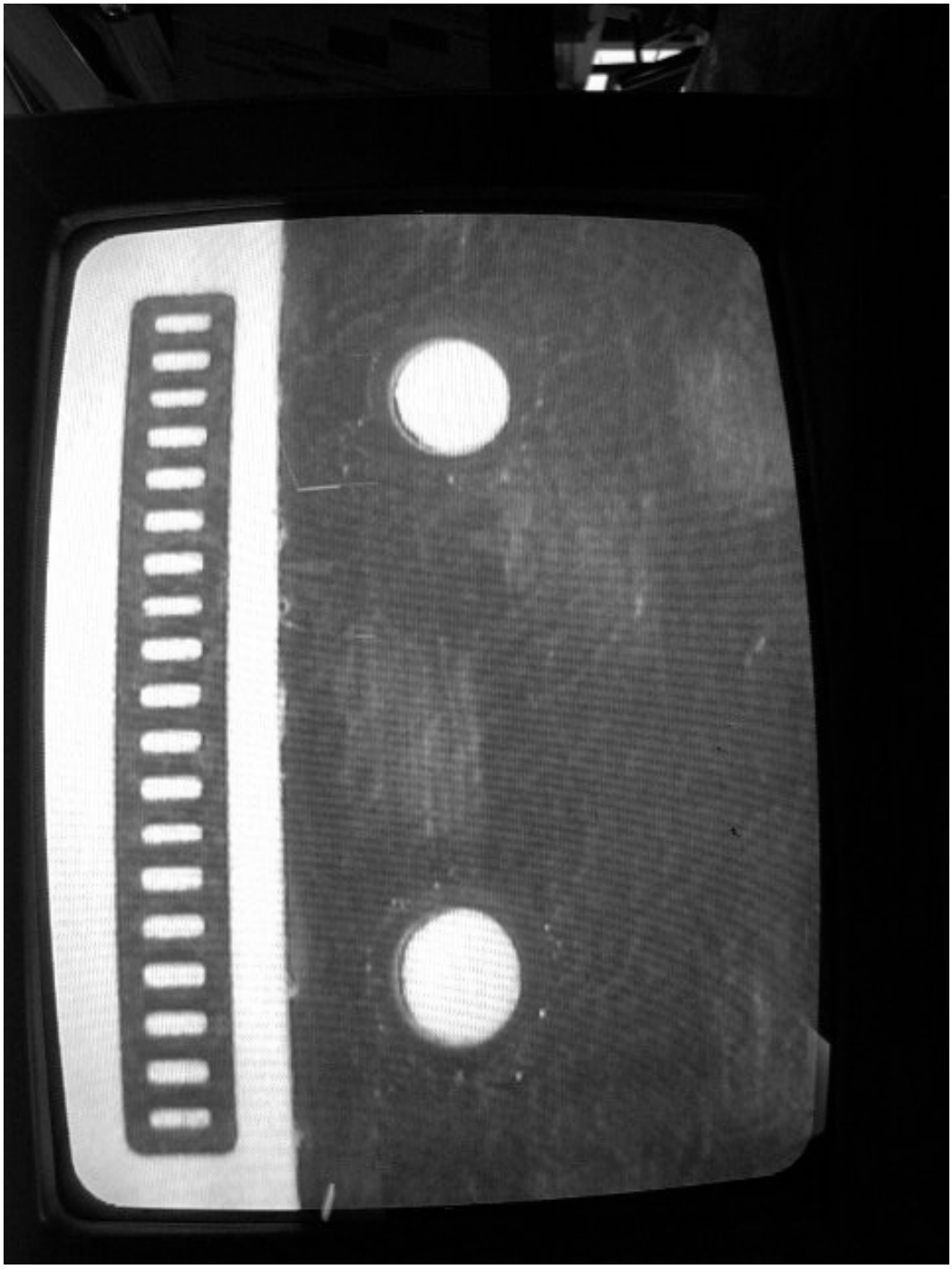

Figure 3.6: Two 1 mm (2.9 arc-sec) diameter holes cut in 0.5 mm thick CF material. The ladder lines are on 0.5 mm centers for scale. Note the clean edges and lack of fiber whiskers in the holes.

3.6 Guide Cameras

3.6.1 Introduction

3.6.1.1 Description of the Guiders

Integral to IMACS are three CCD cameras that are used for acquisition, guiding, and maintenance of the optical system, including control of the primary mirror support system and the secondary position. Each guider accesses a 105" x 105" field-of-view at 0.2"/pixel and carries a single user- accessed filter that can be introduced into the beam. Guider 1 is the principal guider, which tracks a field star and provides offsets for telescope tracking and the secondary tip-tilt system. Guider 2 provides a Shack-Hartman test image that provides information for figure control and fine guiding of the instrument rotator. Guider 3 views the center field of the instrument and a 105" long slit inserted into the beam for the purposed of single object or long-slit observations. The guiders have commercial lenses that can be focused, but the present plan is to fix focus at the focal surface corresponding to the position of the multi-slit mask and always focus the telescope to this point.

Guiders 1 and 2 are used for direct imaging (including Fabry-Perot mode) or in conjunction with multi-slit aperture plates or the integral field unit. A special feature of the mechanical design mechanical rigidity between these guiders and the kinematic mountings for the mask - both have a short, stiff load path to a common mounting bulkhead. Flexure between guider and slit mask will be held to under 0.001-inch (0.07 arcsec) for a several-hour exposure.

Guiders 1 sweeps out an arc of 40 degrees x 105 arcsec at a field radius of approximately 15 arcmin, just outside the 27 arcmin diameter field of the IMACS short camera. A diagonal pick-off mirror, tilted at an angel somewhat greater than 45 degrees to the incoming beam (to align with the curved field of the Nasmyth focus) intercepts the beam in front of the focal surface. Guider 1 sweeps out a fixed radius for a total swept area of 18 sq arcmin. A V=20 star with the Magellan guider and a throughput of 30pole there is on average one such star per guider field, and there are approximately 6 such fields swept out by the guider. (Experience with the COSMIC guider at the 200-inch Hale Telescope, confirms these numbers.)

Guider 2 operates in a comparable fashion on the opposite side of the field from Guider 1. However, Guider 2 is also equipped with a lenslet array that can be introduced into the beam

to provide a Shack-Hartman test of the primary mirror figure and optical alignment. Because the star selected for this test must pass through a small aperture, Guider 2 is also able to move radially one field diameter so that the selected star can be centered up. Whether in direct mode or as a Shack-Hartman test, Guider 2 also provides a guiding signal for the Nasmyth instrument rotator, which must be held to a sub-arcsecond precision over the field diameter during hours- long exposures. Exposures for a Shack-Hartman test are anticipated to last of order 30 seconds in order to average over seeing and build up sufficient signal for centroiding the multiple images, but this is sufficiently often for correction of the angular tracking. Guider 2 is also fitted with a pinhole and light source for calibration of the Shack-Hartman test.

Guider 3 is a fixed camera that views light reflected from a centerfield mirror into which a multi- width long slit is cut (by thin film deposition or EDM). For acquisition of single objects, particularly relatively bright ones, this long-slit mode will enable a simpler, more efficient set-up for spectroscopy. As of this document, the plan is to bring in this mirror, and the optics that transfer this image to the fixed guide camera, on a dedicated mask holder unit. The project will investigate the possibility of bringing in the mirror and optics on a separate robotic stage not requiring use of one of the slit mask slots. If upcoming tests with Magellan 1 show the necessity of frequent on-axis Shack-Hartman tests, Guider 3 will be fitted with a lenslet array in the manner of Guider 2.

3.6.1.2 Operation of the Guiders

The mechanical control of the guiders, including their position, mode (direct or Shack-Hartman), and filter, are controlled by the IMACS instrument. These functions are displayed in the IMACS control window on the UNIX workstation, although software control is accomplished in a LINUX PC which in turn talks to DOS PC's that run the motor controllers.

The imaging from each guider will be controlled by a dedicated PC running DOS, an advanced version of a system already in use at the du Pont telescope developed by Steve Shectman. The settings for the exposure time and other sampling parameters will be entered through a keyboard that can address any one of the guiders (not only the three in IMACS but those of other instrumentation). Error signals generated by these guiders, for correcting the tracking or controlling the tip/tilt control of the secondary , and for adjustment of the primary mirror support or secondary mirror alignment (collimation and focus) will be outside of the

IMACS system and will be fed directly to the TCS (Telescope Control System). The plan is for the guiders to provide error signals which the TCS software will use to apply corrections to the mirror supports, vane end actuators (secondary mirror), secondary tip-tilt, and telescope tracking, Software for these functions is the responsibility of Steve Shectman.

In order to make fine adjustments of the slit positions, and to compensate for atmospheric dispersion changes as fields are tracked to different air masses, it will be necessary for IMACS to be able to modify the cursor position, otherwise set at the DOS PCs. This information will also be sent to the TCS, along with IMACS status, including for example the operating mode of the guider, position angle (guiders 1 & 2 only), radial position (guider 2 only), and parity of the image. Interlocks preventing the moving of the guiders during an IMACS exposure, for example, will be done in the DOS PC software with information fed through the TCS.

For a typical multislit observation, the telescope is given a field position and an expected field rotation angle to achieve alignment of the multislits with targeted objects. Assuming that the field center is known to 30" or better, guide stars can be selected for Guider 1 & 2 as soon as the field is acquired. Guider 2 is run in Shack-Hartman mode to correct primary mirror figure and secondary mirror alignment and focus. A short exposure of the field is taken with the science array and used to identify a number of target galaxies or alignment stars and to compare there positions with the target positions (in CCD coordinates) that have been calculated from an image of the slit mask. These positions are determined before observing; their integrity is assured by the repeatability of 0.001-inch in the mask position. (An alternate approach which has been successfully used at other telescopes is to cut 10" diameter holes in the slit mask at the position of 2 or more target stars and to observe these stars through the slit mask.) A simple software routine, previously developed for COSMIC, calculates the RA and DEC offsets and the correction to the Nasmyth rotator angle required to bring the field into alignment with the mask. These corrections are applied closed loop by requesting the TCS to offset the telescope and Nasmyth rotator and, through the guide camera control computer, to move the cursor to its predicted new location. This procedure, used by COSMIC at the Hale Telescope, routinely achieves moves of 0.1" accuracy, which allows a setup to be accomplished in a single iteration.

This mode of acquisition has been used with COSMIC and the WFCCD at the LCO du Pont telescope. The project hopes that the precision of the IMACS hardware will enable a

more sophisticated approach. Assuming a position uncertainty of the telescope of order 10 arcsec, it should be possible to use the Naval Observatory star catalog and the metrology of the guider system identify and position target guide stars in order to achieve precision of 1 arcsec or better for the initial setup.

The mechanical requirements for the three guide cameras are as follows:

3.6.2 Principal Guide Camera

1. Sweeps out an arc at a fixed radial distance of approximately 16 arcmin from the center of the field.
2. Sweeps out an arc of 40 degrees circumferentially.
3. Is to be located as close as possible to the bottom of the field (perpendicular to the slit length).
4. Flexure between the guider and the slit-mask must be held to less than 25 μm for a several hour exposure (this is equivalent to 0.07 arcsec of motion at the focal plane).
5. Provisions for deployable infrared filter are to be included for guiding during considerable moonlight.

3.6.3 Shack-Hartmann Guide Camera

1. Sweeps out an arc at a radial distance that is variable from approximately 14.5 arcmin to 16 arcmin from the center of the field
2. Sweeps out an arc of 40 degrees circumferentially.
3. Is to be located as close as possible to the top of the field (opposite the principal guide camera for maximum moment arm).
4. Flexure between the guider and the slit-mask must be held to less than 25 μm for a several hour exposure (this is equivalent to 0.07 arcsec of motion at the focal plane).
5. Provision for deployable infrared filter are to be included for guiding during considerable moonlight.

6. The camera is to be designed such that it is switchable from observing mode (same optical design as the principal guide camera) to Shack - Hartmann wavefront sensing mode.

7. Resolution for deployment is to 75 μm. This allows us to center the 2 arcsec aperture of the Shack - Hartmann over the specified star to a resolution of 0.21 arcsec.

3.6.4 Center Field Guide Camera

1. Is to be located in as short a path as possible from the center field.

See Figures 3.7 and 3.8 for top and isometric views of the guide cameras and their positions with respect to the focal surface.

3.6.5 Guide Camera Stages

3.6.5.1 Principal Guide Camera

The principal guide camera is mounted on a table that traverses 40 degrees circumferentially. This is achieved through the use of two circular guide rails (THK) and recirculating ball bearing blocks without any clearance. Three blocks are used - two on the outer rail, and another single block on the inner rail. The radii of the two rails are 500mm and 750mm. Figure 3.9 shows the principal guide camera on its motion stage.

Movement along this degree of freedom is controlled by a single stepper motor. The motor drives a worm gear preloaded on a large radius (600 mm) gear sector. A 4mm pitch has been arbitrarily chosen for now; however, future calculations will be done to show that this pitch will be large enough to support the camera weight, without introducing significant noise to the system. It is likely that the worm will have to be driven through a 90 degree elbow gearhead.

Due to interferences with other structures (specifically the clamps for holding the mask in the focal plane), the camera is mounted on an angle on its table (i.e. It does not point radially inward). Doing this allows us to patrol as close as possible around to the mask clamp; hence, moving as close as possible to the nominal position at the bottom of the field. The result is

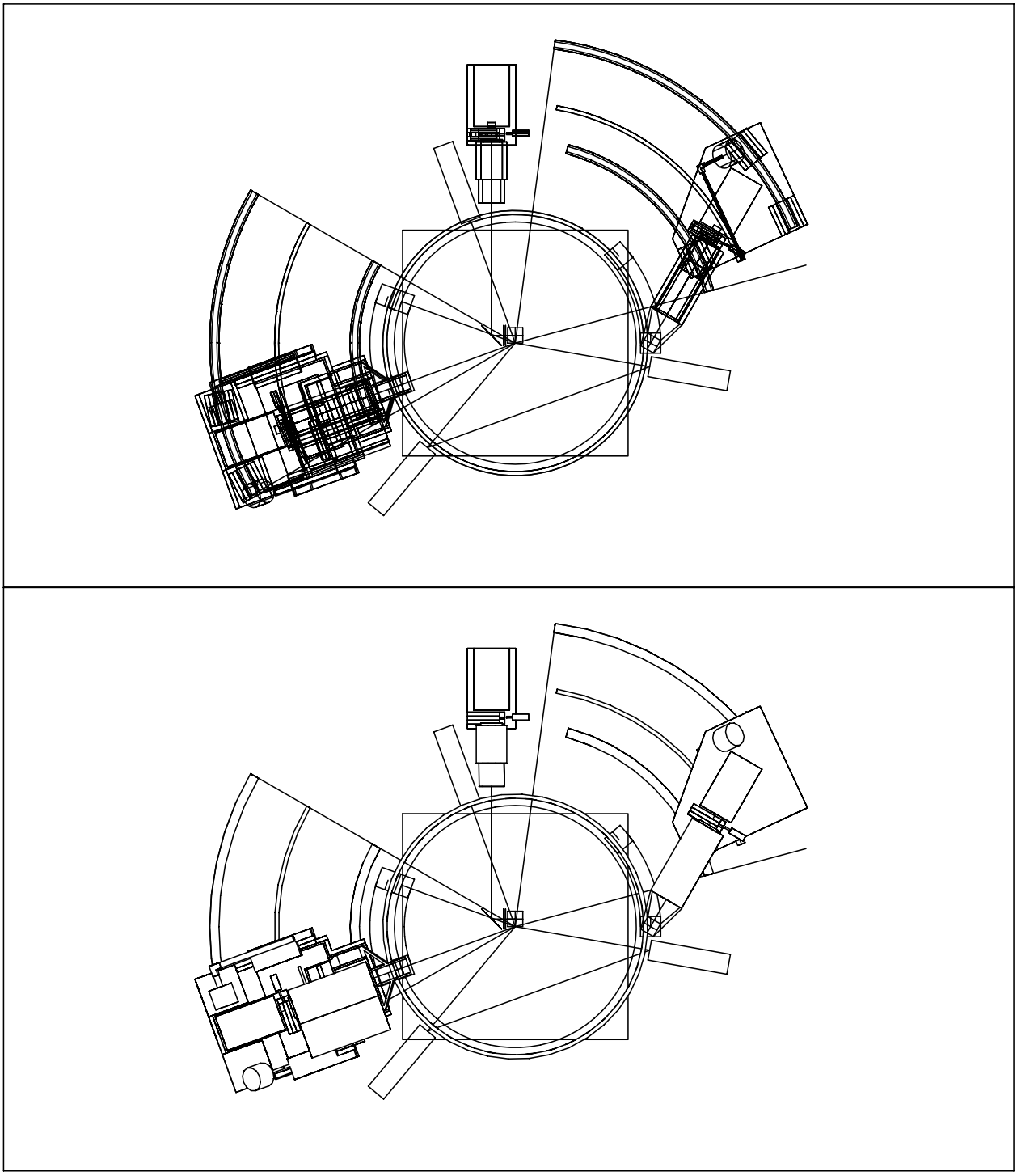

Figure 3.7: Top views of guide cameras.

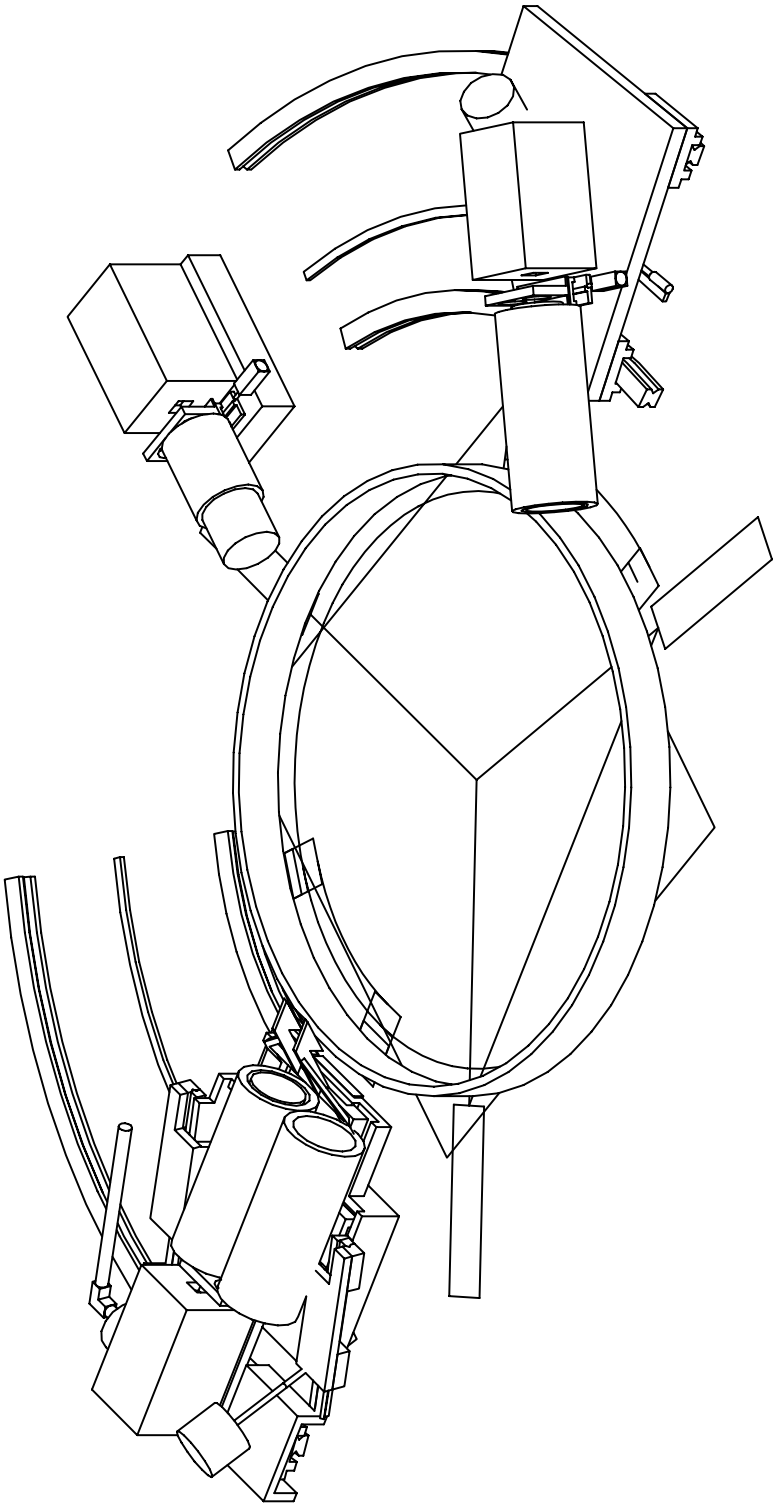

Figure 3.8: Isometric view of guide cameras.

that the pickoff mirror patrols an area starting at the bottom center of the field, through an arc of 40 degrees to the one side. It would be desirable to have the arc centered at the bottom of the field, but the other structures in the area will not permit this.

The camera head itself is mounted directly to the table. Immediately in front of the camera head is a small stage for a filter, and filter dummy. This stage is driven by a small air cylinder against two hard stops. This setup yields stiff and repeatable positioning of the two elements.

In front of the filters is a barrel arrangement that contains the pickoff mirror, pickoff arm, field lens, and re-imaging lens (proprietary Canon lens). Due to the availability of space around these elements, it is felt that it will be quite simple to build an extremely stiff structure to hold these elements.

The center of gravity of the camera head, filter mechanism and barrel is slightly forward of the center of gravity of the table. It is expected however that the separation of the three rail block supporting the table will add stiffness to the system. As can be seen, the load path of the camera in any of its orientations is directed through quite robust cross-sections. It is felt that the weakest point in the system will be the stiffness through the worm gear.

3.6.5.2 Shack - Hartmann Guide Camera

The Shack - Hartmann guide camera is also mounted on a table that traverses a full 40 degrees circumferentially. Again two circular guide rails are used; however, the radii are 400mm and 750mm. In this case, the table is mounted on four recirculating ball bearing blocks without any clearance. Figure 3.10 shows the Shack-Hartmann guide camera and its motion stage.

Similar to the principal guide camera, movement along this degree of freedom is controlled by a single stepper motor. The motor drives a worm gear preloaded on a large radius (600 mm) gear sector. Again the worm gear will be driven through a 90 degree elbow gearhead. In this case, the gear sector will be recessed slightly below the plane defined by the surface of the FOSS. This is due to the fact that the second stage of the SH camera moves in such a way that most of the clearance between the bottom of the first table and the FOSS surface is inaccessible.

The second stage of the SH camera moves radially on linear rails. These rails are mounted

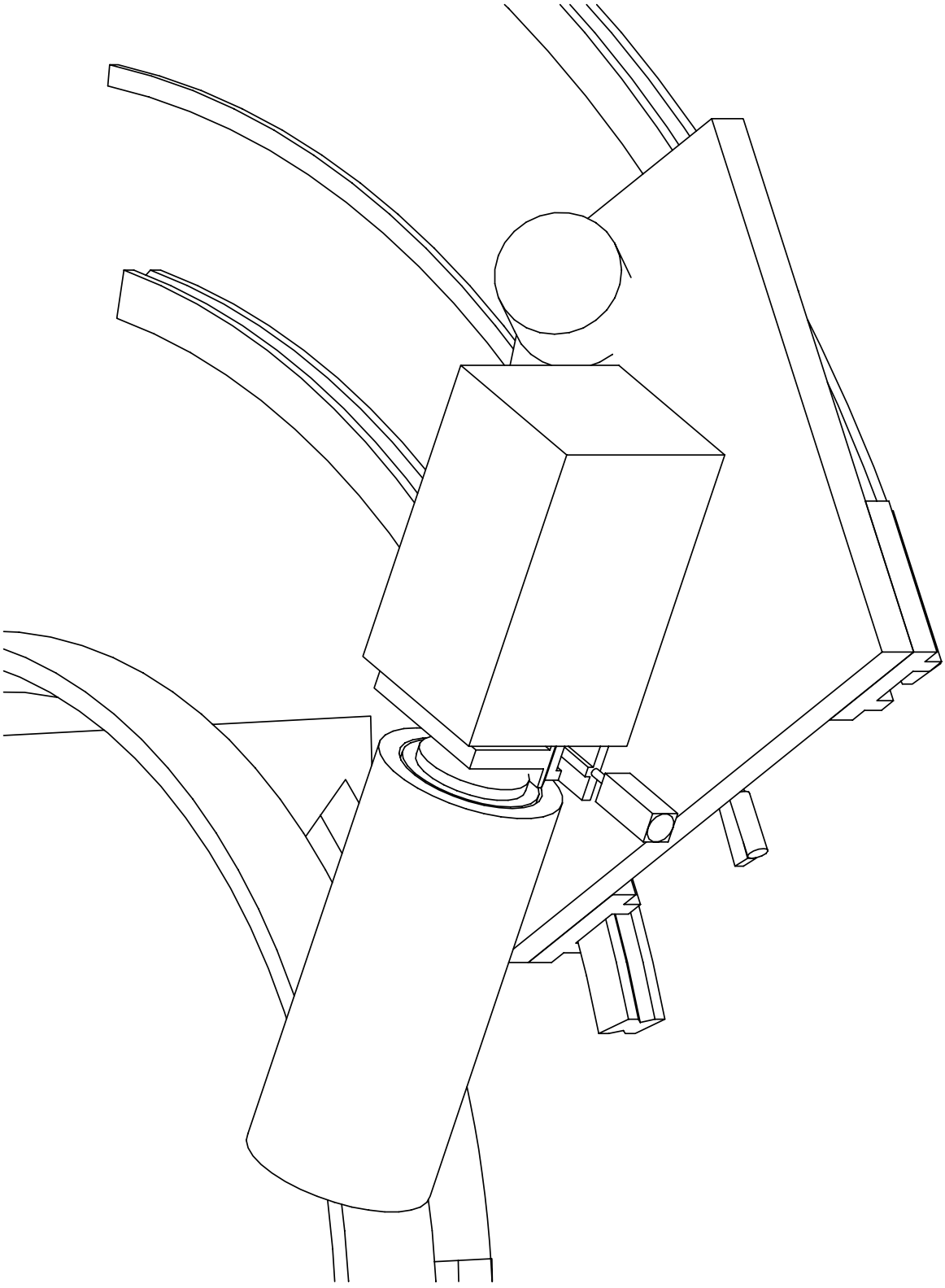

Figure 3.9: The principal guide camera and its motion stage.

at an angle tangent to the focal plane at the middle of the pickoff mirror travel. In this way, as the mirror remains approximately the correct distance from the focal plane during it's radial movement. The second table is driven with a stepper motor and lead screw arrangement.

With the two drive types used for these stages, their design was considered with stiffness as a consideration. A result of this is that both drives should easily meet the resolution requirements for positioning. In the case of the worm gear, an angular rotation of 13.5 degrees results in a 75 μm motion at the pickoff mirror. Similarly for the radial stage, a lead screw with a 2mm pitch would also result in a 75 μm motion for a 13.5 degree rotation of the shaft. These numbers are will within the abilities of today's common stepper motors.

The camera head itself is mounted onto the top stage of the table along with the filter mechanism, barrel selector, pickoff arm, and pickoff mirror. The filter mechanism is identical to the mechanism used on the principal guide camera. It utilized a single air cylinder driving a linear stage against two hard points (at each end of travel). Mounted on the stage are the filter, and dummy filter.

A major difference between the principal guider, and the SH guider is the presence of two barrels on the camera. These are mounted on an air cylinder driven stage similar to the filter mechanism. The first of these barrels contains the Shack - Hartmann optical elements, and the second barrel is identical to the barrel used in the principal guider for imaging.

Another major difference between the principal guider and the SH guider is that the SH pickoff arm cannot be constructed as an integral portion of the barrel due to the aforementioned mechanism. There are however, plenty of locations in which stiffening members may be added if it is found that the pickoff arm is not stiff enough (i.e. back to the camera head).

3.6.5.3 Center Field Guide Camera

The center field guide camera is mounted in a fixed location, outside of the instrument FOV and immediately to the side of the long slit. It mounted as close as possible to the plane defined by the FOSS, but is raised slightly in order to peer over the lip of the mask. See Figure 3.11 for a view of the CF camera on its base.

The center field guide camera is equipped with a filter mechanism identical to the ones used in the principle guider, and the SH guider.

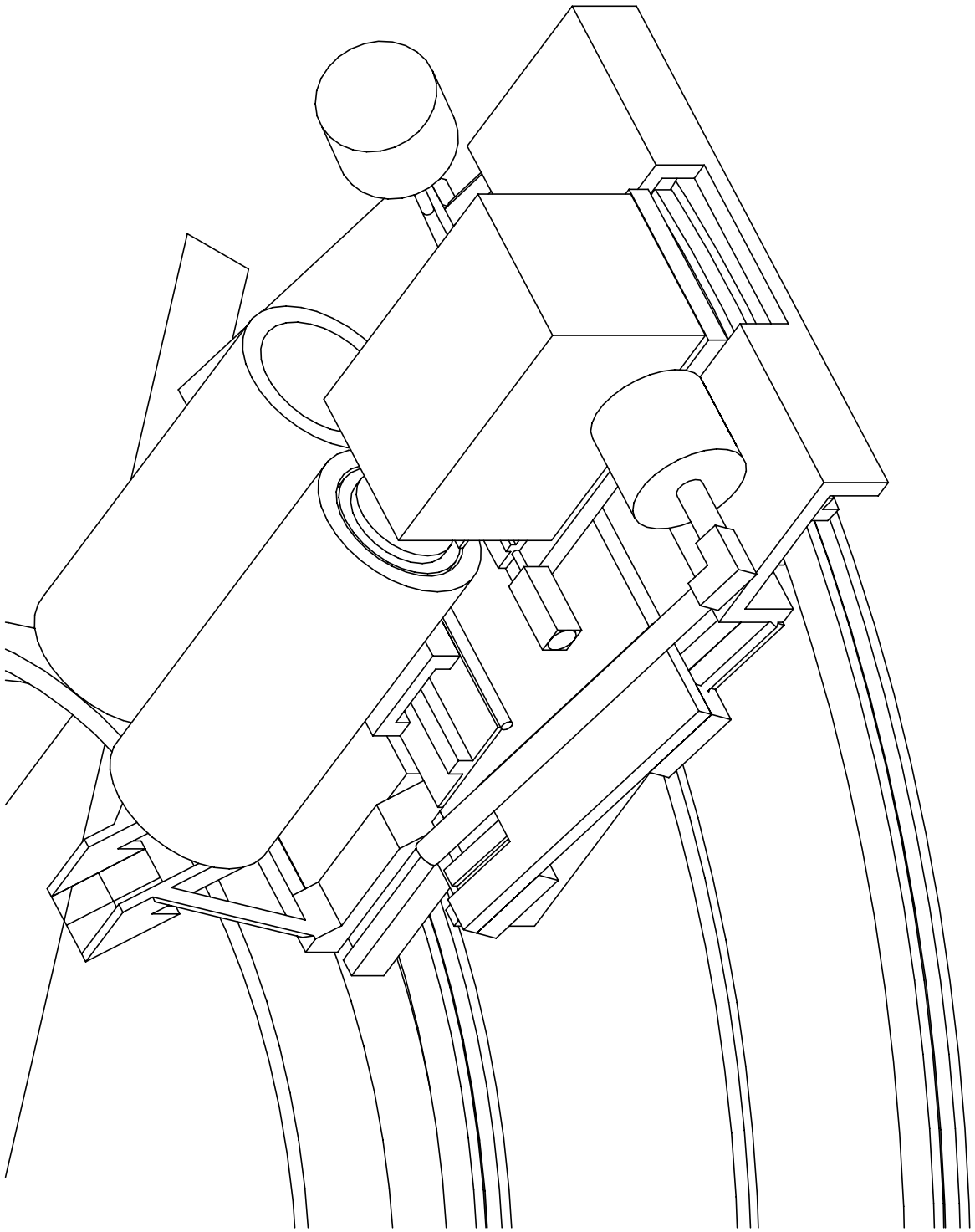

Figure 3.10: The Shack-Hartmann guide camera and its motion stages.

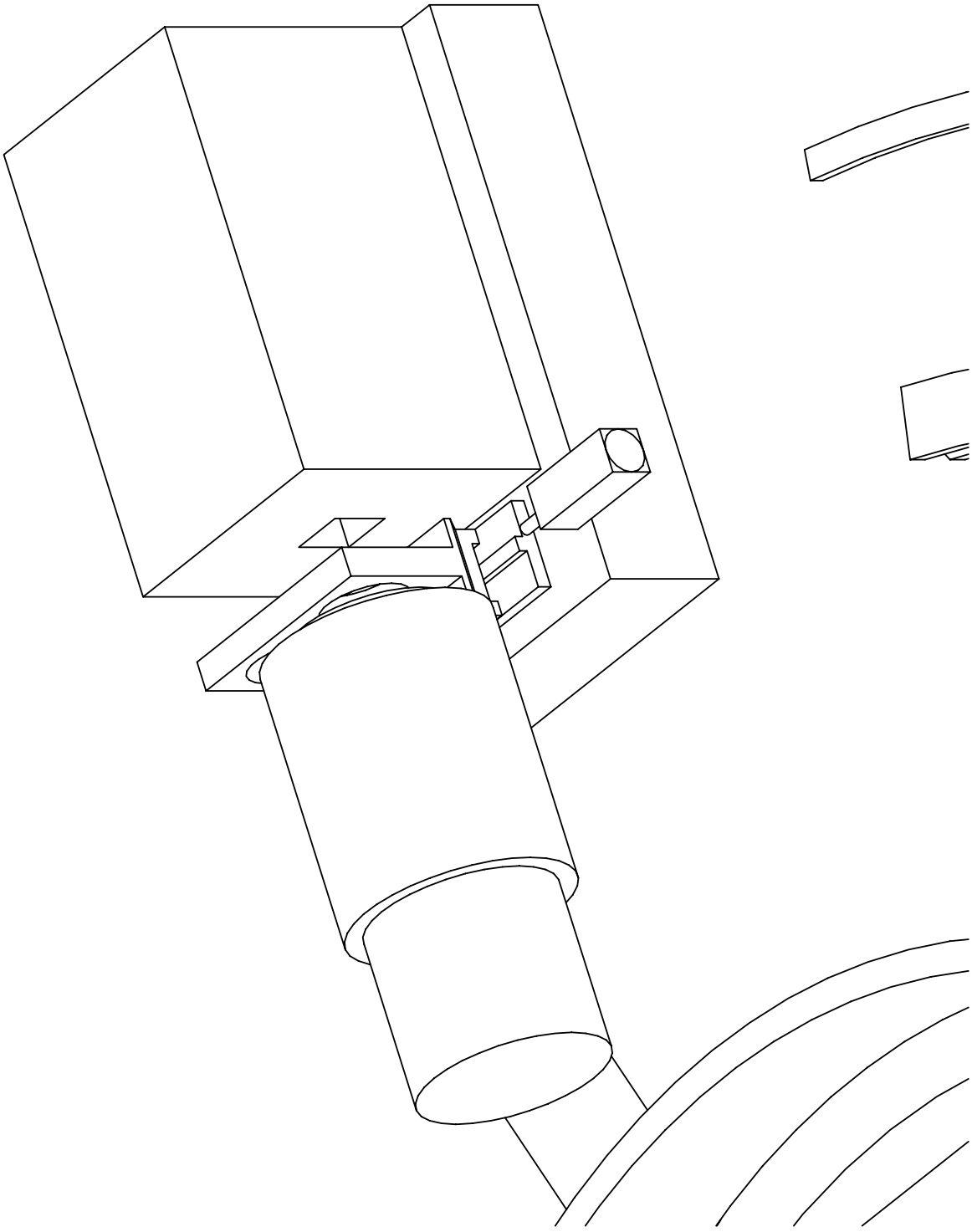

Figure 3.11: The center-field guide camera and its mount.

3.7 Calibration Systems

3.7.1 Introduction

Light sources will be provided for wavelength and flat-field calibration. To maximize flexibility, simplify the instrument design, and make full use of the Magellan optical design, both internal and external calibration sources will be available. Only the internal calibration sources will be provided by the IMACS project.

3.7.2 Internal Calibration

A set of calibration lamps will be mounted in the forward optical area (near the focal surface). The lamps will be mounted in holders on a common stage. The instrument hatch will be coated with a non-specular material which will reflect calibration light from the lamps back to the focal surface. This illumination will not accurately simulate the telescope, and will be less representative than the external calibration system. But it will allow for testing and calibration during the day, or when other the telescope is not available to IMACS.

3.7.3 External Calibration

The Gregorian optical configuration of the Magellan F/11 focus produces a pupil near the surface of the secondary mirror. This location has been identified as an ideal location to place a screen for reflecting calibration and flat-field light to the Cassegrain and Nasmyth foci. Although not yet designed, a common calibration system will be provided by the telescope project.

3.8 Field Lens Mounting

3.8.1 Introduction

Immediately following the slit-mask in the optical path is a large fused-silica field lens. This will be mounted on the opposite (back) side of the FOSS structure. The lens itself is 650mm

in diameter, and 91mm thick at the center. The edge thickness is approximately 8mm.

3.8.2 Lens Mounting

The method chosen for mounting field lens will be to adhere it into a machined bezel, with a finger-stock type arrangement extending to the lens. The fingers wil actually extend past the edge of the lens, forming a protective snout. Figure 3.12 shows the field lens and its bezel.

The element alone is approximately 36kg in mass and has to be supported in such a way that it does not move by more than 25 μm in any direction. Preliminary calculations have shown that mounting the element via this method yields sags as little as 4 μm due to gravity.

Specifications on the opto-mechanics are such that operation temperatures range from -5 to +10 degrees Celsius, and the survival range is from -15 to +35 degrees Celsius.

Athermalization is achieved by flexure of the fingers in the radial direction. The cross section of the fingers is such that they are compliant in the radial direction; however, quite stiff in the axial, and tangential directions.

The initial alignment is also specified such that the element is mounted to within 25 μm of its nominal position. Through proper machining and mechanical alignment techniques, it is anticipated that this should simple to accomplish.

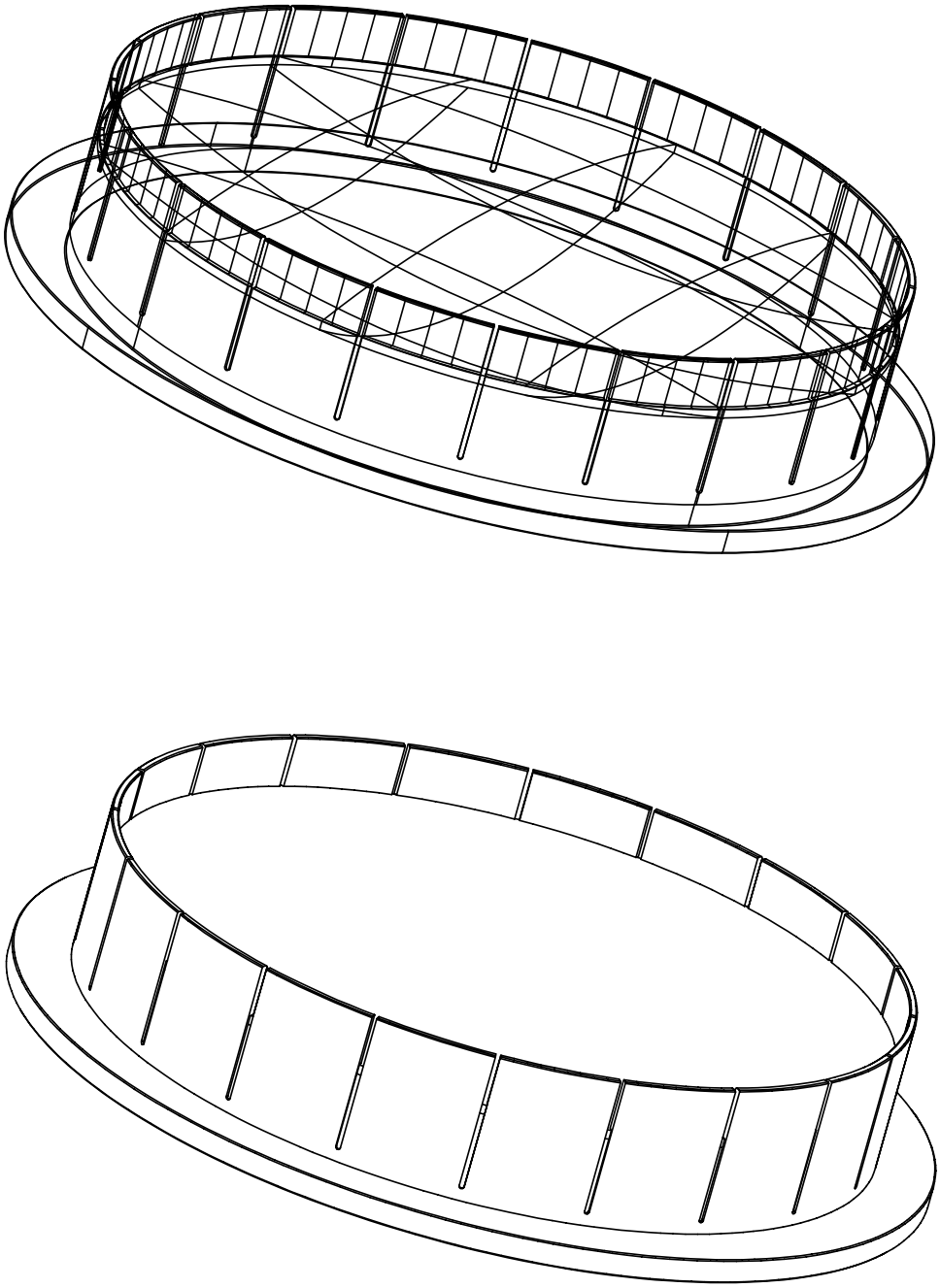

Figure 3.12: Field lens and finger-stock lens bezel.

3.9 Collimator Barrel

3.9.1 Introduction

The collimator is comprised of two singlets and a doublet. It is located 900mm past the field lens in the optical train, and is mounted on the face of the MOSS. The collimator barrel itself is designed to be supported at approximately its center of gravity by a flange on the outside of the barrel.

The barrel itself is made in two separate sections; a body and a nose cone bolted and pinned at mating flanges. The flange for the nose cone has three cutaway sections for the mounting points of the middle element. The barrel is fabricated from aluminum in order to take advantage of its high CTE for de-spacing of the elements during temperature changes. Figures 3.13 and 3.14 show a cross-sectional view and and isometric view of the collimator barrel.

3.9.2 Collimator Lens Mountings

The first element of the collimator is a singlet, and is mounted in a similar fashion as the field lens. The lens is adhered into a bezel with fingerstock protrusions. This provides a stress-free mounting that is also athermalized radially. The bezel is then mounted to the barrel at three hard points. These hard points are in reality three pucks - bolted and pinned from both sides. It is our intention that these pucks will not need to be machined when initially assembled; however, their presence does allow us to make any adjustments if found to be necessary later.

The middle singlet is also mounted on a fingerstock arrangement for radial athermalization purposes. This bezel is however, mounted inside an axial flexure. The axial flexure chosen to use is one utilizing two diaphragms separated by some distance. It was determined that a large portion of the scale change due to temperature changes could be corrected by "de-spacing" this element within the collimator. As it turns out, a good portion of the defocus is corrected by this as well.

The final group in the barrel is a doublet, separated by a liquid couplant. The lenses are to be adhered into a CTE matching subcell. The gap between the glass and the subcell will be tuned according to the CTE of the glass, cell, and adhesive. The subcells will then be adhered

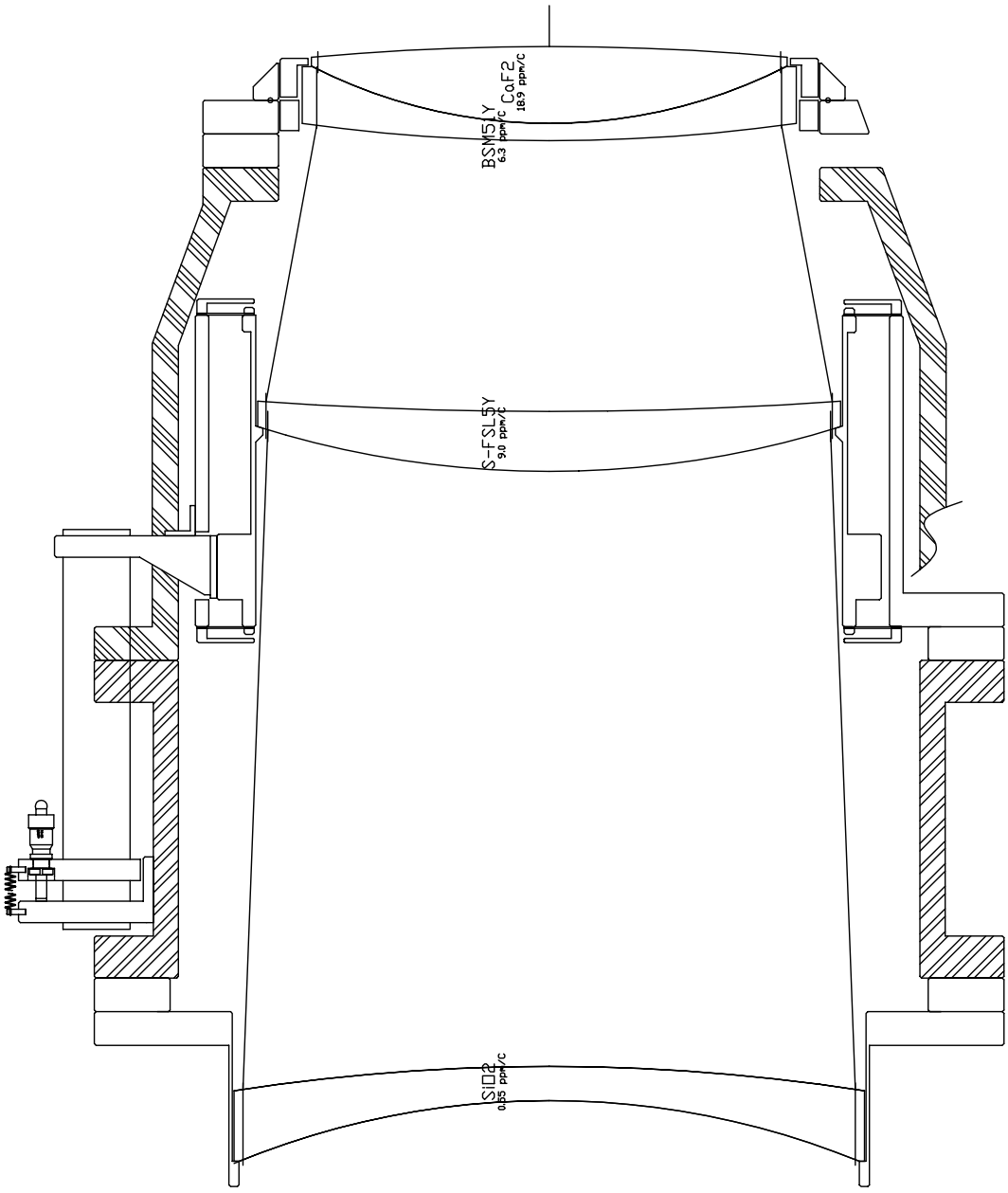

Figure 3.13: Cross-section of the collimator barrel.

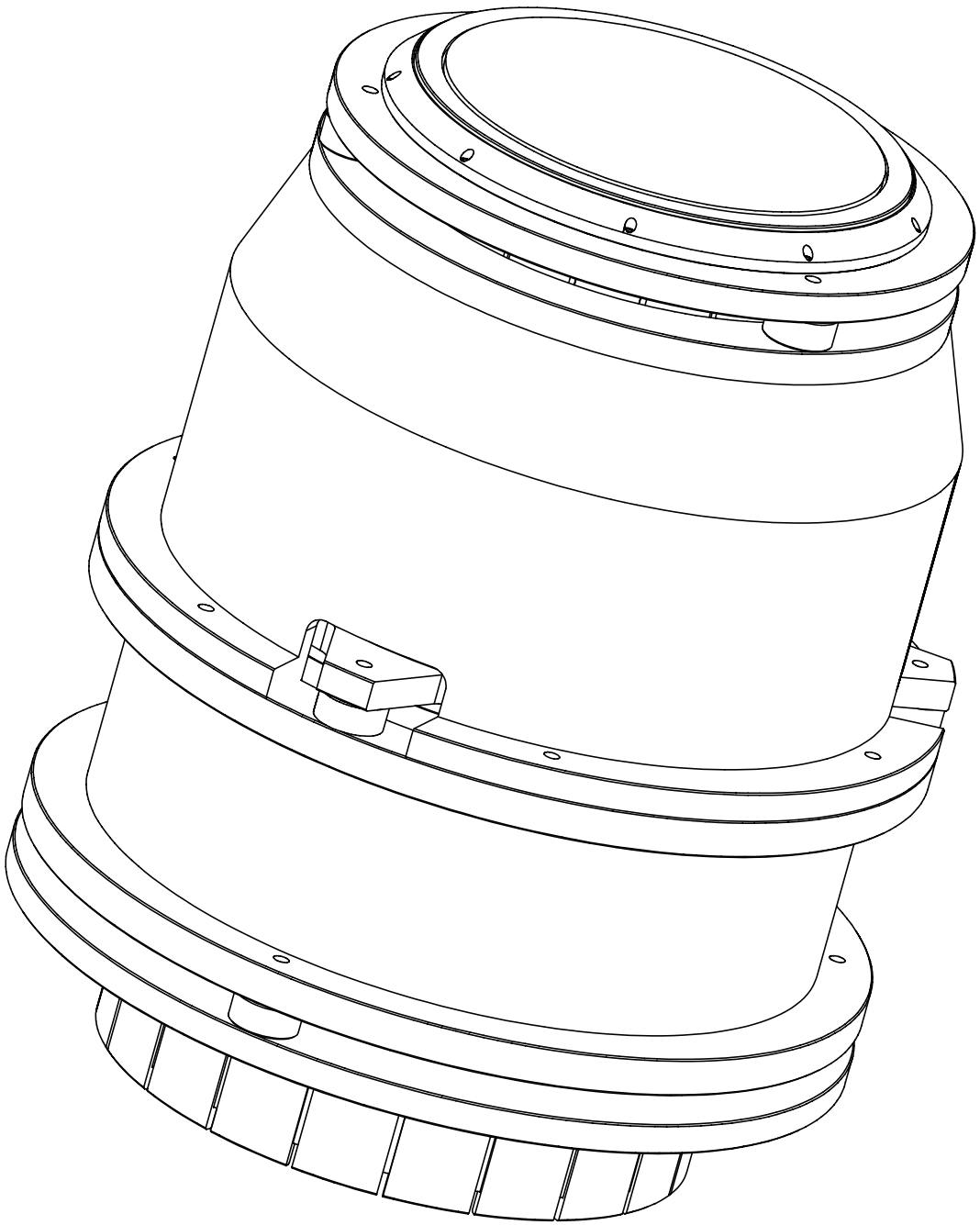

Figure 3.14: Isometric view of the collimator barrel.

into an aluminum cell with a structural adhesive. Sealing (by a single o-ring) is accomplished between these outer cells. The resulting group is then attached to the end of the barrel in a similar fashion as the first singlet was - via three pucks, bolted and pinned from both sides.

3.9.3 Axial Athermalization

The de-spacing is accomplished by the use of a delrin rod mounted on the outside of the barrel. Great care will be taken to make sure that the temperature of the delrin rod remains close to that of the barrel and lenses within (i.e. barrel and delrin will be wrapped in insulation). A micrometer/clamp arrangement is used for the initial alignment of this middle element.

3.9.4 Baffles

Ample space has been left on the inside of the barrel for baffles. A scheme has been devised which incorporates a series of annular rings cut from a sheet of carbon fiber, placed in blocks with a series of slices in them.

3.9.5 Couplant

It is anticipated that the couplant used in the final doublet will require a bellows type arrangement in order to compensate for the expansion/contraction of the fluid during temperature changes. Precautions will be taken to ensure that the doublet can be bled properly, and the bellows arrangement is accessible, yet protected.

3.9.6 Alignment

It is required that all of the elements are to be assembled into their nominal locations to within 25 μm. If is felt that through the use of proper machining, and mechanical alignment techniques, this should not be a problem.

Initial calculations have shown deflections in the barrel due to gravity of approximately 15 μm (below the 25 μm tolerance allowable). Initial calculations have also determined a mass of approximately 115 kg for the barrel (including lenses).

3.10 Long Camera Barrel

3.10.1 Introduction

The long camera is comprised of three singlets and a triplet. It is located at a 45 degree spectrograph angle from the collimator, immediately following the dispersion grating in the optical train. The "snout" of the long camera comes in very close proximity with the "snout" of the collimator, and some adjustment to the optical design is anticipated.

The barrel is designed to be mounted from two points onto the MOSS. A truss (designated the long camera truss) extend from the surface of the MOSS back to a flange that holds the dewar and one end of the barrel. The other end of the barrel protrudes into the MOSS and is supported by a smaller radial truss. Figures 3.15 and 3.16 show two views of the long camera barrel.

3.10.2 Lens Mountings

The barrel itself is made in two separate sections; a body and a nose cone, bolted and pinned at mating flanges. The end of the nose cone also has a flange to accommodate three mounting points for the first singlet. The opposite end of the nose cone has three slots machined in it to serve as clearances for three arms supporting the triplet onto the flange of the body. The opposite end of the body has similar slots in it for the mounting of the next singlet in the series.

The final singlet is mounted to the rear flange of the body at four locations. Four points were chosen to make the load path from the 4 legged truss to be as stiff as possible. It is through four pucks on the back of the final element's flange, that the end of the barrel attaches to the long camera truss flange.

The first element is mounted in a similar fashion as the field lens. It is supported in a bezel in a fingerstock arrangement. The bezel itself is mounted to the front flange of the nosecone via three pucks - bolted and pinned from both sides.

The second group of elements is a fluid coupled triplet. This group is constructed using the same design and assembly techniques as the doublet in the collimator. The group is then

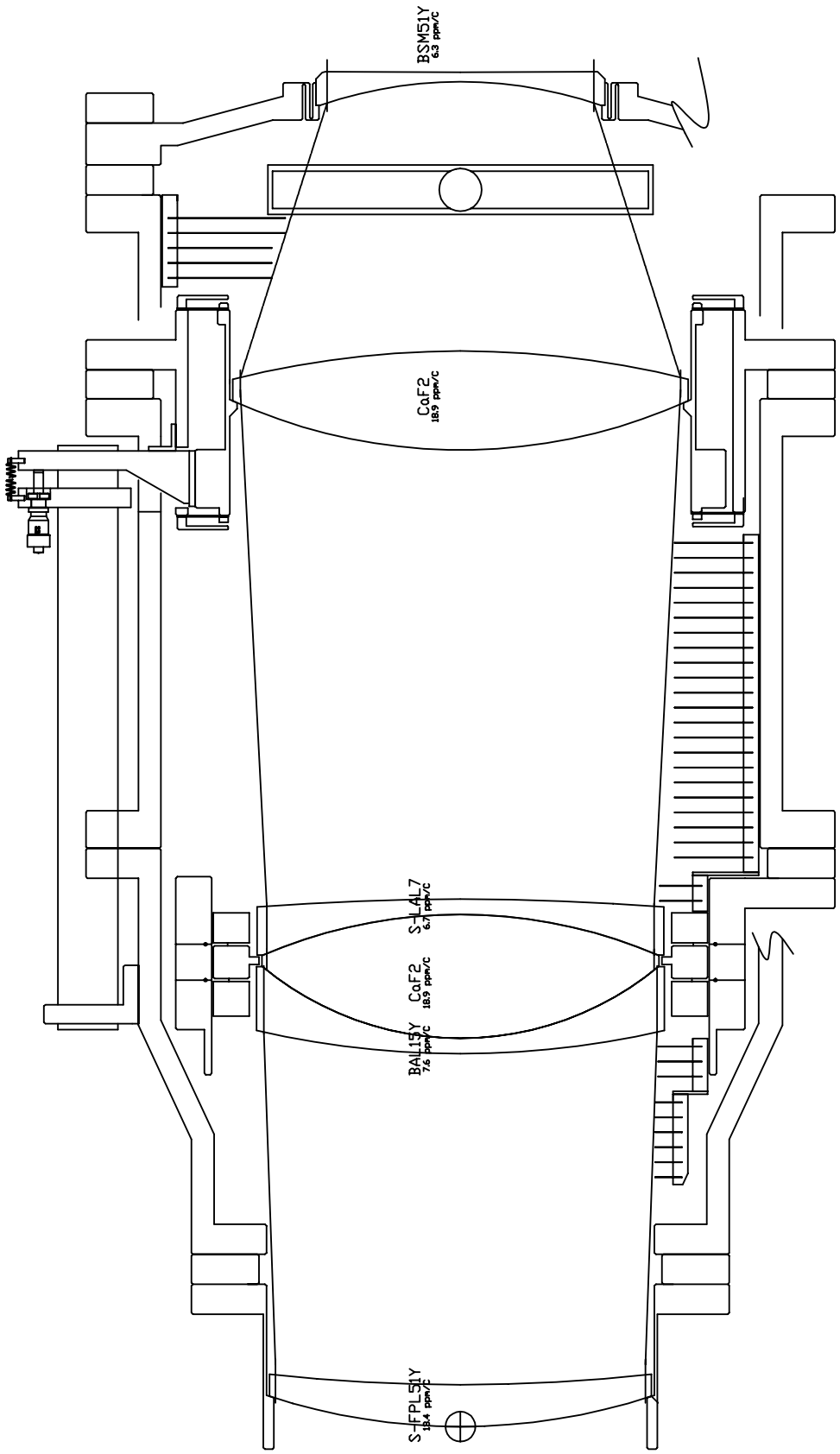

Figure 3.15: Cross-section of the long camera barrel.

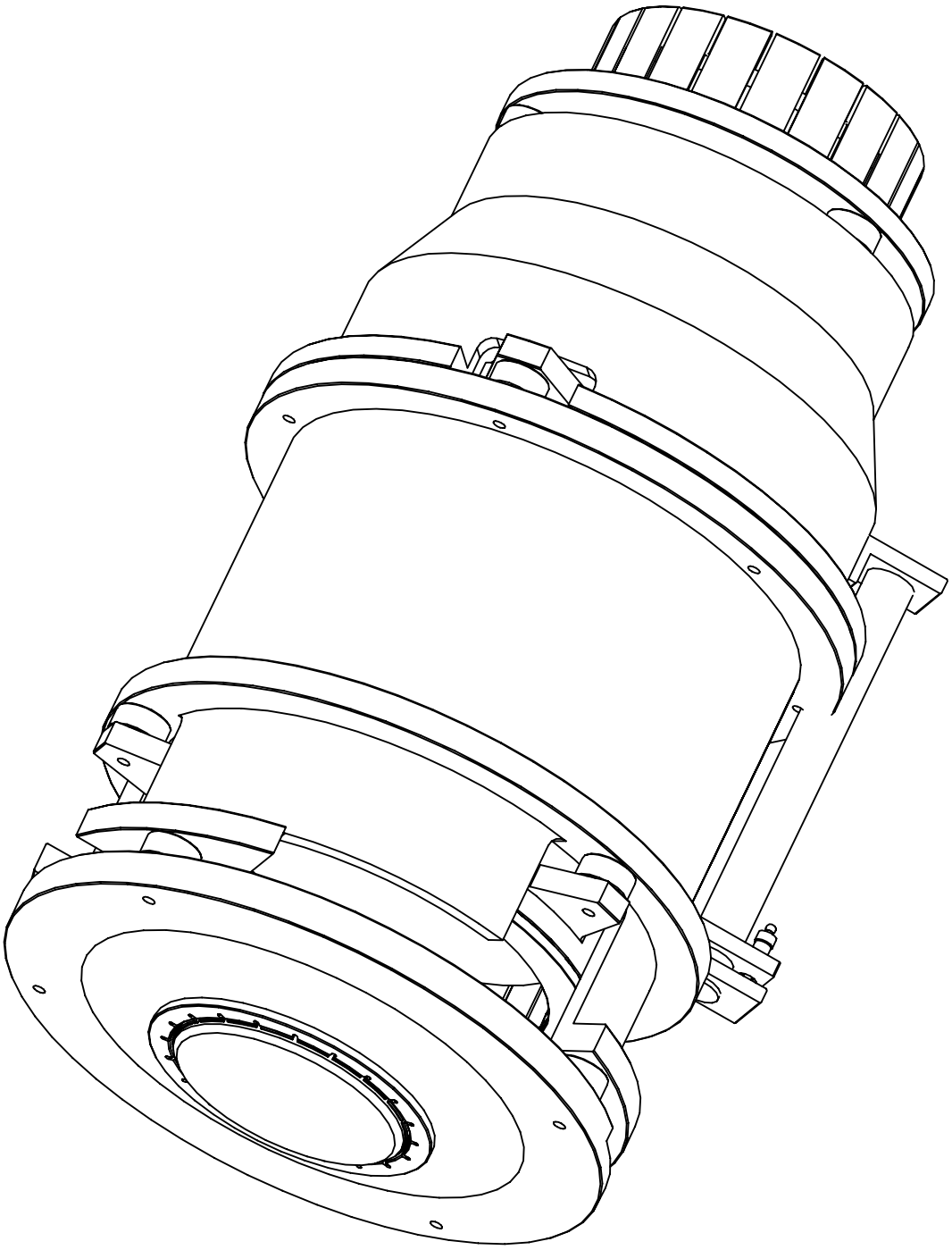

Figure 3.16: Isometric view of the long camera barrel.

mounted to the body section via three pucks - bolted and pinned from both sides.

The third group in the long camera is a large calcium fluoride singlet. It was determined that a large portion of the scale change due to temperature changes could be corrected by "de-spacing" this element within the camera. As a result, a large portion of the focus shift is also corrected. All of this is accomplished by mounting the element in a radial flexure (fingerstock type) and then mounting the radial flexure within an axial flexure.

3.10.3 Axial Athermalization

The axial flexure is accomplished by again utilizing two diaphragm flexures in parallel (similar to the mechanism used in the collimator). The de-spacing of this element is controlled by a large delrin rod (cross section must also be large enough to support the mass in this case) on the outside of the barrel. Again, the delrin rod and barrel will be wrapped with insulation in order to ensure that the delrin stays at a temperature close to that of the barrel. This singlet and its flexure stages are then mounted to a central flange on the body via three pucks - bolted and pinned on both sides.

The final element is a singlet again mounted into a radial fingerstock type flexure. This element is supported on the end of the body section via four pucks (again bolted and pinned on both sides).

Ample space has been left on the inside of the barrels for the baffles. The same arrangement is to be used here as was used in the collimator.

It is required that all of the elements are to be assembled into their nominal positions to within 25 μm. As with the collimator, the use of proper machining and mechanical alignment techniques should make this straightforward.

Initial calculations have shown deflections in the barrel due to gravity of approximately 10 μm (below the 25 μm tolerance allowable). Initial calculations have also determined a mass of approximately 155 kg for the barrel (including the lenses).

3.11 Short Camera Barrel

The short camera has not been developed other than to confirm that space is allocated to the packaging of the elements, and that it will be possible to implement the proposed shutter and filter mechanism as designed for the long camera. Similar methods will also be used to support the short camera as are utilized in the long camera (i.e. support in two places: at the front with a radial truss and at the back on a flange that also supports the dewar).

It is anticipated that similar methods will be used in the mounting of the optical elements as are used in the collimator, and long camera.

3.12 Camera Shutters

3.12.1 Introduction

A common shutter design will be used in both the long and short cameras. The shutter is an air-powered design, which uses two blades. The first blade moves across the optical beam to start the exposure, and second follows to end the exposure. The shutter specification calls for one second minimum exposure, and linearity of 1% for all exposures.

3.12.2 Preliminary Shutter Design

In keeping with the IMACS design goal of making use of proven existing designs, the IMACS shutters are based on the UCO/Lick Observatory shutter design used in the Shane telescope Prime Focus Camera and the Keck ESI instrument. The ESI shutter is very close in size to the IMACS shutters. The shutter blades are made of titanium for light weight and high ultimate strength and fatigue resistance. The air-cylinders include internal dampers to reduce shock forces at the end of the stroke.

The shutters pass through clearance holes in the long and short camera barrels. A gasket of sealing material creates a light-tight barrier between the shutter and barrel. To reduce shock and vibration loads in the cameras, the shutter loads will be carried by brackets to the dewar mounting flange.

3.13 Filter Server System (FSS)

3.13.1 Introduction

The filter server system provides a selection of filters for both the long and short cameras. The will be two complete server mechanisms, but one set of filters which is switched with the dewar to the active camera.

The mechanical requirements for the Filter Server System are as follows:

1. Nominal filter size is 165mm by 165mm by 12 mm thick.
2. Filter exchange is limited to 30s.
3. There are to be spaces for 15 filters in the server mechanism.
4. Filters are to be repositioned repeatably to 25 μm (goal of 10 μm).
5. All filters can be removed from the mechanism to be switched to an additional (identical) mechanism on the other camera.

3.13.2 Filter Server Components

The filter server system is supported by a bracket, back to the flange that also supports the dewar. The system also has a separate frame that is mounted on the inside of the barrel. This inner structure holds the filter and its frame within the light path immediately behind the shutter. It is located as close to the dewar as possible to yield the smallest filter size possible. Figure 3.17 shows top and end views of the filter server mechanisms.

The frame that holds each individual filter is approximately 200mm square with V guides machined on two sides of the frame. This allows the frame to travel from it's storage location (in the selector), to its final position (in the beam) by a series of grooved rollers. In it's final position, two of the rollers that support the frame are "hard mounted" to the support structure, while all of the remaining rollers are "spring loaded". Without complex alignment procedures, and a minimum amount of adjustments, the filter frames are rigidly held in place, yet not over constrained.

Although two hard points are provided by the rollers, a third is required and is achieved through the use of a permanent magnet - mounted near a hard point at the end of the masks travel. The actuator that moves the frame to it's final position is engaged with a clearance fit in a key way. This clearance is large enough that when in it's final position, the frame will be close enough for the magnet to pull it tightly against its hard stop. The force of the actuator should be strong enough to disengage the magnet when the frame is to be moved back to its storage location. During filter use, the actuator that drove the frame to its final position remains in its key way, fully extended.

The key way on the mask serves two purposed. The first - to engage the actuator that drives it to and from the light beam. The second is to engage with a rail system back in the storage compartment, in order to lock it into the storage box. There is also a magnet for each slot in the storage box, in order to prevent the frames from "rattling" on the clearance that the rail is engaged with. As the storage box is moved to a new position for selecting a new filter, the old filter is moved onto the rail (from the actuator) and the new filter is moved off of the rail on to the key on the actuator.

The actuator that will drive the filter and frame to and from the beam is an air cylinder. The cylinder itself will have to be properly baffled, tuned, and cushioned in order to prevent the filters from being damaged. All testing will be done on a filter test blank and frame. A linear ball bearing table with an integrated lead screw moves the entire bank of filters in order to select a new filter. The motor travels with the table top in this case.

The storage box for the filters is constructed in such a way that by simply removing the rear cover, and attaching a handling bar to the back of each individual filter, one is able to lift all of the filters out of the mechanism for storage or replacement into a similar mechanism on the short camera. Preliminary calculations have determined the mass of the structure (including 15 masks) to be approximately 50 kg.

Figure 3.18 shows a filter frame at the end its travel. Figure 3.19 shows an isometric view of the FSS.

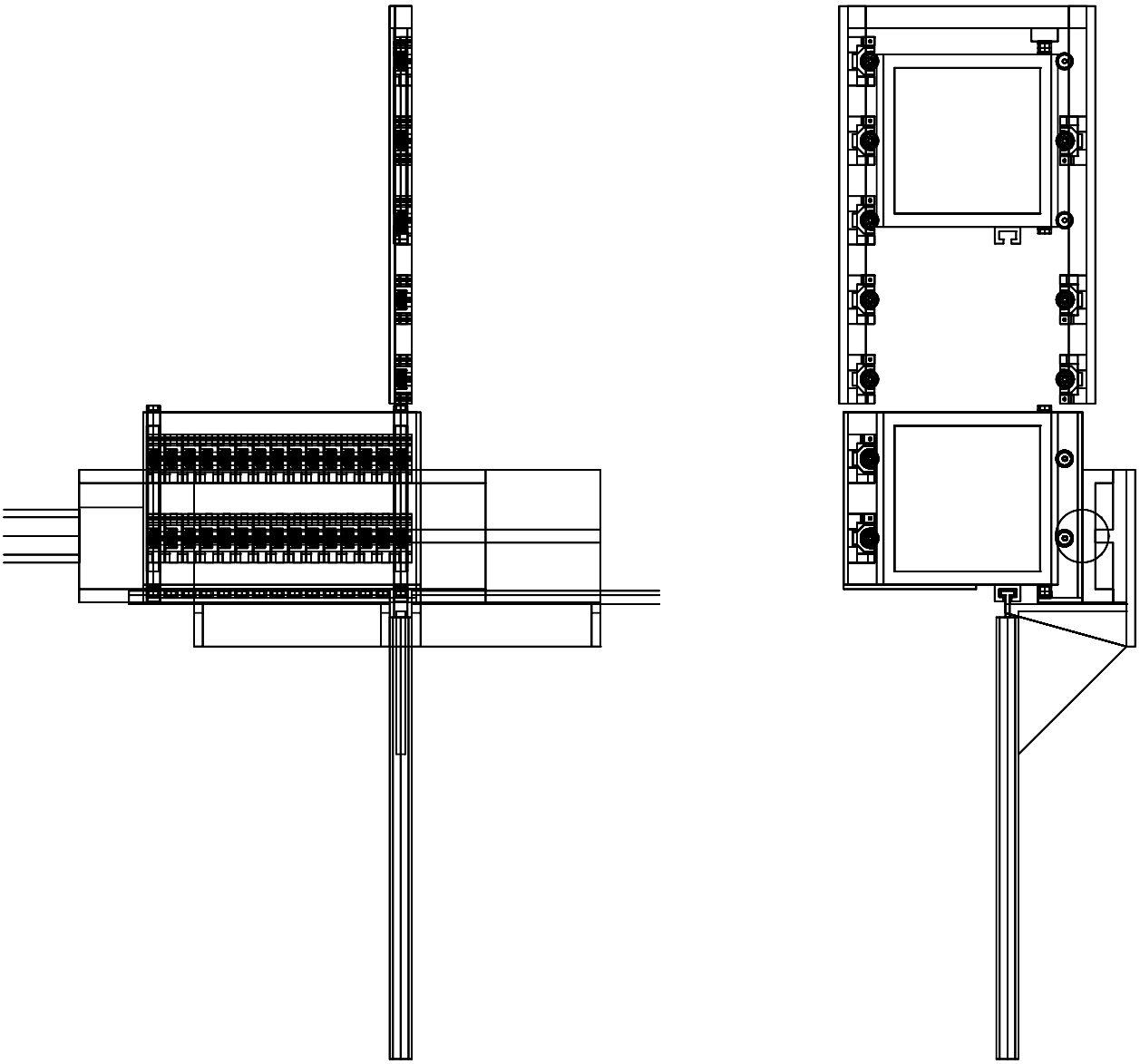

Figure 3.17: Top and end views of the filter server system.

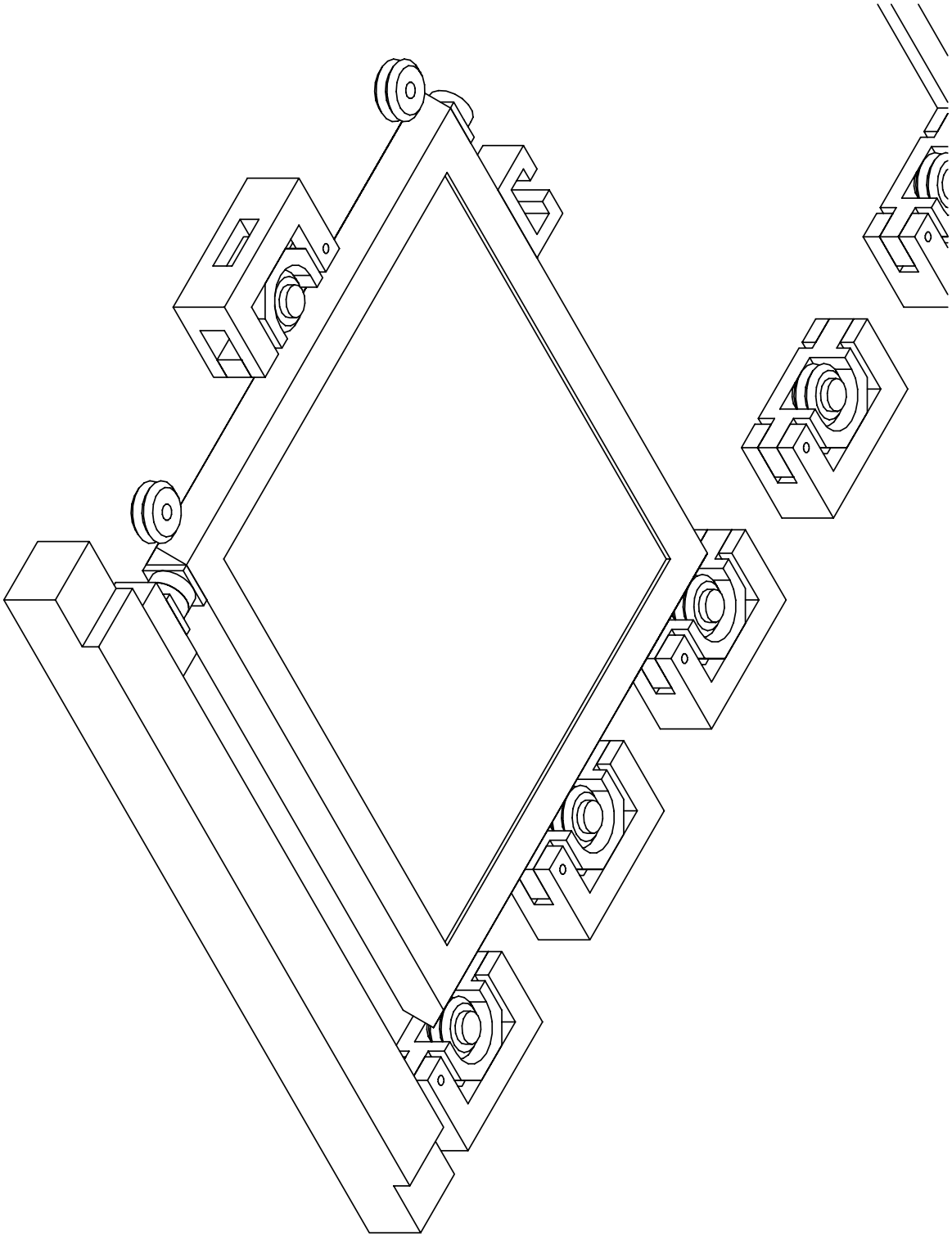

Figure 3.18: Filter frame at resting position in the camera barrel.

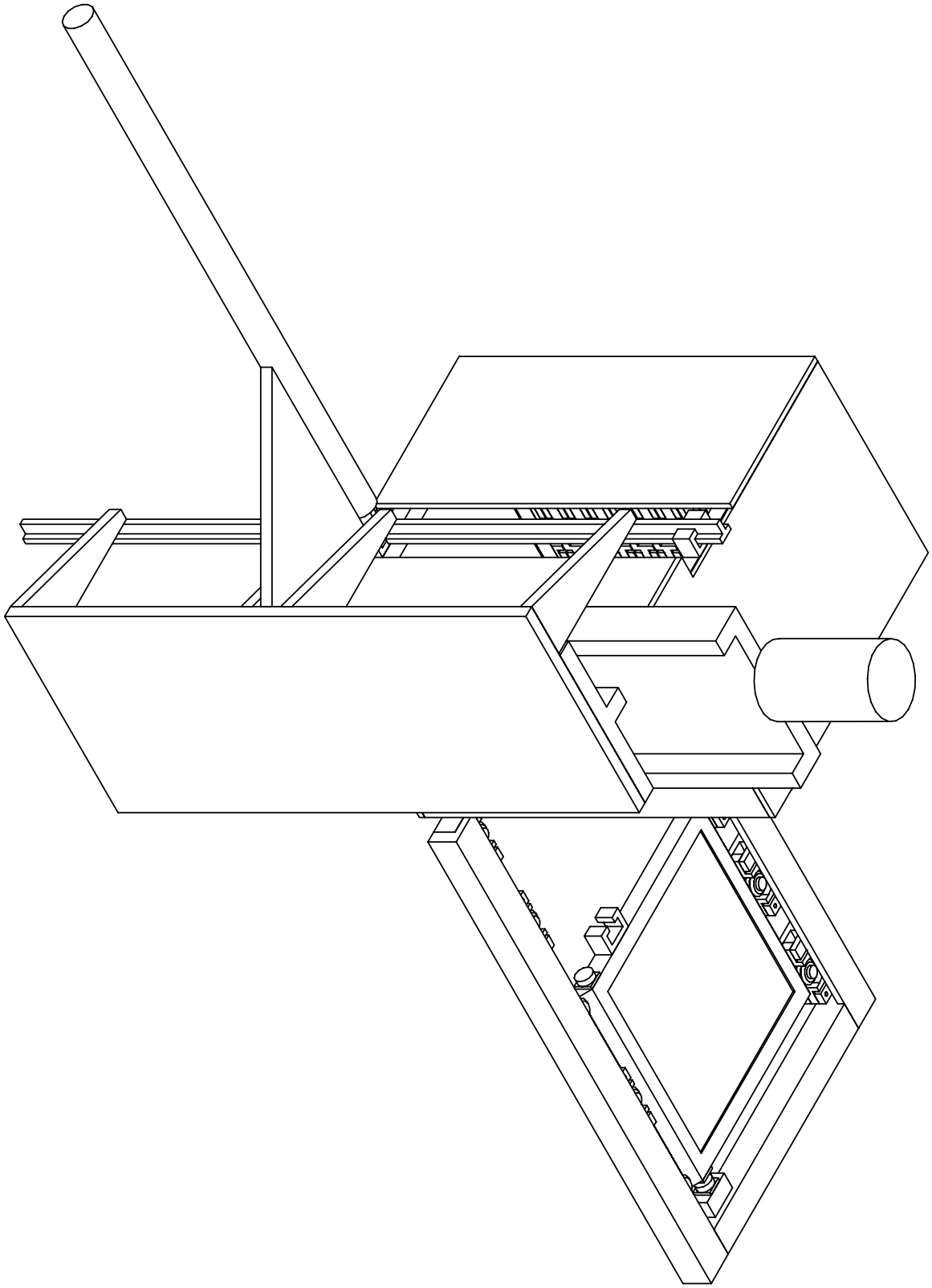

Figure 3.19: Isometric view of the filter server system. The insertion air cylinder extends out from the motion stage.

3.14 Instrument Structures

3.14.1 Introduction

The following sections describe the structural interface to the Magellan telescopes, and the main segments of the instrument structure. The three main structure elements, the forward optical support structure (FOSS), main optical support structure (MOSS), mainframe, and instrument carriage are described. A preliminary finite element model of the mainframe and MOSS is presented, and image motions due to structure deflections are calculated for two orthogonal gravity vectors representing rotations of the instrument about the optical axis. Finally, a brief description of the instrument carriage and auxiliary support system are given.

3.14.2 The Telescope/Instrument Interface

The Magellan telescopes provide two main interfaces to the Nasmyth instrument foci. The first is through the Nasmyth instrument rotator (NIR), a round plate attached to the sides of the elevation disks. The NIR is friction-driven and encoded in order to provide derotation of the focus relative to the Nasmyth deck, as required by Altitude-Azimuth telescopes.

The second structural interface is through the Nasmyth deck itself. Smaller instruments may practically use just the NIR, and make few or no requirements on the deck itself. IMACS will make use of both the NIR and Nasmyth deck for support.

3.14.3 Structure Concepts

The primary function of the instrument structures is to support the optical sub-systems such that image motions due to variations in the gravity vector will be less than the 0.1 pixel flexure specification. A variety of approaches, described below, have been taken in the structure design to meet that objective.

There are other constraints on the structure which bias the design as well. The instrument structure must attach efficiently and effectively to the Nasmyth instrument mount. Although routine removal and re-installation of the instrument are not required, it is a goal to be able to remove the instrument completely from the telescope in one day. The structure should

allow easy access to the internal components, especially those that require frequent changes, principally the mask server, but also the filter servers, and the disperser server. The structure should be relatively versatile, such that future modifications or additions to the instrument are as simple as possible. The self weight of the structure will affect its deflections, and hence should be as light in weight as possible. The cost of the structure will be somewhat dependent on its weight, as well as its geometry; simple weldments of plates and tubes will ease manufacture and help to minimize cost.

Three distinct structure concepts have been investigated. The first was a plate-weldment design proposed and developed by Steve Gunnels of Paragon Engineering, and shown in Figure 3.20. The benefits of this design include simplicity of fabrication, compactness, relative ease of analysis and fabrication. The principal weaknesses of this design include difficult access to internal components, and assembly complications due to the fact that the structure would have to be disassembled to reach some internal components such as the collimator.

The second concept was a space frame design, where all the instrument sub-systems are attached to each other with determinate trusses. The primary benefit of this design is the ability to put structure mass exactly where it is most effective. The truss elements carry only axial loads, and the element cross-sections can be tuned to minimize weight while still providing the required stiffness. A space frame also provides perhaps the highest level of access to the supported components. Weaknesses include relatively more complicated design effort, more complicated fabrication,

A third concept has been adopted, which is a hybrid of the first two, and is shown in Figure 3.21. The primary objective for this structure concept was to meet the flexure specifications by using the best features of the monocoque and plate weldment designs. A plate weldment structure (called the main optical support structure, or MOSS) is used to carry the collimator, disperser server, and cameras. A space frame is used to carry components in the slit area, and is called the forward optical support structure (FOSS). Finally, a determinate truss, called the mainframe, is used to attach the MOSS to the instrument mounting flange and the NIR.

The hybrid structure was selected as the preferred design, and the development of the FOSS, MOSS, and mainframe, is described in the following sections.

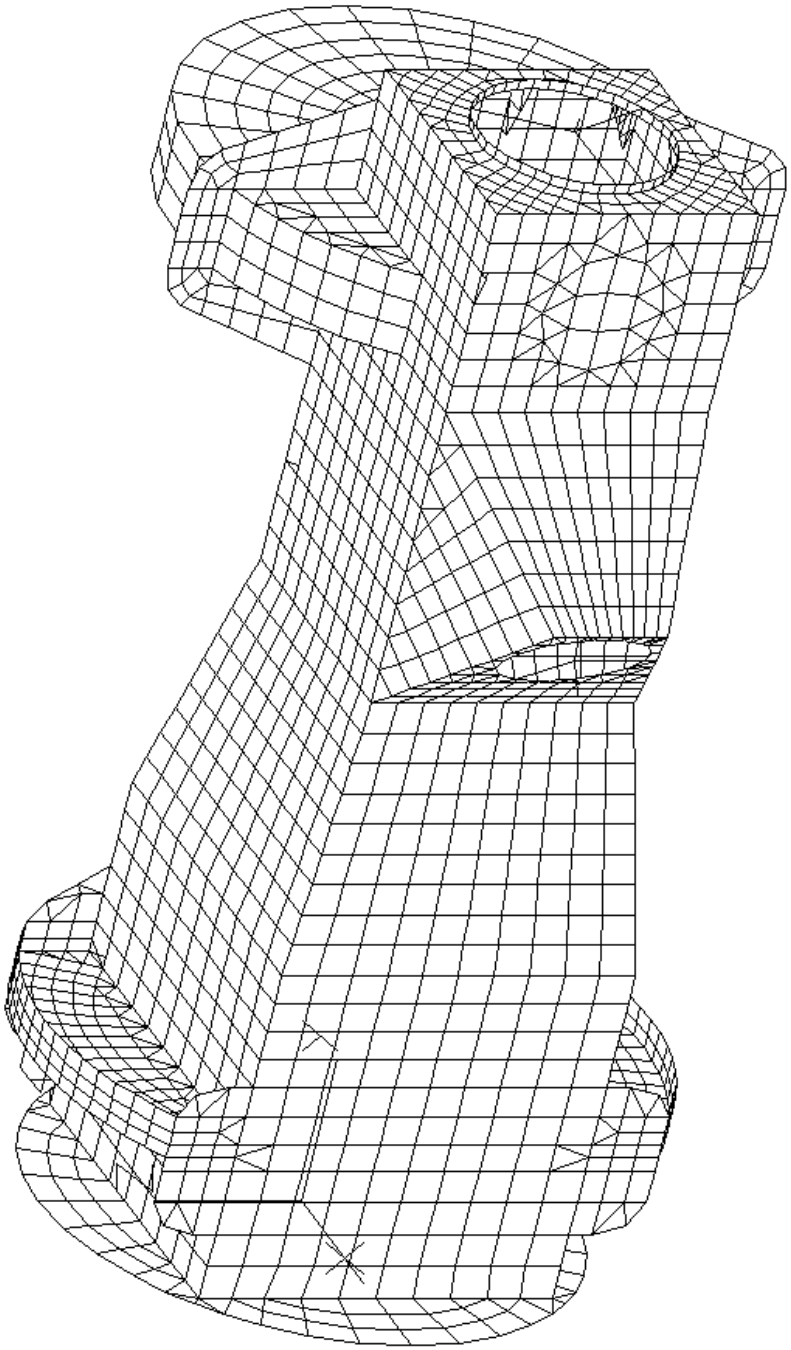

Figure 3.20: Plate weldment structure by Gunnels. The circular section at the top was for a disperser wheel, the lower disk is the mounting flange.

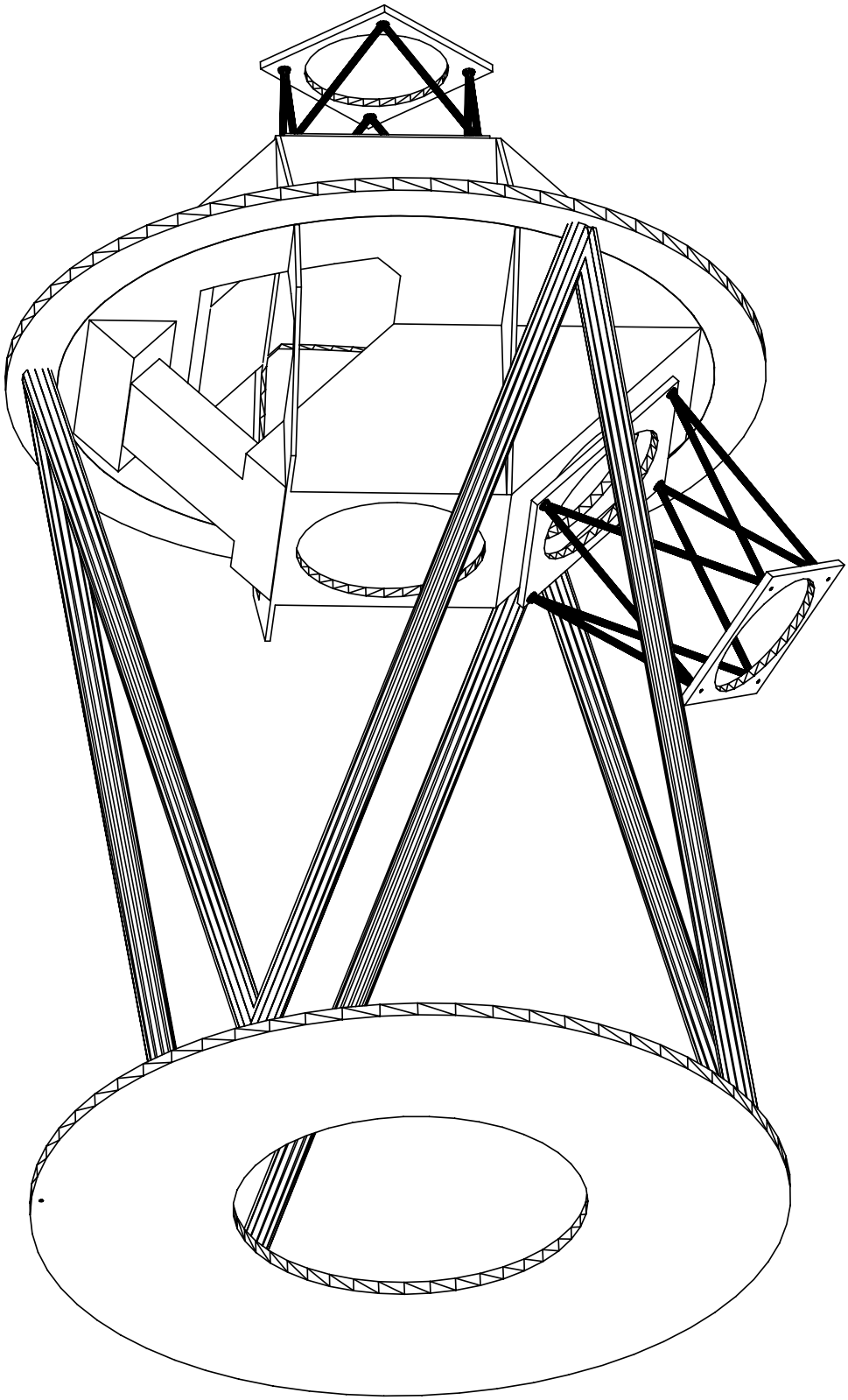

Figure 3.21: Hybrid structure

3.14.4 Forward Optical Support Structure (FOSS)

The region of the instrument closest to the NIR contains the mask server system (MSS), guide and Shack-Hartmann cameras with associated motion stages, the calibration lamps, and the field lens. Figure 3.22 shows the forward area components and FOSS. The primary function of the FOSS is to support the local optics and motion stages such that the resulting flexures meet the image motion specifications. Of particular importance is the rigid connection between the slit masks and guide cameras. Flexure between the guide cameras and the slit masks will result in erroneous guide signals to the telescope, and mis-registration of the field on the slit mask. For those reasons, a single, rigid structure is used to carry both. Due to its proximity to the slit mask, the field lens is also carried by the FOSS. The primary features of the FOSS are the stiffened bulkhead to which the cameras, slit mask, and field lens attach, and the determinate truss which attaches the bulkhead to the mainframe.

3.14.5 Main Optical Support Structure (MOSS)

The majority of the optical mass in IMACS is concentrated in the region around the collimator exit pupil. The main optics, including the collimator, disperser server, long camera, and short camera are all carried by a single weldment, called the main optical support structure, or MOSS. The machined faces of the MOSS establish the optical axes between the collimator and the two cameras. The primary objective for the MOSS is to maintain the integrity of the angles between the collimator, disperser, and long camera - the image motion sensitivities for tilts about the grating axes are the largest in the instrument.

Figure 3.23 shows the MOSS. The primary features include the central disk, which attaches to the mainframe through a bolted flange, and the plate weldments which together carry the flanges for mounting the collimator, long camera, and short camera. The disperser server attaches to the fixed post at the front of the MOSS. The auxiliary support acts through the rim of the central disk. The structure finite element model includes the MOSS, and can be seen in Section 3.14.7

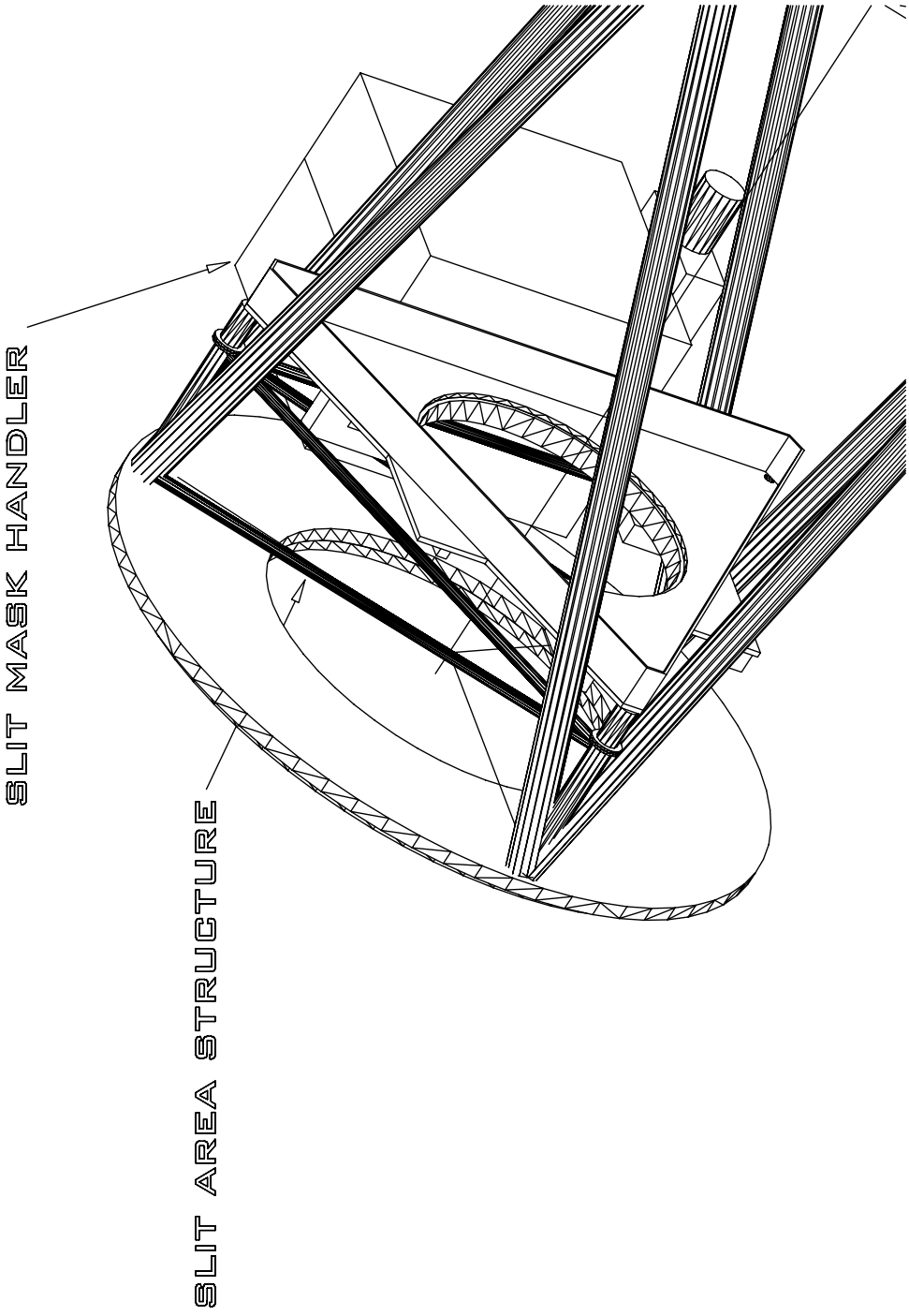

Figure 3.22: Forward optical support structure (FOSS).

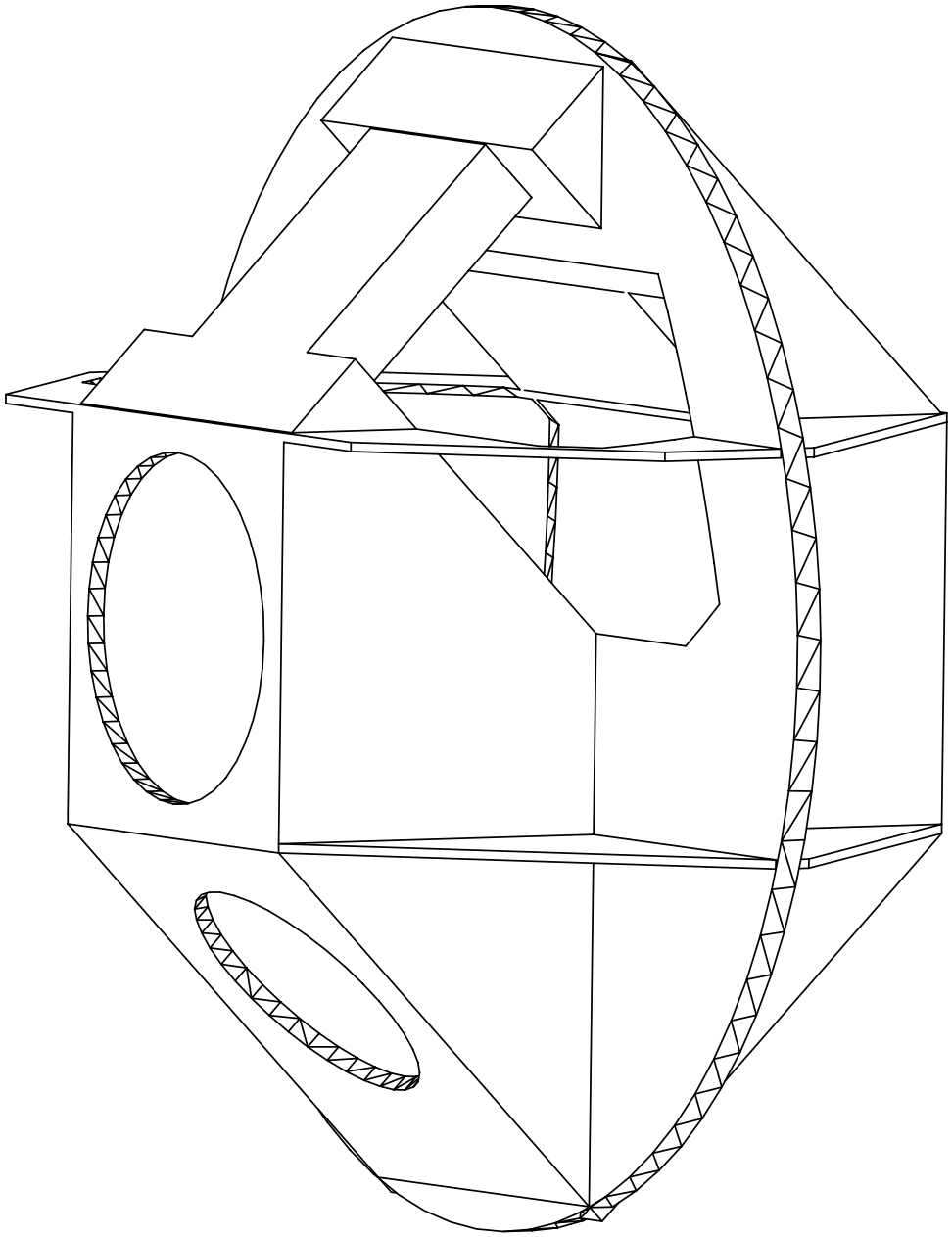

Figure 3.23: Main optics support structure.

3.14.6 Mainframe Structure

The mainframe provides the connection between the two principal regions of the instrument - the slit area and the main optics area. The mainframe consists of the instrument mounting flange, the six struts, which together form a determinate truss, and the MOSS mounting flange. The mainframe also provides the mounting points for the slit area structure.

Figure 3.24 shows the mainframe structure. The mainframe also provides the mounting points for the instrument enclosures, and the cable wrap (from the rotating instrument to the fixed Nasmyth platform). The structure finite element model includes the mainframe, and can be seen in Section 3.14.7.

3.14.7 Preliminary Finite Element Analysis

A parametric finite element model of the MOSS and mainframe structures has been generated to examine the flexural behavior of the concept. The model is parametric in the sense that virtually all the structure parameters are defined by variables in an input file. The variables, which define the gross structure dimensions, the geometry of the plates and tubes, and the material properties, can be changed easily. Then, by varying the parameters and re-running the input file, new finite element models can be generated automatically, which simplifies refinement and optimization of the structure.

Figure 3.25 shows a perspective view of the finite element model. Note that the model currently does not include the slit area or field lens. Dummy trusses have been included in the model to input the loads for the collimator and an installed disperser. Nodes at the center of the dummy trusses are used to sense the deflections and rotations of the centroids of the optical assemblies. Additional loads for the camera assembly masses (camera/filter-server/shutter/dewar) are applied at the free ends of the long and short camera trusses. Point masses are attached to the MOSS post to simulate the loads of the disperser server.

A starting point, all-steel design, which used 6 mm plates for the MOSS, 35 mm plates for the two mainframe disks, 100 $\times$ 6 mm round tubes for the mainframe, and 50 $\times$ 5 mm tubes for the camera trusses, was analyzed for two gravity vectors orthogonal to the Nasmyth optical axis. The two load cases represent the gravity-off to gravity-on deflections of the structure, which can be doubled to give the deflections for a 180 degree rotation of the

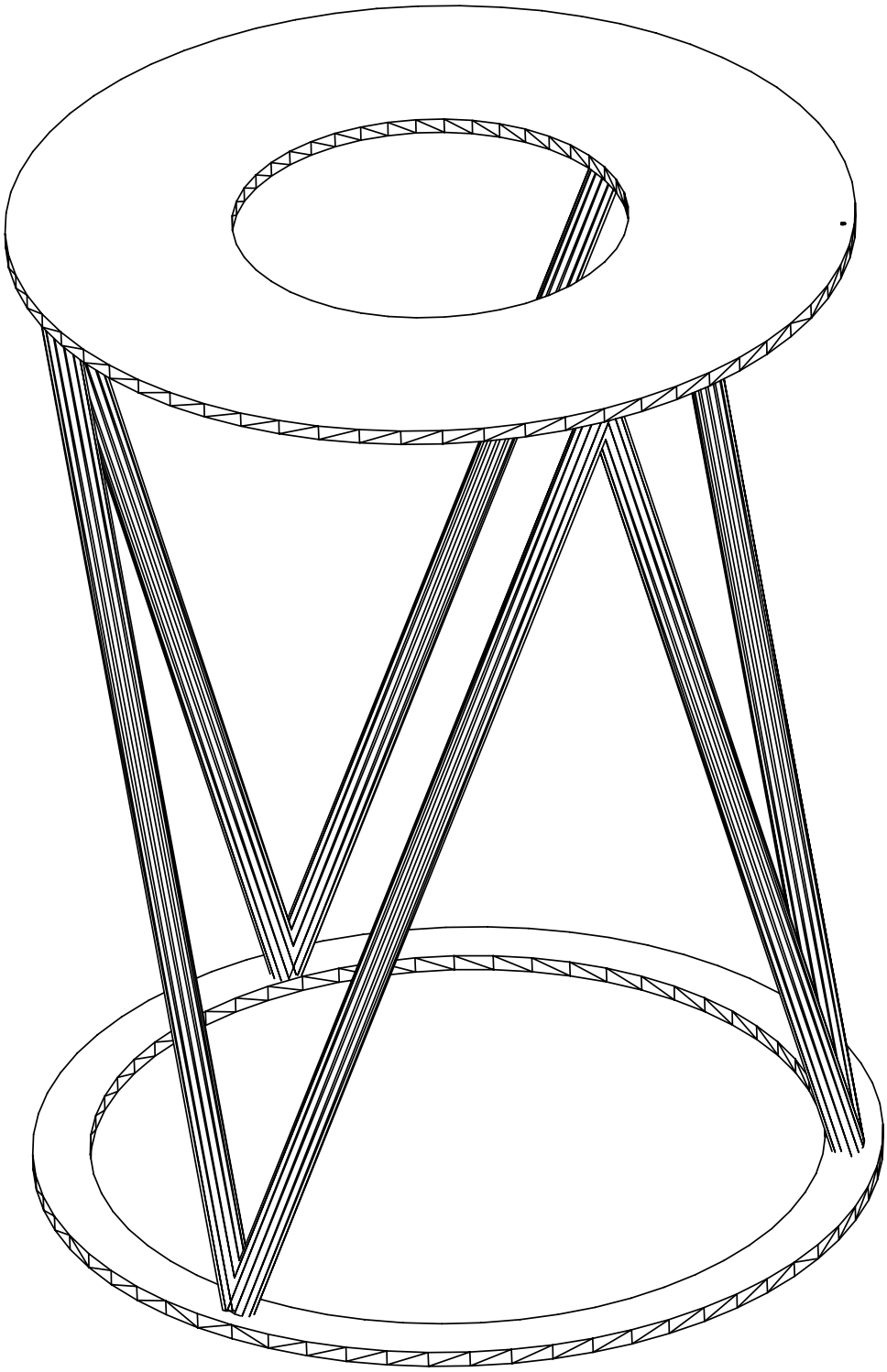

Figure 3.24: Mainframe structure.

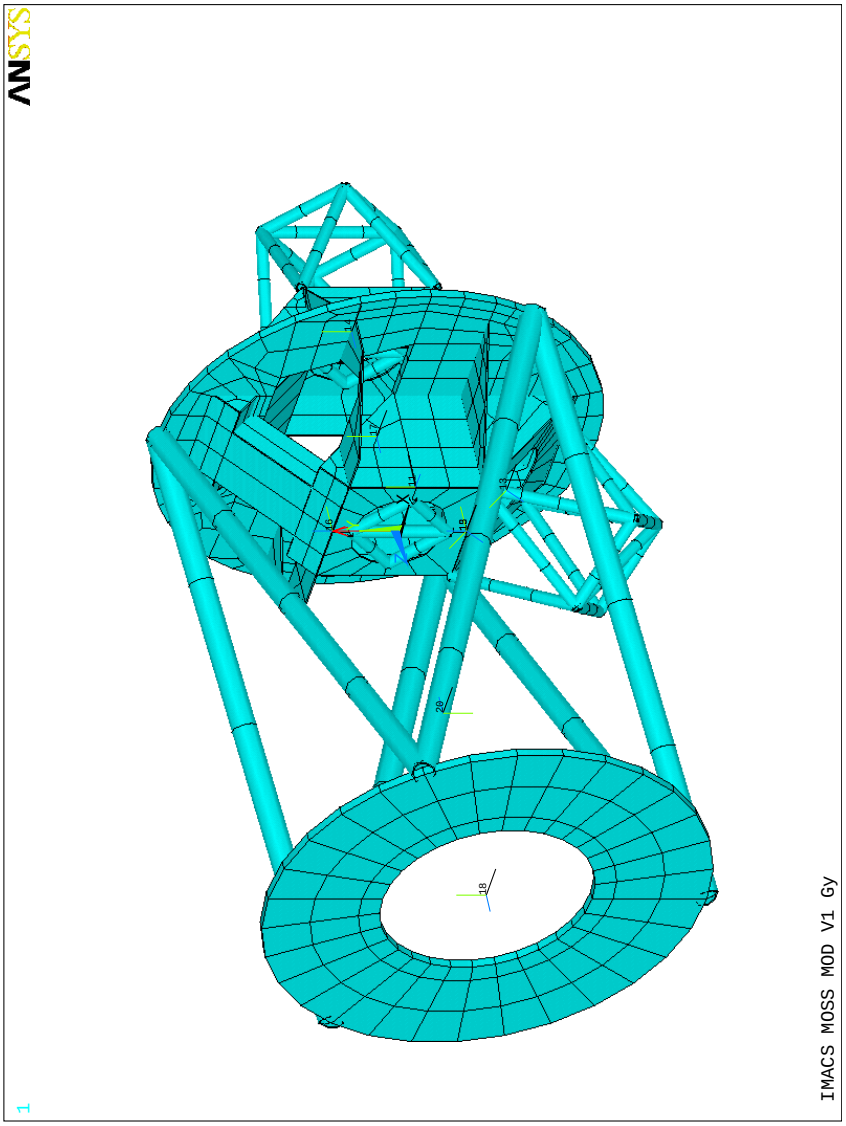

Figure 3.25: Finite element model of the mainframe and MOSS structures.

structure. Figures 3.26 and 3.27 show the structural deflections, in the direction of the gravity vector, for two 90 degree rotations of the instrument.

The tables shown in Figures 3.28, 3.29, 3.30 and 3.31 show the sensitivities of the various optical elements, and the calculated allowable translations and rotations for each element, assuming that each element is given the entire 0.1 pixel error budget. Also shown in the tables are the relevant translations and rotations of each optical element for the long and short cameras, and for two gravity vectors, from the finite element models. The upper half of each table shows the resultant image motion from the sensitivities and the FEA results for the flexure-control and no-flexure-control cases.

Note that the sensitivities and the deflections currently are unsigned. The errors are simply added and the linear sums are shown as totals. These results are thus worst-case, and it is expected that in fact many of the errors compensate, or can be forced to compensate each other by later tuning of the structure.

The preliminary results show that for a 360 degree rotation of the instrument, image motions due to flexure in the structure are approximately 70 microns, or a little under 5 pixels peak-to-peak. This is a very encouraging result, given that no effort has been made to optimize the starting-point design. The image motion errors in the structure are dominated by rotations of the point representing the grating or grism in the long and short camera models respectively. If in fact the image motions are adding linearly, future optimization will be directed at reducing the disperser mounting point rotations.

3.14.8 Instrument Carriage

The instrument carriage serves several functions. First, it will provide a test and assembly stand for the instrument during construction in Pasadena. It will serve as a storage fixture for the instrument when not installed on the telescope. It will aid installation and removal of the instrument from the telescope. It will provide the mounting interface between the instrument and the telescope at the Nasmyth platform. The carriage will include the auxiliary support mechanisms for the MOSS disk. The carriage will feature clips or brackets for constraining the structure during installation or storage (earthquake clips). Finally, the carriage will support the instrument electronics racks, provide access features for changing slit masks, dispersers,

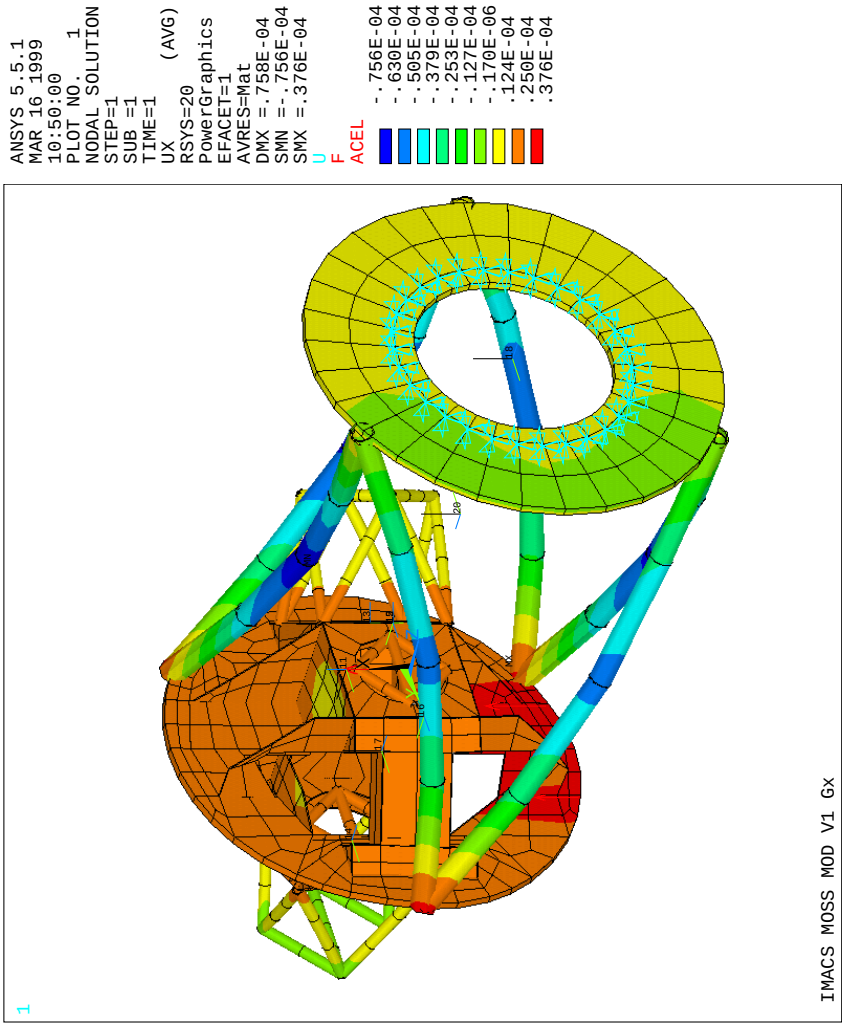

Figure 3.26: Deflections for the Gx gravity vector.

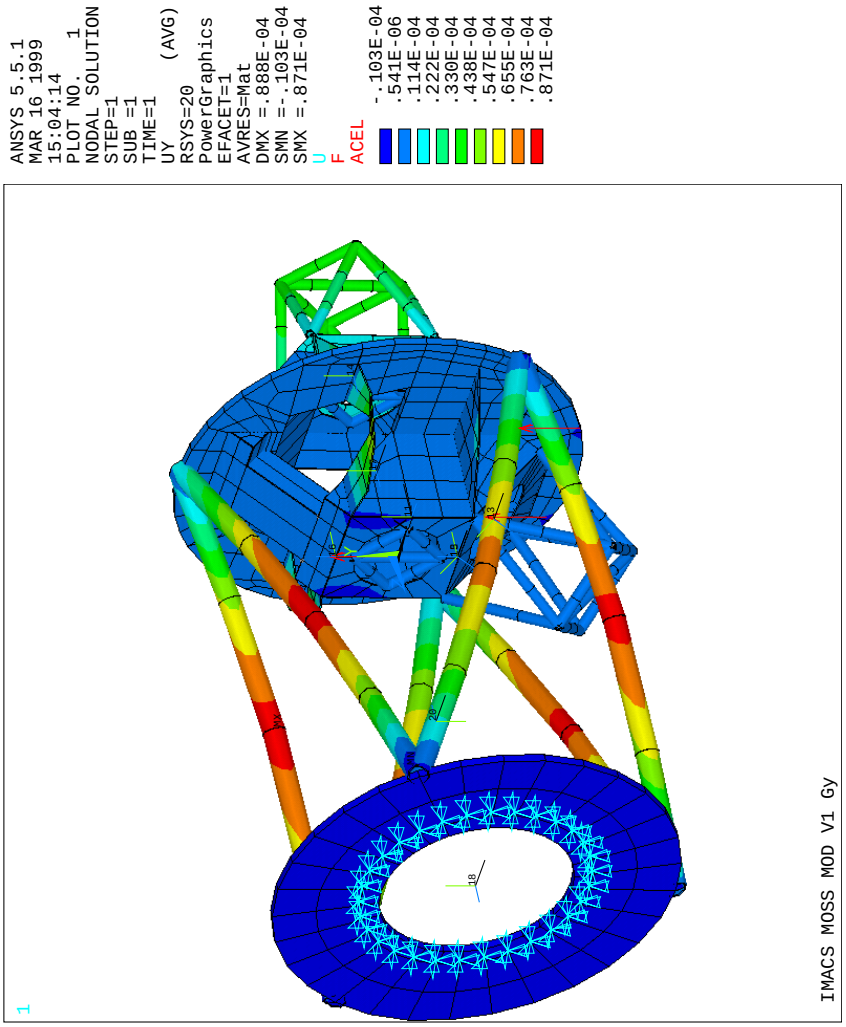

Figure 3.27: Deflections for the Gy gravity vector.

IMACS									
Image motions from structure finite element model									
file: scam_gx.xs3									
BCB 3/10/99									
15 micron pixels									
0.1 Px image motion spec. − 1.5 microns									
long camera									
600 l/mm grism									
gravity on, Gx									
				allowed					
				error for		**FEA**		**image**	**image**
	no flex.			**a single**		**dipl/rot**		**motion**	**motion**
Optic error	**sensit.**		**1/sens.**	**source**		**radians−meter**	**arcsec−um**	**microns**	**pixels**
field lens Rx	0.1269	um/arcsec	7.880	11.820	arcsec	0.000e+00	0.0000	0.0000	0.00
field lens Ry	0.1246	um/arcsec	8.026	12.039	arcsec	0.000e+00	0.0000	0.0000	0.00
field lens Tx	0.0150	um/um	66.667	100.000	um	0.000e+00	0.0000	0.0000	0.00
field lens Ty	0.0153	um/um	65.359	98.039	um	0.000e+00	0.0000	0.0000	0.00
coll Rx	0.6697	um/arcsec	1.493	2.240	arcsec	1.032e−05	2.1291	1.4258	0.10
coll Ry	0.6595	um/arcsec	1.516	2.274	arcsec	7.192e−06	1.4835	0.9784	0.07
coll Tx	0.2094	um/um	4.776	7.163	um	6.289e−06	6.2894	1.3170	0.09
coll Ty	0.2067	um/um	4.838	7.257	um	4.525e−07	0.4525	0.0935	0.01
grism Rx	0.2172	um/arcsec	4.604	6.906	arcsec	4.268e−06	0.8804	0.1912	0.01
grism Ry	0.0476	um/arcsec	21.008	31.513	arcsec	2.357e−05	4.8621	0.2314	0.02
grism Rz	0.4944	um/arcsec	2.023	3.034	arcsec	1.377e−06	0.2839	0.1404	0.01
camera Rx	1.7649	um/arcsec	0.567	0.850	arcsec	1.277e−06	0.2634	0.4648	0.03
camera Ry	1.7574	um/arcsec	0.569	0.854	arcsec	2.482e−05	5.1203	8.9985	0.60
							totals	13.8411	0.92
				allowed					
				error		**FEA**		**image**	**image**
	with flex.			**single**		**dipl/rot**		**motion**	**motion**
Optic error	**sensit.**		**1/sens.**	**source**		**radians−meter**	**arcsec−um**	**microns**	**pixels**
field lens Rx	0.0305	um/arcsec	32.787	49.180	arcsec	0.000e+00	0.0000	0.0000	0.00
field lens Ry	0.0281	um/arcsec	35.587	53.381	arcsec	0.000e+00	0.0000	0.0000	0.00
field lens Tx	0.0020	um/um	500.000	750.000	um	0.000e+00	0.0000	0.0000	0.00
field lens Ty	0.0022	um/um	454.545	681.818	um	0.000e+00	0.0000	0.0000	0.00
coll Rx	0.0510	um/arcsec	19.608	29.412	arcsec	1.032e−05	2.1291	0.1086	0.01
coll Ry	0.0274	um/arcsec	36.496	54.745	arcsec	7.192e−06	1.4835	0.0406	0.00
coll Tx	0.0064	um/um	156.250	234.375	um	6.289e−06	6.2894	0.0403	0.00
coll Ty	0.0156	um/um	64.103	96.154	um	4.525e−07	0.4525	0.0071	0.00
grism Rx	0.1294	um/arcsec	7.728	11.592	arcsec	4.268e−06	0.8804	0.1139	0.01
grism Ry	0.0448	um/arcsec	22.321	33.482	arcsec	2.357e−05	4.8621	0.2178	0.01
grism Rz	0.2417	um/arcsec	4.137	6.206	arcsec	1.377e−06	0.2839	0.0686	0.00
camera Rx	0.0389	um/arcsec	25.707	38.560	arcsec	1.277e−06	0.2634	0.0102	0.00
camera Ry	0.0369	um/arcsec	27.100	40.650	arcsec	2.482e−05	5.1203	0.1889	0.01
							totals	0.7961	0.05

Figure 3.28: Short Camera and Gx image motions.

IMACS									
Image motions from structure finite element model									
file: scam_gy.xs3									
BCB 3/10/99									
15 micron pixels									
0.1 Px image motion spec. − 1.5 microns									
long camera									
600 l/mm grism									
gravity on, Gy									
				allowed					
				error for		**FEA**		**image**	**image**
	no flex.			**a single**		**dipl/rot**		**motion**	**motion**
Optic error	**sensit.**		**1/sens.**	**source**		**radians−meter**	**arcsec−um**	**microns**	**pixels**
field lens Rx	0.1269	um/arcsec	7.880	11.820	arcsec	0.000e+00	0.0000	0.0000	0.00
field lens Ry	0.1246	um/arcsec	8.026	12.039	arcsec	0.000e+00	0.0000	0.0000	0.00
field lens Tx	0.0150	um/um	66.667	100.000	um	0.000e+00	0.0000	0.0000	0.00
field lens Ty	0.0153	um/um	65.359	98.039	um	0.000e+00	0.0000	0.0000	0.00
coll Rx	0.6697	um/arcsec	1.493	2.240	arcsec	1.192e−05	2.4579	1.6460	0.11
coll Ry	0.6595	um/arcsec	1.516	2.274	arcsec	1.381e−09	0.0003	0.0002	0.00
coll Tx	0.2094	um/um	4.776	7.163	um	1.144e−09	0.0011	0.0002	0.00
coll Ty	0.2067	um/um	4.838	7.257	um	1.890e−07	0.1890	0.0391	0.00
grism Rx	0.2172	um/arcsec	4.604	6.906	arcsec	2.940e−05	6.0650	1.3173	0.09
grism Ry	0.0476	um/arcsec	21.008	31.513	arcsec	6.911e−10	0.0001	0.0000	0.00
grism Rz	0.4944	um/arcsec	2.023	3.034	arcsec	5.571e−11	0.0000	0.0000	0.00
camera Rx	1.7649	um/arcsec	0.567	0.850	arcsec	2.975e−05	6.1354	10.8283	0.72
camera Ry	1.7574	um/arcsec	0.569	0.854	arcsec	7.839e−10	0.0002	0.0003	0.00
							totals	13.8314	0.92
				allowed					
				error		**FEA**		**image**	**image**
	with flex.			**single**		**dipl/rot**		**motion**	**motion**
Optic error	**sensit.**		**1/sens.**	**source**		**radians−meter**	**arcsec−um**	**microns**	**pixels**
field lens Rx	0.0305	um/arcsec	32.787	49.180	arcsec	0.000e+00	0.0000	0.0000	0.00
field lens Ry	0.0281	um/arcsec	35.587	53.381	arcsec	0.000e+00	0.0000	0.0000	0.00
field lens Tx	0.0020	um/um	500.000	750.000	um	0.000e+00	0.0000	0.0000	0.00
field lens Ty	0.0022	um/um	454.545	681.818	um	0.000e+00	0.0000	0.0000	0.00
coll Rx	0.0510	um/arcsec	19.608	29.412	arcsec	1.192e−05	2.4579	0.1254	0.01
coll Ry	0.0274	um/arcsec	36.496	54.745	arcsec	1.381e−09	0.0003	0.0000	0.00
coll Tx	0.0064	um/um	156.250	234.375	um	1.144e−09	0.0011	0.0000	0.00
coll Ty	0.0156	um/um	64.103	96.154	um	1.890e−07	0.1890	0.0029	0.00
grism Rx	0.1294	um/arcsec	7.728	11.592	arcsec	2.940e−05	6.0650	0.7848	0.05
grism Ry	0.0448	um/arcsec	22.321	33.482	arcsec	6.911e−10	0.0001	0.0000	0.00
grism Rz	0.2417	um/arcsec	4.137	6.206	arcsec	5.571e−11	0.0000	0.0000	0.00
camera Rx	0.0389	um/arcsec	25.707	38.560	arcsec	2.975e−05	6.1354	0.2387	0.02
camera Ry	0.0369	um/arcsec	27.100	40.650	arcsec	7.839e−10	0.0002	0.0000	0.00
							totals	1.1518	0.08

Figure 3.29: Short Camera and Gy image motions.

IMACS									
Image motions from structure finite element model									
file: lcam_gx.xs3									
BCB 3/10/99									
15 micron pixels									
0.1 Px image motion spec. − 1.5 microns									
long camera									
1200 l/mm grating									
gravity on, Gx									
				allowed					
				error for		**FEA**		**image**	**image**
	no flex.			**a single**		**dipl/rot**		**motion**	**motion**
Optic error	**sensit.**		**1/sens.**	**source**		**radians−meter**	**arcsec−um**	**microns**	**pixels**
field lens Rx	0.1112	um/arcsec	8.993	13.489	arcsec	0.000e+00	0.0000	0.0000	0.00
field lens Ry	0.1578	um/arcsec	6.337	9.506	arcsec	0.000e+00	0.0000	0.0000	0.00
field lens Tx	0.0206	um/um	48.544	72.816	um	0.000e+00	0.0000	0.0000	0.00
field lens Ty	0.0144	um/um	69.444	104.167	um	0.000e+00	0.0000	0.0000	0.00
coll Rx	0.6698	um/arcsec	1.493	2.239	arcsec	1.032e−05	2.1291	1.4260	0.10
coll Ry	1.0267	um/arcsec	0.974	1.461	arcsec	7.192e−06	1.4835	1.5231	0.10
coll Tx	0.3328	um/um	3.005	4.507	um	6.289e−06	6.2894	2.0931	0.14
coll Ty	0.2128	um/um	4.699	7.049	um	4.525e−07	0.4525	0.0963	0.01
grating Rx	4.6085	um/arcsec	0.217	0.325	arcsec	4.268e−06	0.8804	4.0571	0.27
grating Ry	4.4402	um/arcsec	0.225	0.338	arcsec	2.357e−05	4.8621	21.5886	1.44
grating Rz	3.0516	um/arcsec	0.328	0.492	arcsec	1.377e−06	0.2839	0.8665	0.06
camera Rx	2.7833	um/arcsec	0.359	0.539	arcsec	3.425e−07	0.0706	0.1966	0.01
camera Ry	2.7940	um/arcsec	0.358	0.537	arcsec	5.292e−06	1.0915	3.0496	0.20
							totals	34.8971	2.33
				allowed					
				error		**FEA**		**image**	**image**
	with flex.			**single**		**dipl/rot**		**motion**	**motion**
Optic error	**sensit.**		**1/sens.**	**source**		**radians−meter**	**arcsec−um**	**microns**	**pixels**
field lens Rx	0.0257	um/arcsec	38.911	58.366	arcsec	0.000e+00	0.0000	0.0000	0.00
field lens Ry	0.0376	um/arcsec	26.596	39.894	arcsec	0.000e+00	0.0000	0.0000	0.00
field lens Tx	0.0036	um/um	277.778	416.667	um	0.000e+00	0.0000	0.0000	0.00
field lens Ty	0.0020	um/um	500.000	750.000	um	0.000e+00	0.0000	0.0000	0.00
coll Rx	0.0708	um/arcsec	14.124	21.186	arcsec	1.032e−05	2.1291	0.1507	0.01
coll Ry	0.1258	um/arcsec	7.949	11.924	arcsec	7.192e−06	1.4835	0.1866	0.01
coll Tx	0.0370	um/um	27.027	40.541	um	6.289e−06	6.2894	0.2327	0.02
coll Ty	0.0172	um/um	58.140	87.209	um	4.525e−07	0.4525	0.0078	0.00
grating Rx	0.1801	um/arcsec	5.552	8.329	arcsec	4.268e−06	0.8804	0.1586	0.01
grating Ry	0.1540	um/arcsec	6.494	9.740	arcsec	2.357e−05	4.8621	0.7488	0.05
grating Rz	0.1909	um/arcsec	5.238	7.858	arcsec	1.377e−06	0.2839	0.0542	0.00
camera Rx	0.0146	um/arcsec	68.493	102.740	arcsec	3.425e−07	0.0706	0.0010	0.00
camera Ry	0.0200	um/arcsec	50.000	75.000	arcsec	5.292e−06	1.0915	0.0218	0.00
							totals	1.5622	0.10

Figure 3.30: Long Camera and Gx image motions.

IMACS									
Image motions from structure finite element model									
file: lcam_gy.xs3									
BCB 3/10/99									
15 micron pixels									
0.1 Px image motion spec. − 1.5 microns									
long camera									
1200 l/mm grating									
gravity on, Gy									
				allowed					
				error for		**FEA**		**image**	**image**
	no flex.			**a single**		**dipl/rot**		**motion**	**motion**
Optic error	**sensit.**		**1/sens.**	**source**		**radians−meter**	**arcsec−um**	**microns**	**pixels**
field lens Rx	0.1112	um/arcsec	8.993	13.489	arcsec	0.000e+00	0.0000	0.0000	0.00
field lens Ry	0.1578	um/arcsec	6.337	9.506	arcsec	0.000e+00	0.0000	0.0000	0.00
field lens Tx	0.0206	um/um	48.544	72.816	um	0.000e+00	0.0000	0.0000	0.00
field lens Ty	0.0144	um/um	69.444	104.167	um	0.000e+00	0.0000	0.0000	0.00
coll Rx	0.6698	um/arcsec	1.493	2.239	arcsec	1.192e−05	2.4579	1.6463	0.11
coll Ry	1.0267	um/arcsec	0.974	1.461	arcsec	1.381e−09	0.0003	0.0003	0.00
coll Tx	0.3328	um/um	3.005	4.507	um	1.144e−09	0.0011	0.0004	0.00
coll Ty	0.2128	um/um	4.699	7.049	um	1.890e−07	0.1890	0.0402	0.00
grating Rx	4.6085	um/arcsec	0.217	0.325	arcsec	2.940e−05	6.0650	27.9506	1.86
grating Ry	4.4402	um/arcsec	0.225	0.338	arcsec	6.911e−10	0.0001	0.0006	0.00
grating Rz	3.0516	um/arcsec	0.328	0.492	arcsec	5.571e−11	0.0000	0.0000	0.00
camera Rx	2.7833	um/arcsec	0.359	0.539	arcsec	5.365e−06	1.1065	3.0798	0.21
camera Ry	2.7940	um/arcsec	0.358	0.537	arcsec	1.288e−08	0.0027	0.0074	0.00
							totals	32.7257	2.18
				allowed					
				error		**FEA**		**image**	**image**
	with flex.			**single**		**dipl/rot**		**motion**	**motion**
Optic error	**sensit.**		**1/sens.**	**source**		**radians−meter**	**arcsec−um**	**microns**	**pixels**
field lens Rx	0.0257	um/arcsec	38.911	58.366	arcsec	0.000e+00	0.0000	0.0000	0.00
field lens Ry	0.0376	um/arcsec	26.596	39.894	arcsec	0.000e+00	0.0000	0.0000	0.00
field lens Tx	0.0036	um/um	277.778	416.667	um	0.000e+00	0.0000	0.0000	0.00
field lens Ty	0.0020	um/um	500.000	750.000	um	0.000e+00	0.0000	0.0000	0.00
coll Rx	0.0708	um/arcsec	14.124	21.186	arcsec	1.192e−05	2.4579	0.1740	0.01
coll Ry	0.1258	um/arcsec	7.949	11.924	arcsec	1.381e−09	0.0003	0.0000	0.00
coll Tx	0.0370	um/um	27.027	40.541	um	1.144e−09	0.0011	0.0000	0.00
coll Ty	0.0172	um/um	58.140	87.209	um	1.890e−07	0.1890	0.0032	0.00
grating Rx	0.1801	um/arcsec	5.552	8.329	arcsec	2.940e−05	6.0650	1.0923	0.07
grating Ry	0.1540	um/arcsec	6.494	9.740	arcsec	6.911e−10	0.0001	0.0000	0.00
grating Rz	0.1909	um/arcsec	5.238	7.858	arcsec	5.571e−11	0.0000	0.0000	0.00
camera Rx	0.0146	um/arcsec	68.493	102.740	arcsec	5.365e−06	1.1065	0.0162	0.00
camera Ry	0.0200	um/arcsec	50.000	75.000	arcsec	1.288e−08	0.0027	0.0001	0.00
							totals	1.2859	0.09

Figure 3.31: Long Camera and Gy image motions.

and filters, and will carry a tool-box and storage containers for instrument sub-systems.

Figure 3.32 shows the instrument carriage with the the mainframe and forward optical support structure. Rollers at the NIR end of the structure will support the NIR mounting flange when the instrument is not attached to the NIR. The rollers will be adjustable in height, so that the NIR mounting flange can be raised or lowered for mating to the NIR.

3.14.8.1 Auxiliary Structure Support

IMACS will violate the mass, bending moment, and moment of inertia limits of the Nasmyth instrument rotator (NIR). In order to reduce flexure in the structure, and protect the NIR from overloading, an auxiliary support for the instrument is provided under the MOSS disk. This support does not constrain the structure, but simply applies a reaction force sufficient to minimize or eliminate moment loads on the NIR. The function of the auxiliary support is thus to provide a continuous upward force, without over-constraining the structure.

Several approaches have been considered for applying the auxiliary forces. Simple counter-balancing levers, hydraulic cylinders, air cylinders, coil springs, and air springs have all been identified as options. The current concept uses air-springs, which can apply a constant force over a range of inches, and provide no transverse stiffness or restoring force.

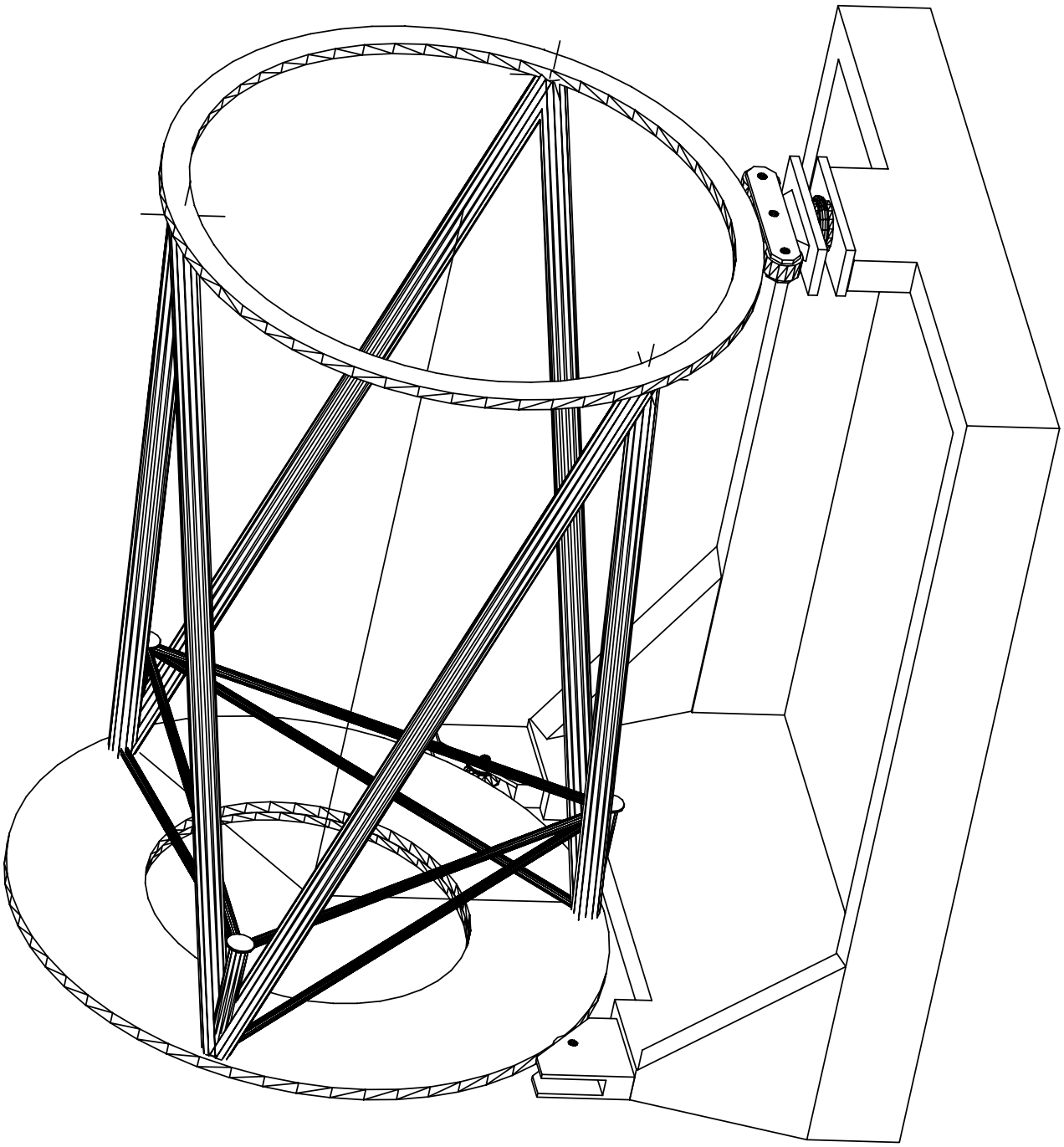

Figure 3.32: Mainframe mounted on instrument carriage.

3.14.9 Instrument Enclosures

3.14.9.1 Introduction

The instrument enclosure will provide several functions; it provides a light-tight seal around the optical system, protects the optics from dust and damage, provides a thermal barrier to rapid temperature changes in the dome, and protects the interior of the instrument from outside activities.

3.14.9.2 Hatch

The Nasmyth instrument rotator (NIR) has a 863 mm diameter aperture. A hatch at the front of the instrument will cover the entrance aperture whenever the instrument is not in use. The hatch will have a diffusive coating on the instrument side, for reflecting calibration light from the lamps into the slit area. The hatch will be a retracting screen, potentially a commercial slide or overhead screen, driven by an air cylinder.

3.14.9.3 Light Baffles and Seals

The instrument will enclosure will support internal light baffles between the field lens and collimator, and in the area around the disperser server system. The exact dimensions of the baffles and their locations are TBD. Additionally, care will be taken to provide light-tight seals at all joints in the enclosure, and around the access ports.

3.14.9.4 Instrument Enclosures

Figure 3.33 shows the instrument enclosure with some panels removed for clarity. The largest portion of the enclosure surrounds the mainframe, and is composed of insulated panels which mount to rails between the instrument mounting flange and the MOSS disk. The panels will sit on sills which are baffled and made light tight with adhesive gaskets. The panels will be of composite construction, with insulation and low thermal-conductivity skins. The panels will be attached with quarter-turn fasteners, to simplify their removal when servicing the instrument.

The second part of the enclosure protects the short camera and the rear of the MOSS.

The panels that make up the cone-shaped end are of similar construction to the main enclosure panels. These shells are readily removable as with the main enclosure panels. Near the MSS, DSS, and short camera, the panels will have protrusions, and access ports for changing masks, dispersers, and filters.

3.14.10 Electronics Enclosures

There will be racks of electronics mounted on the instrument carriage as close as possible to the instrument. These enclosures will be commercial, insulated electronics cabinets.

3.14.10.1 Thermal Control System

Currently, there are no substantial sources of heat within the instrument enclosure, except for the guide and SH cameras, which are liquid cooled. The major heat producing components will be located in the electronics racks which will also be liquid cooled. Sensors will monitor the guide cameras and cabinet temperatures. Liquid cooling will be provided by the telescope, and fed into the instrument through the telescope cable wrap system.

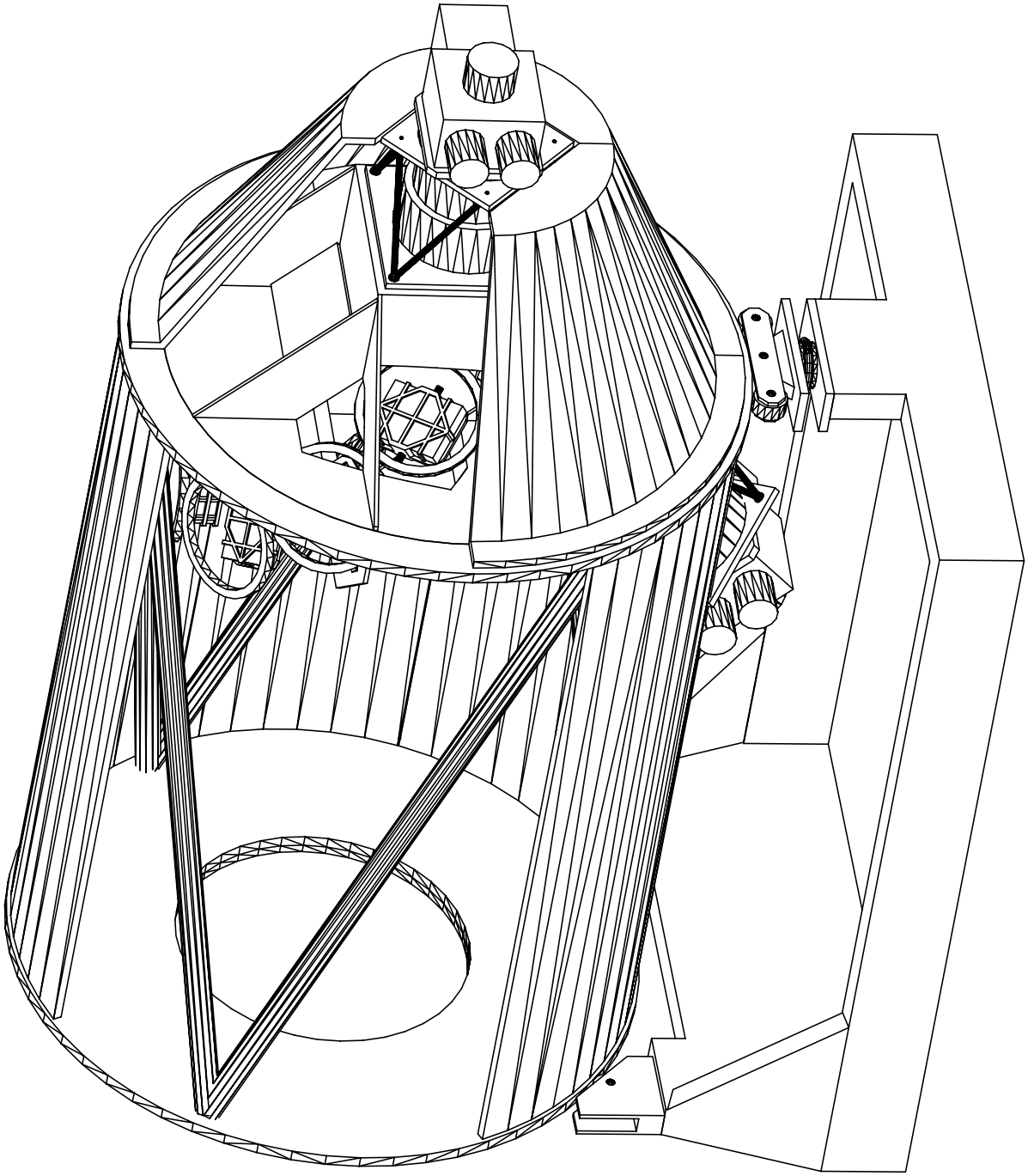

Figure 3.33: Instrument enclosure with some panels removed for clarity.

3.15 Disperser Server System (DSS)

3.15.1 Introduction

The disperser server system is an automated system for selecting optical elements in the instrument. The elements are mostly dispersers; gratings and grisms. There is one position occupied by a mirror, for direct imaging with the long camera. The grism positions will be counter-weighted until the short camera systems are implemented. Figure 3.34 shows the an isometric view of the DSS wheel.

The mechanical requirements for the disperser Server System are as follows:

1. The system must be able to select from one of eight positions. The elements to choose from include three gratings (with adjustable tilts), a mirror, three grisms, and an empty position (up-gradeable for a Fabry-Perot etalon).

2. Angle stability must be maintained to better than 0.1 pixel image motion. This translates to better than 0.46 arcsec tip and tilt of the element, and better than 0.25 arcsec rotation about the optical axis.

3. The mechanism must be able to exchange gratings without changing tilt angle, in order to allow switching between spectrographic and imaging mode.

4. The repeatability spec for removal and replacement of an element is to have spectral features return to their original positions within 5 pixels (75 μm and a goal of 1 pixel (25 μm). This translates to angular changes of the element of 14.1 arcsec (with 2.8 arcsec goal). This further translates to 10.2 μm (with goal of 2.0 μm) displacement over 150 mm.

5. The time required to remove a dispersion element, and to replace it with another must be less than one minute.

6. Tilt angles range from 20 degrees to 65 degrees.

7. The resolution of grating tilt settings is to be one degree or better.

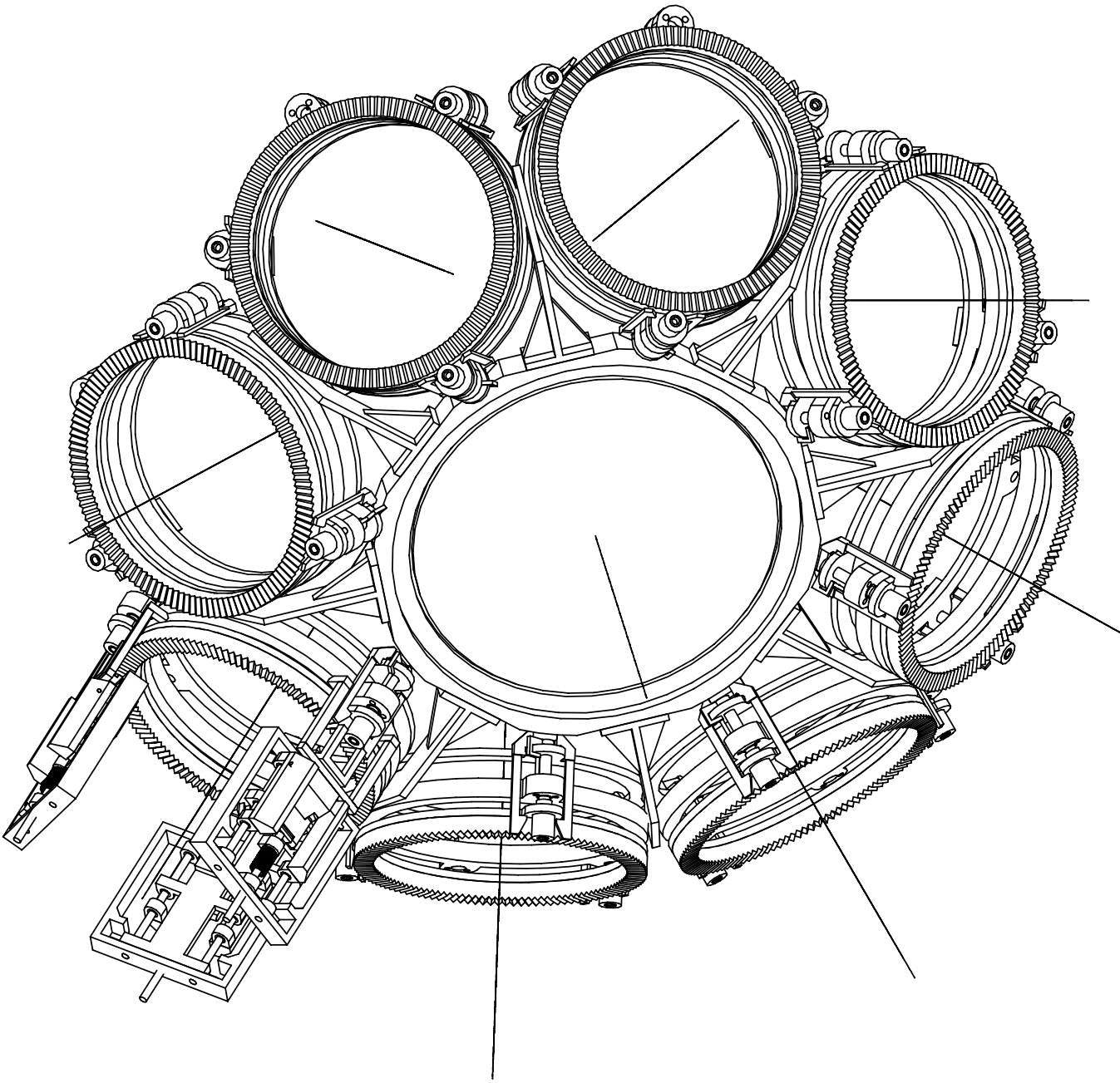

Figure 3.34: Isometric view of the disperser server system.

3.15.2 Disperser Server Components

The disperser server system is comprised of a large annular wheel mounted on an axis opposite to that of the long camera, and above the collimator. In mounting the disperser in this fashion, it is expected that the space envelope will be reduced, with the additional benefit of having the mass of the server offset the mass of the long camera, about the instrument axis. Around the periphery of the wheel are mounted the eight different elements (and their tilt mechanisms where required).

The heart of the system is based on the utilization of a commercially available "matrix ring" that allows us to separate and engage again repeatably at the micron level. One half of this ring will be mounted rigidly within the MOSS and the other half will be attached to the dispersing element (each element will have its own second half of the matrix ring). Once the wheel is in its proper location for serving up a specified element, a mechanism transfers that disperser, its matrix ring, and tilt mechanism onto the other half of the matrix ring where it is clamped into position. Figure 3.35 shows a detail of an index ring.

The larger wheel that carries all of the elements is made of a separable annular ring that is driven by on a set of cam followers. In this configuration, we are able to make the MOSS a single large weldment, without the requirement of a removable hub for placement of bearings. All of the rollers can be added after the MOSS is complete and the ring assembled onto the rollers. The ring is driven by a belt through a large stepper motor equipped with a power-off brake. There is a single home position on the wheel activated by a knife-edge passing through a photo-electric sensor. "Homing" the wheel is an operation required upon initialization only.

Each dispersing element is held on the wheel on a set of forks, equipped with a spring-loaded latch. It is not possible for the element to be removed from the wheel without first tripping the latch mechanism that retains the element. An air cylinder is used to slide the element (and latch) along the fork until it is pressed against the MOSS half of the indexing ring. At this point three clamps are activated - engaging the matrix rings tightly together, as well as releasing the latch mechanism from the forks to the element. The forks are now free to be retracted from the element, thus removing any contact between the wheel and the element.

The clamps are designed in such a way that they are "powered" open and spring loaded

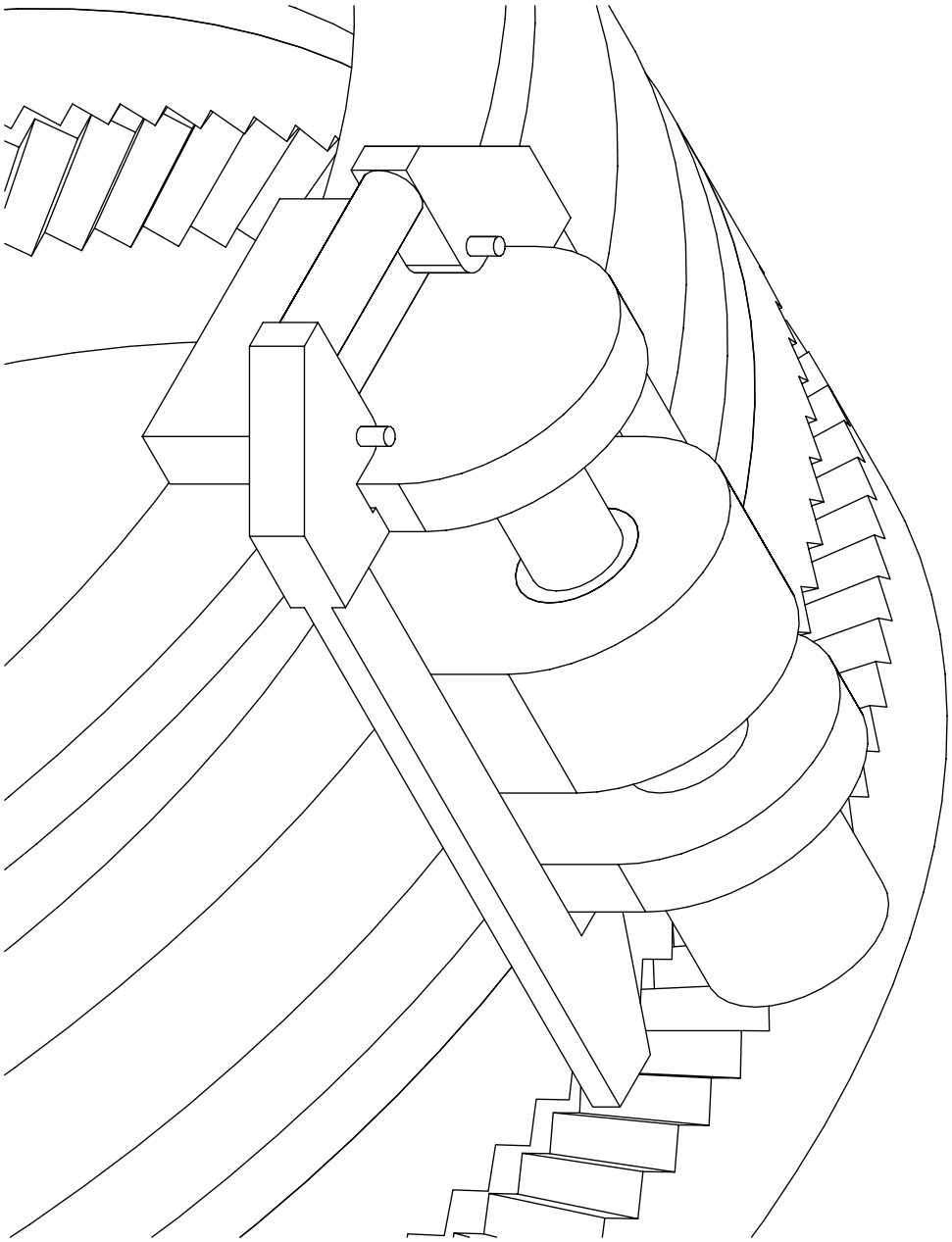

Figure 3.35: Index ring fork and latch mechanism.

closed in the event of any type of power failure. It is not possible to remove the disperser element from its forks without first clamping it to the matrix ring. In order to load the matrix ring back onto the wheel, the forks are driven back into the element, and the clamps are released. Releasing the clamps allows the latch on the forks to engage the element again, and as the forks are retracted, the element moves back with it.

In this arrangement, it is possible to do all of the element selection through the use of four air cylinders. One to drive the forks, and one for each of the three clamps (all on one circuit).

The clamps are designed in such a way that the portion of the clamp that pulls on the element's matrix ring must also retract out of the way when the selection wheel is being turned. The other half of the clamp jaws is designed to disengage the latch on the fork as it travels forward to meet the back half of the matrix ring. Essentially the clamping mechanism is "free floating" on a set of rails. This ensures that all of the clamping force is directed through the mechanism and the matrix rings, and none is passed through the MOSS.

In the case of the grisms, the cell that holds the grism can be mounted rigidly to the actual matrix ring half. In the cases of the gratings, and the imaging mirror, the cell must be mounted on to the matrix ring through a structure that houses two bearings and allows tilting of the cell with respect to the ring. A ceramic bearing is to be used for maximum stiffness, and it will be preloaded appropriately.

The cells are designed to place the center of gravity on the axis of the bearing, thus removing any load from the mechanism that drive the tilt, and placing all of the load through the bearings and support structure. The requirements for flexure of the structure (i.e. stability during observation) are quite stringent; however, they are viewed more as goals than requirements as it is expected that some of the errors due to displacements of other elements, and structures can be used to offset the errors due to flexure of the disperser mechanism.

The mechanism to be used for driving the tilt of the element is a worm gear driving a sector, located behind the element. A small linear spring will be used to keep the sector loaded against the worm. Each element that requires tilt will have its own stepper motor, power off brake, worm, and sector. Thus, several of the positions on the disperser wheel will require an umbilical to the disperser tilt mechanism.

The gratings are to be mounted within their cell on a series of flexures. Three pillars on

the back of the cell are adhered to the back of the grating. These three pillars are compliant in two directions, but stiff along the axis of the pillar. These will define the plane that the grating sits in, and three mode hard points are required to fix the grating in that plane. These are located on the sides of the cell, two on the long side, and one on the short side.

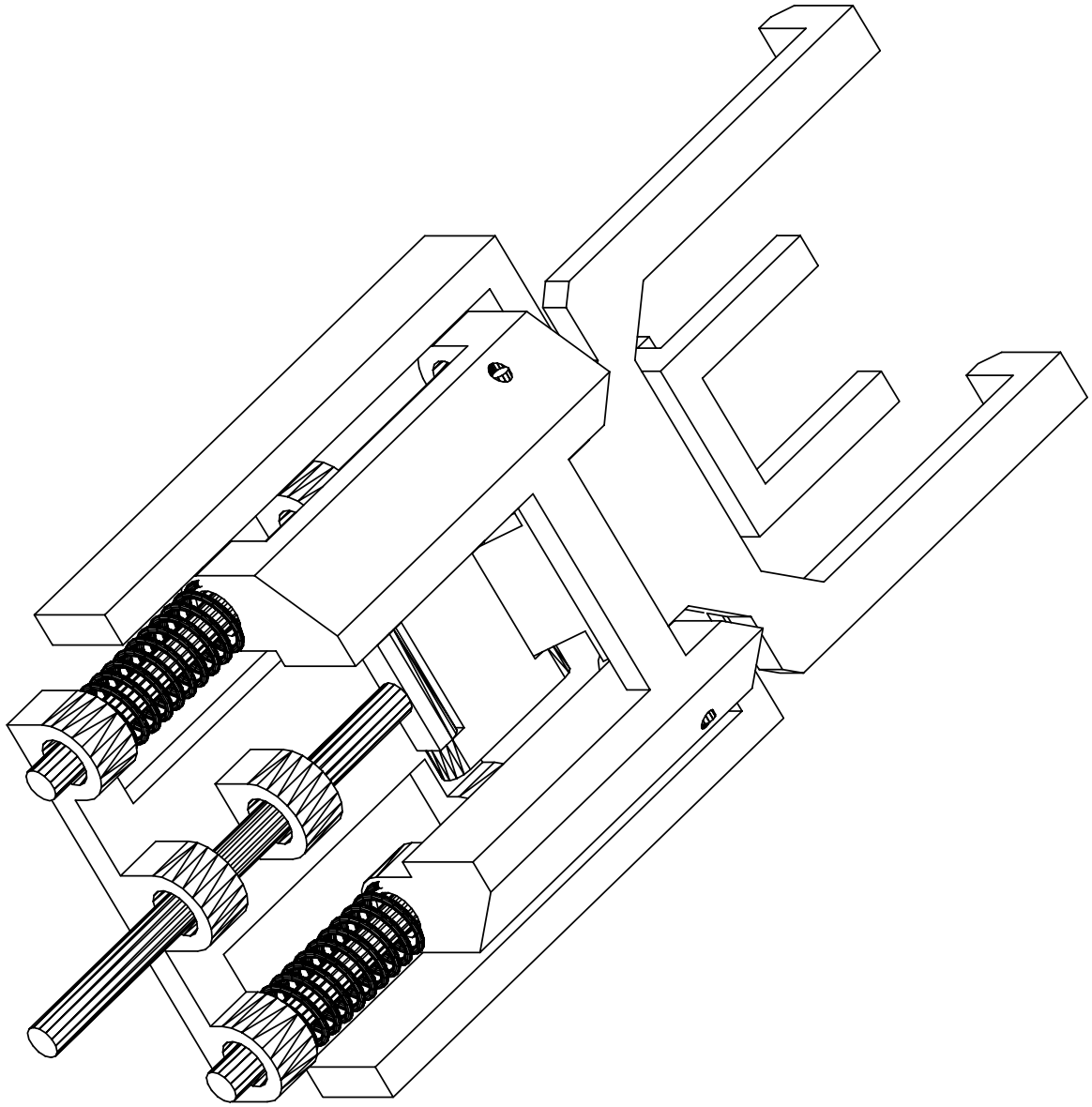

Figure 3.36: Index ring clamp mechanism.

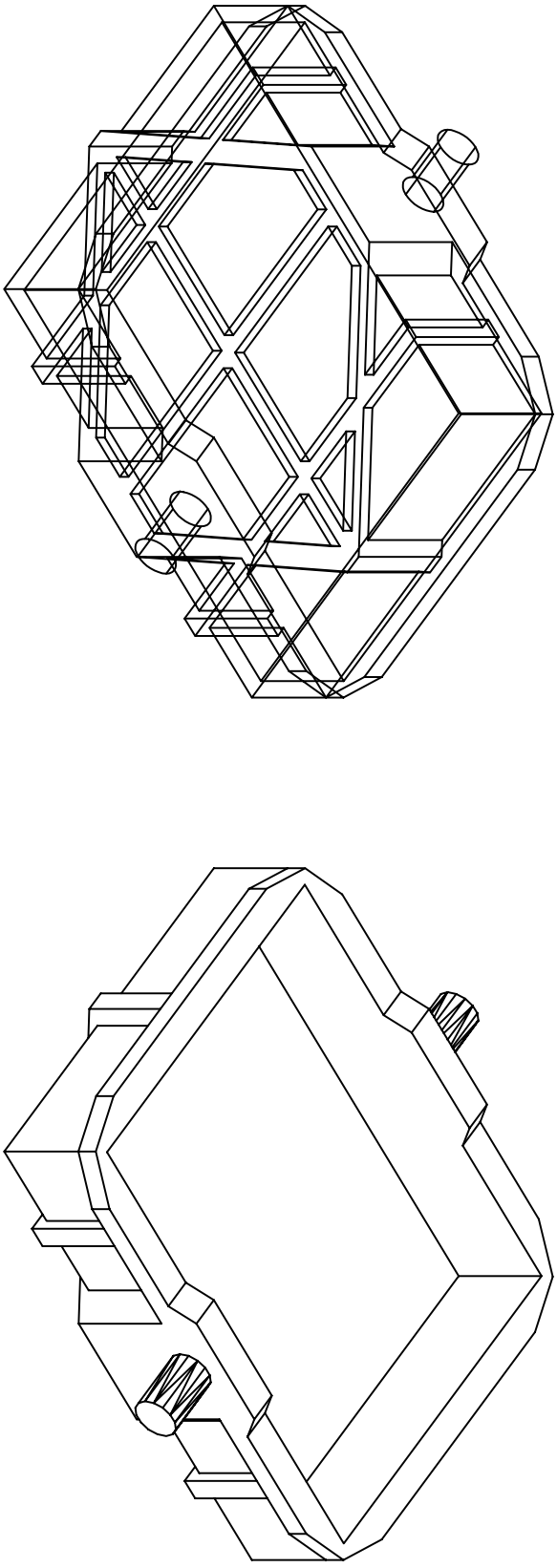

Figure 3.37: A grating cell.

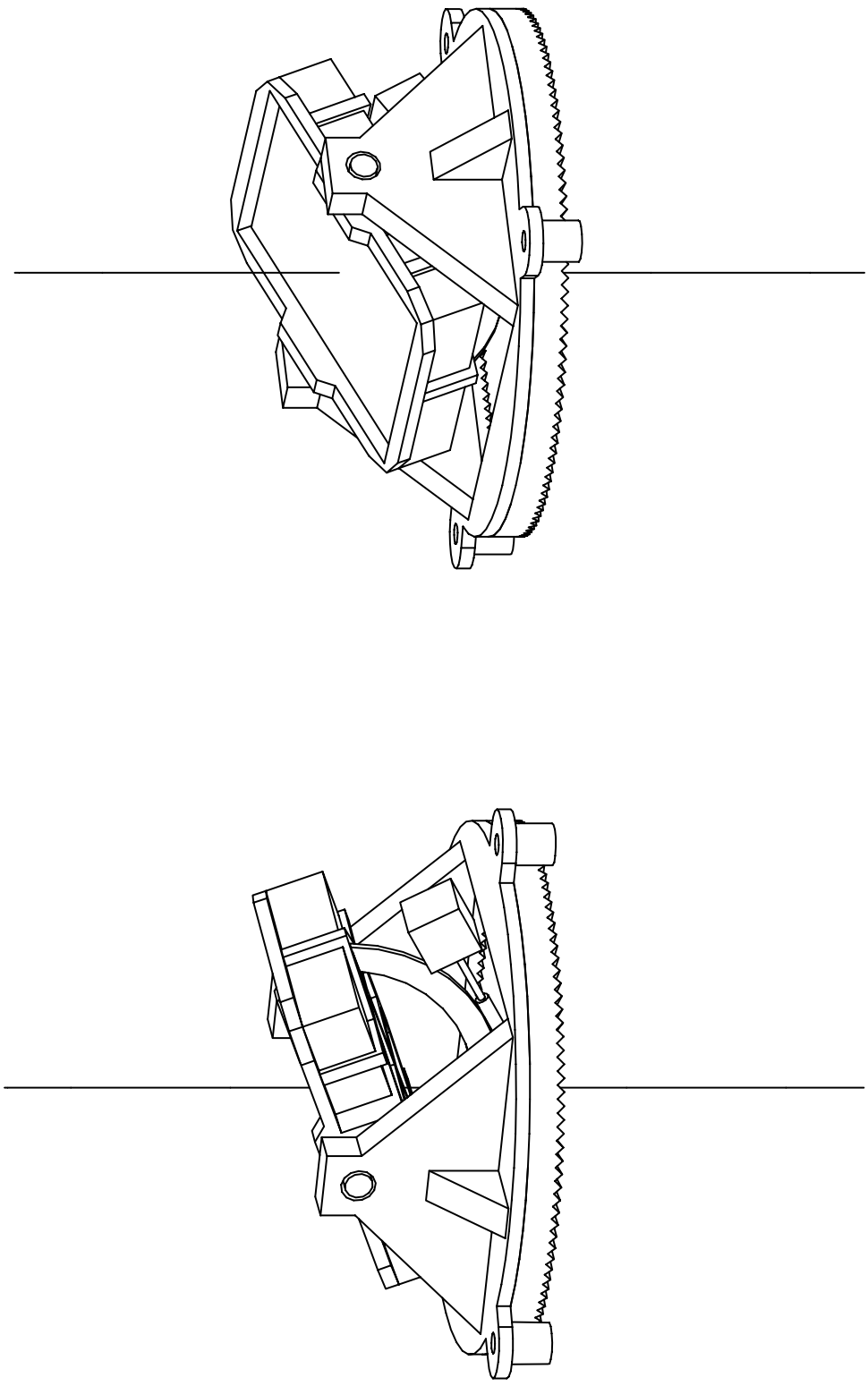

Figure 3.38: A grating cell mounted on its index ring.

Chapter 4

Guide Camera Head Design

4.1 Magellan Guider Camera Description

The guide camera heads used in IMACS are of a common design to be used by most of the Magellan instruments. A description of the design is included here for reference.

The guider camera is designed to use a frame-transfer CCD detector with low read-noise and fast readout. It supports a full-frame imaging mode, a fast subraster imaging/centroid mode, and a slow Shack-Hartmann wavefront sensing mode.

With a nominal 100 ms exposure time, the camera is designed to work with 19th magnitude guide stars.

The full documentation package is on-line at http://www.ociw.edu/~burley/ccd/guider.html.

4.2 Mechanical Layout

Physically, the guider camera consists of six circuit boards

- CCD header board (with preamps)
- DSP timing generator board
- Signal processing board
- Clock driver board
- Power supply board

- Backplane board

in a package with dimensions of 3.75″ x 3.5″ x 6.0″.

Figure 4.1 shows the mechanical arrangement of the camera. The imaging area of the array is located in the center of the faceplate. The position of the CCD is referenced to the heat sink, through the thermo-electric cooler and spacer block.

The header board is not shown in the diagram.

A space of about 2.5″ behind the camera will be required for the serial connector (HD-15), the power connector (DB-9), and two fluid connectors (1/4″ OD).

4.3 CCD Detector

The detector for the guider camera is the EEV CCD-47 frame transfer CCD. The frame transfer architecture is required for shutterless operation. The array is made up of two sections of 1024×1024 pixels, each independently clocked. The read-out section is covered with an opaque aluminum mask.

The device is backside illuminated with high quantum efficiency and low read-noise (useful for faint guide stars). The typical quantum efficiency of the CCD-47 is shown in Figure 4.2.

Properties of the guider camera and detector are given in Table 4.1.

4.4 CCD Cooling System

The CCD operates within a sealed, dry gas filled housing with thermo-electric (TE) cooling. The cooling system uses a two-stage TE cooler attached to a liquid-cooled heat sink. The CCD temperature is monitored with a sensor mounted near the cold side of the TE cooler.

The EEV CCD is available in either a standard 32-pin device package, or in a special hermetically-sealed package. For the prototype camera, we plan to contain the dry gas with a housing built around the standard package.

4.5 CCD Controller Electronics

The design of the CCD controller is based on a digital signal processor, to provide software programmable binning, subrasters, and so on.

The preamplifiers and signal processing are optimized for fast settling time to take advantage of the high speed readout capability of the EEV CCD.

The CCD controller is suitable for a frame transfer CCD with one or two output amplifiers. The digital-signal processor generates the CCD clocking sequences, providing parallel, serial and frame transfer clocks. All of the clock voltages and timing are software programmable, as are the signal processing gain and offsets. Other programmable features include the exposure time, subraster size and position, binning, and temperature control. The controller has two 14-bit signal processing channels, each capable of 500 kpix/sec conversion rates (2 μs per pixel). The digitized image data is transfered by a 10 Mbps serial link to a PCI interface in the host computer.

4.6 Computer Interface

Each guider camera is controlled from a host PC, which has software to set the parameters for the CCD and to accept the digitized image data. The host computer sends control commands and receives the CCD data on a bidirectional serial link.

The guider camera computer receives the image data from the CCD controller. It generates position error signals, and sends them to the TCS. It can also export the images to the image analysis system.

The display for the user is driven from the guider camera computer.

The interconnect between the guider cameras, the guider camera computers, and the telescope system are shown in Figure 4.3. It is possible that each guider camera computer will be able to support a few guider cameras with one PCI interface board and monitor per camera. As drawn, each guider camera has its own computer.

Table 4.1: Guider Camera and Detector Properties.

Parameter	Value	Units	Notes
Array Size	1024×2060	pixels	
Image Area	1024×1024	pixels	
Pixel size	13	μm	
Quantum efficiency	90	% peak	(at 500 nm)
Estimated read-noise	< 10	e^-	(at 500 kpix/s)
	2	e^-	(at 20 kpix/s)
Dark current	100	e^-/pix/s	(at 293 K)
	$< .2$	e^-/pix/s	(at 243 K)
FOV	$103'' \times 103''$		(at f/4.1)
Resolution	0.1	arcsec/pixel	
Full Frame readout	200	ms	(binned 2×2)
Subraster readout	25	ms	(50×50 pixels)

4.7 Guider Camera Software

The software for the guider camera consists of several sets of code:

DSP code – routines used by the DSP to generate serial and parallel clock waveforms for the CCD, read out and digitize the image data, and to send or receive over the serial link.

Device drivers – routines to interface the PCI card into the host computer operating system. There will eventually be drivers for DOS, Linux, and NT.

Interface library – routines to handle low-level interaction between the guider computer and the DSP. These include downloading the program code to the DSP at power-up, sending controller parameters (image size, binning, gain, clock and bias voltages, etc.), reading and formatting the image data, and so on.

DSP test suite – a series of programs to exercise the various functions of the CCD controller, such as the serial ports, ADC, DAC, serial and parallel clock generators, and timers. These are designed to be used at the test bench with an oscilloscope to verify the hardware.

Guider software – a program which does the image processing, centroiding, user display, and handles interaction with the user. This will be based on the software currently operating on the Dupont 100″ telescope.

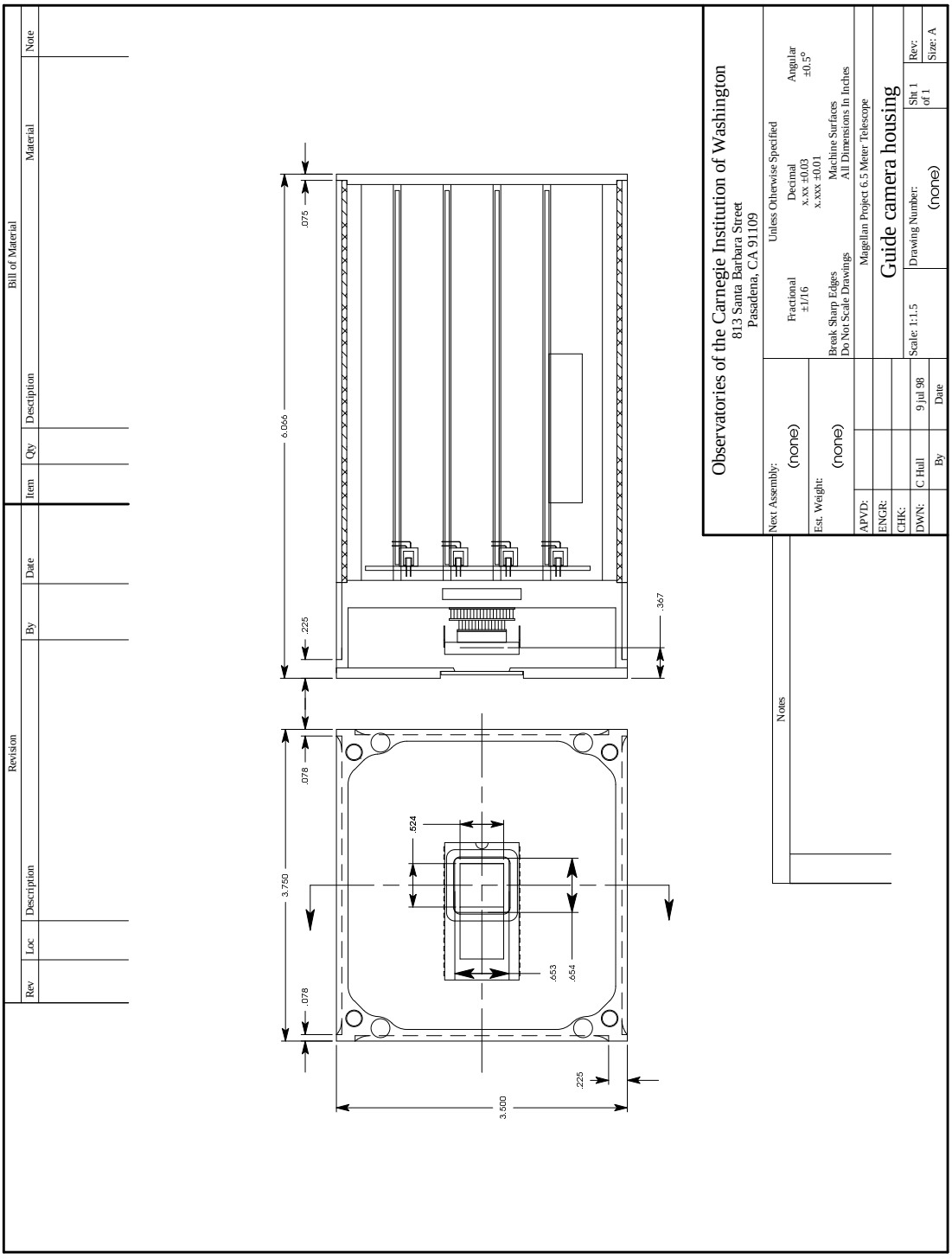

Figure 4.1: Magellan Guider Camera Mechanical Layout.

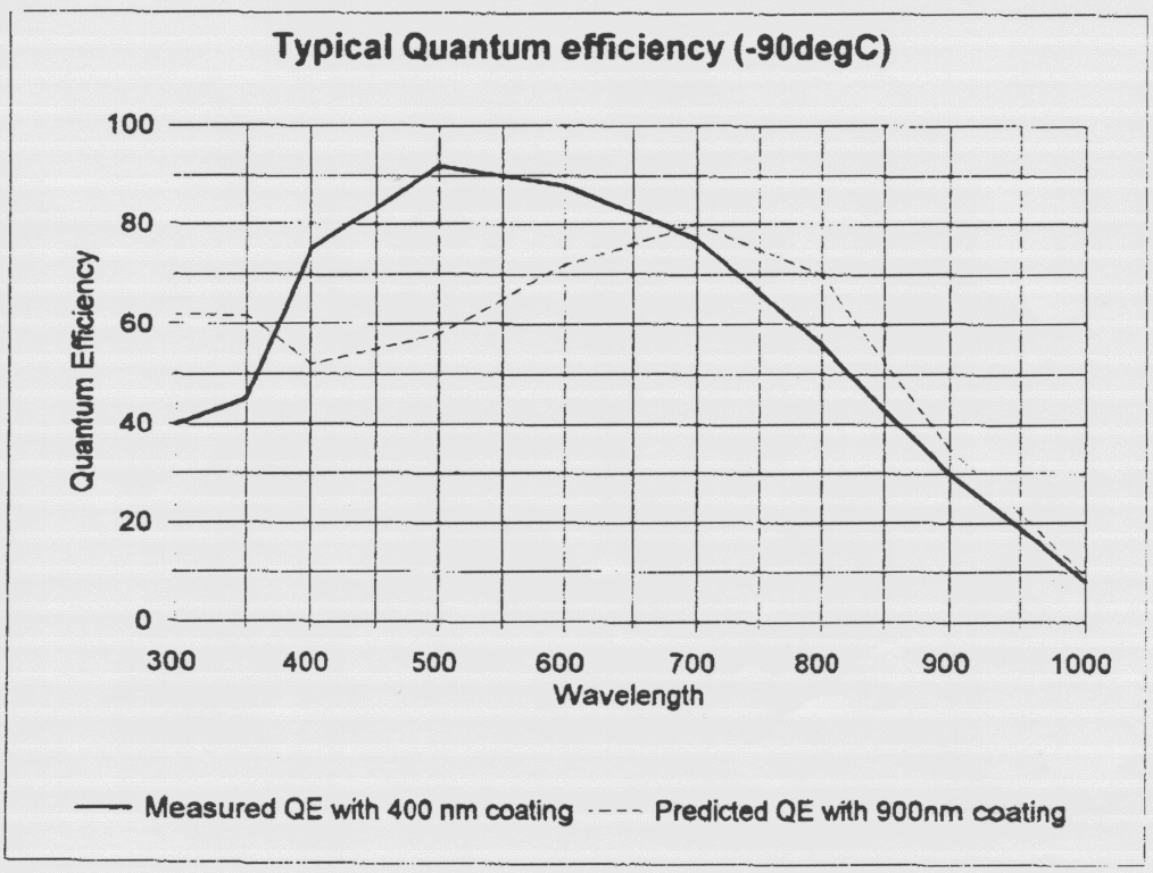

Figure 4.2: EEV CCD-47 Typical Quantum Efficiency.

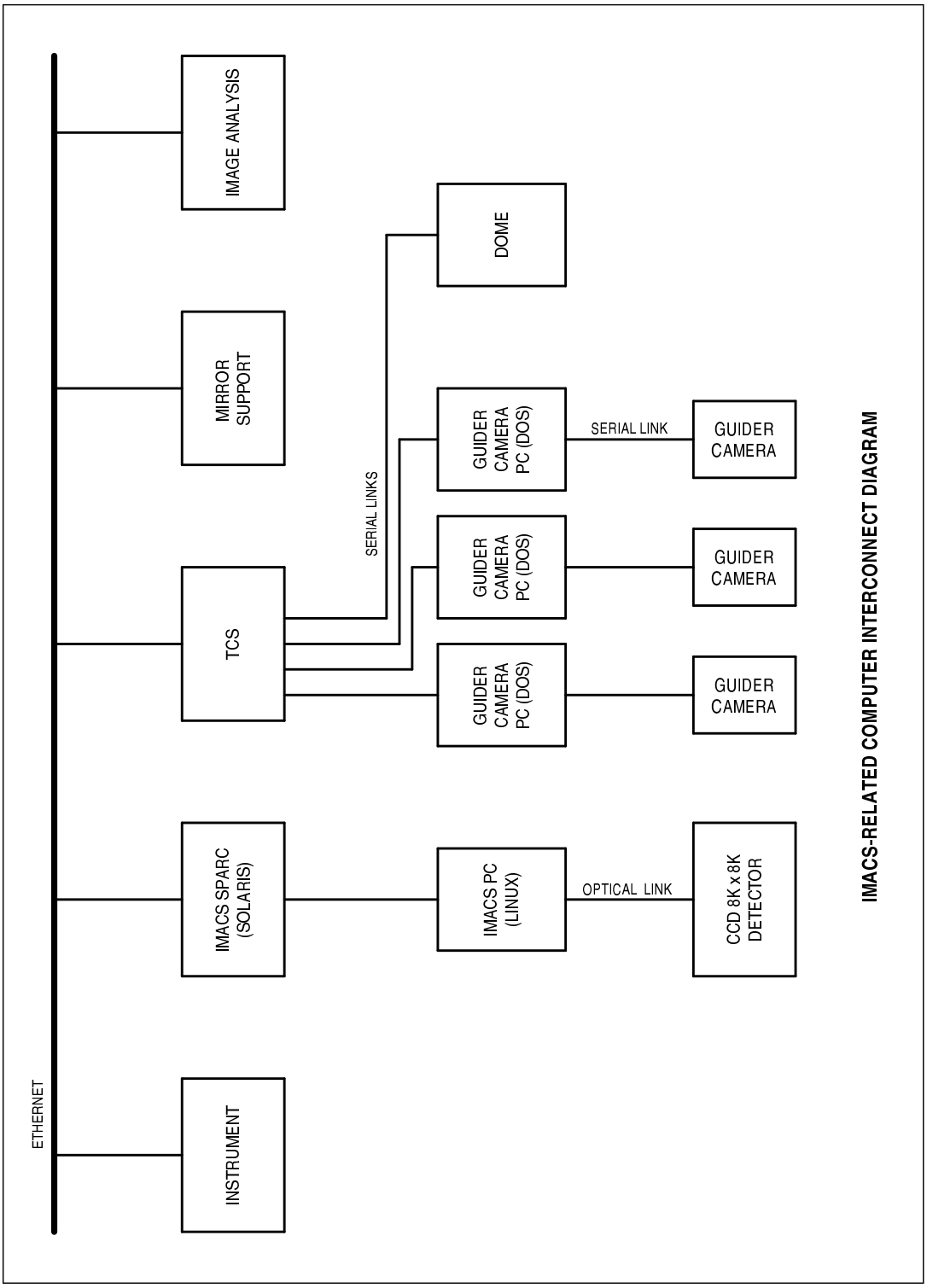

Figure 4.3: Guider Camera Interconnect diagram.

Chapter 5

Preliminary Dewar Design

5.1 Preliminary Detector Array System Design

5.1.1 Science Array Mechanics

5.1.1.1 Cryostat Window

The dewar window is a plano/concave lens (whose flat back faces the CCD focal plane and serves as the vacuum sealing surface for the cryostat. The lens is the final element in the camera lens assembly. The cryostat front plate contains a recess about 2/3 the edge thickness of the lens. The small lip in the front plate contains an o-ring that contacts the back surface of the lens and provides the vacuum seal. A bezel fits around the remaining portion of the lens that protrudes from the front-plate, and is flush with the front lip of the lens (see Figure 5.1). This bezel serves to protect the lens, retains it when the cryostat is not evacuated, and allows easy removal of the lens when necessary.

5.1.1.2 Cryostat Body

The body of the camera cryostat is based on the successful design used for the CFHT 8Kx12K camera. Rather than using a camera with cylindrical symmetry, the square CFH12K design is more suited to the natural geometry of the focal plane. The camera body is approximately 330mm x 330mm in cross section and approximately 200mm thick, and is shelled to a wall

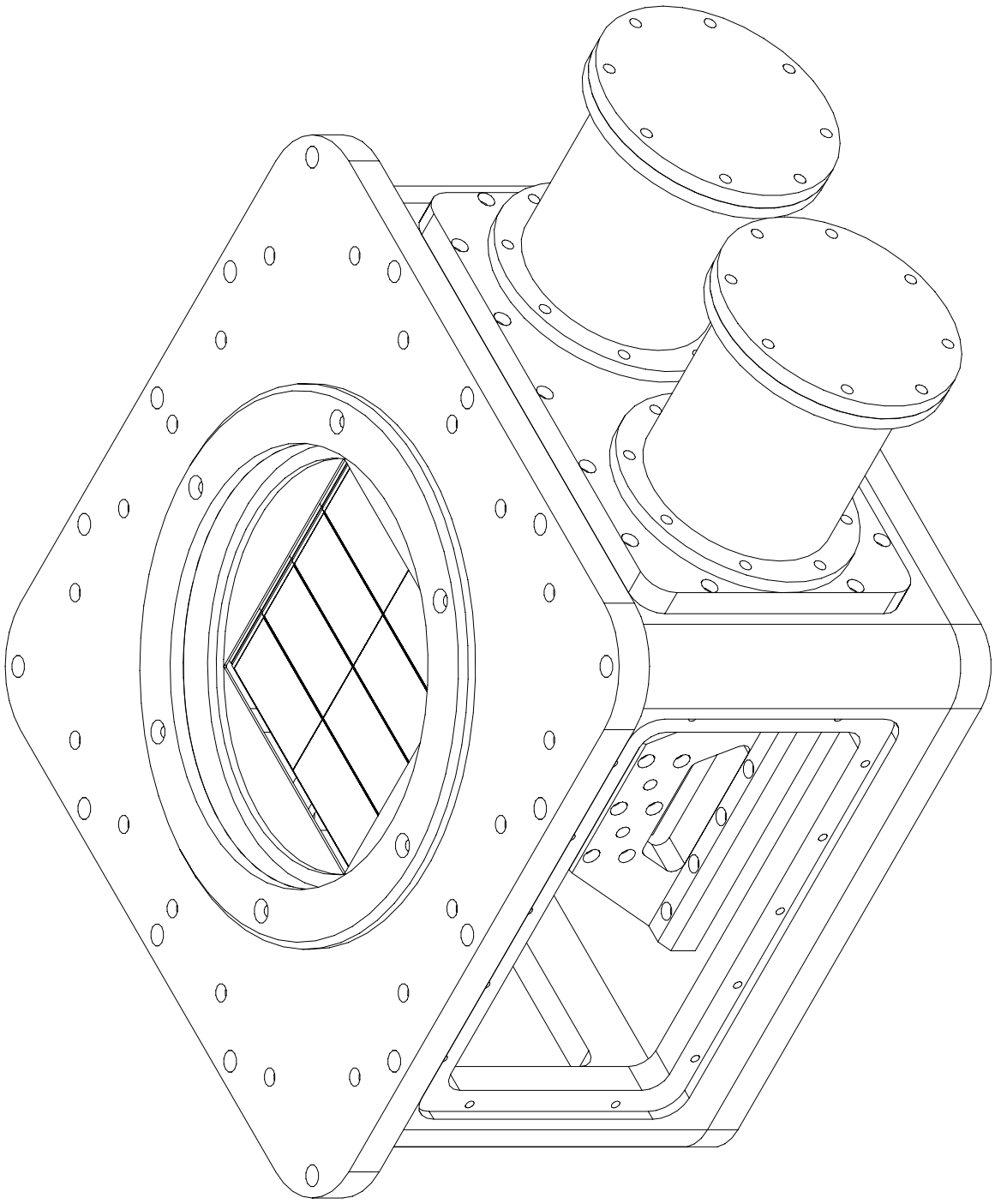

Figure 5.1: Isometric view of dewar exterior.

thickness of approximately 25 mm. This large aluminum frame is hogged out of a single billet of aluminum. The CCD sits in the center of the 330mm x 330mm square at the nominal focal plane position 8.5 mm behind back surface of the window. All four side walls have large access ports (see Figure 1). Similar previous mosaic camera designs (UH8K, CFH12K, AAO WFI) had the focal plane attached to the inner walls of the camera body, allowing rigid mechanical attachment and easy access to all sides of the focal plane. In the IMACS camera, this was not possible because of the need for the X-Y-Z translation stages for focus and flexure compensation. In this design, the X-Y-Z stages attach to the camera backplate (see Figure 5.2). Easy accessibility is still maintained with all focal plane and stage hardware attached to this back plate, except for the electronics cabling and cooling straps, both of which attach to points on the side-walls. Still, because of the numerous large access ports, assembly and adjustment of internal parts should be straightforward.

5.1.1.3 CCDs and CCD Mosaic Focal Plane

The CCDs used in the IMACS 8K camera are the SITe ST-002A 2048 $\times$ 4096 devices with 15 μm pixels. The CCDs are packaged in 3-edge buttable, invar packages designed to be used in mosaic arrays. The package is a simple invar slab with a small circuit board along the short edge containing a 37-pin Nanonics connector. The slab is machined flat on the backside and has four 4-40 tapped holes for attaching the CCD to a mounting surface. The CCD and package are illustrated in the mosaic drawing shown in Figure 5.3.

Note: the CCDs as provided by SITe need to have two minor modifications:

1. The device is provided with a wire bond cover that sticks up high enough to possibly cause problems. This cover serves little useful purpose and should be removed.

2. The SITe package is provided with a flat cable mated with the Nanonics connector. This is provided so as to avoid having to mate and disconnect the fragile Nanonics connector. Unfortunately, the flat cable provided by SITe uses rather large wires that will certainly cause additional unnecessary thermal load on the focal plane. This flat cable should definitely be removed and replaced with a flex cable that uses 5-mil wide 0.5 oz copper traces.

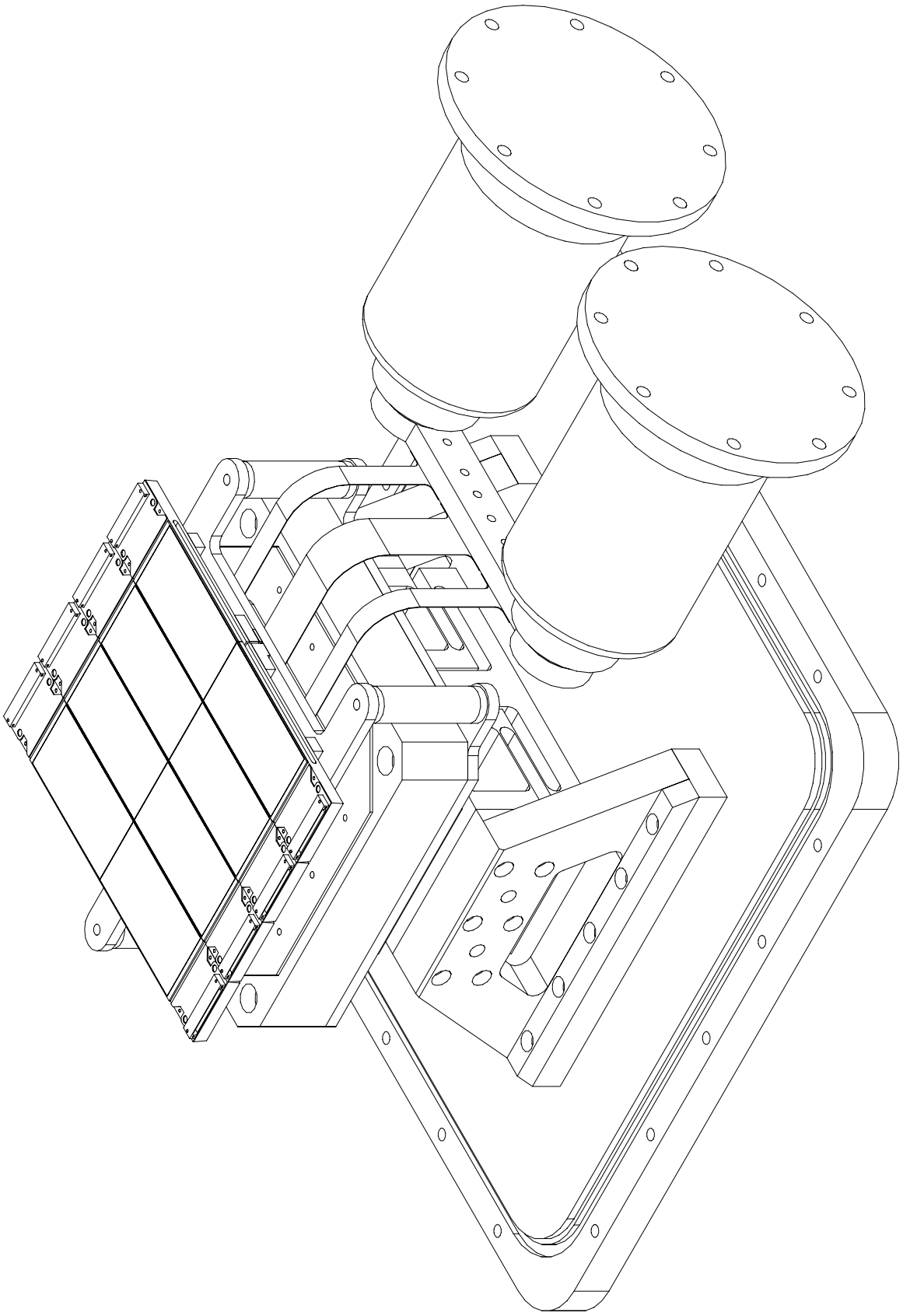

Figure 5.2: Isometric view of dewar interior.

> Similar flex circuits have been used for other CCDs and they work quite well and provide thermal isolation as good as a conventional wire harness made from 5-10 mil constantan. The mating and unmating of the Nanonics connectors is a real concern. These very same connectors are used on on the LL CCID-20 packages, and we have considerable experience mating and unmating hundreds of them. Mating cycles should be avoided. The best approach would be to attach the new low-thermal-load flex cable to the CCD and *leave it there.*

The simplest approach for a focal plane design would have been to screw the 8 SITe CCDs to a flat plate, but this would not have allowed adjustment for height and tilt variations from CCD to CCD which is expected to be larger than the desired flatness for the assembled focal plane. To compensate for these possible height and tilt variations, a sub-package was designed that can be adjusted for each CCD to enable the construction of a flat, aligned focal plane. The sub-package attaches to the CCD package via the four 4-40 mounting screws. The sub-package/CCD assembly is then attached to a flat plate (the focal plane mounting plate) at three points. Contact to the plate is made on three feet, each of which can be ground to adjust for the overall piston and tilt of a given CCD.

In order to know how much each CCD sub-package must be adjusted, each CCD must be have its height measured at various positions on the imager. This can be done using a high powered video microscope to a precision of about $\pm$5-10 μm. This technique was employed with the LL CCID-20 CCDs used in the CFH12K camera. Although the surface of the chips were planar ($\pm 10 \mu$m), the chip to chip heights and tilts for these devices varied by tens to hundreds of microns and adjustments had to be made to achieve a flat focal plane. The height of each device was measured at 6 points along the edge of the imaging array. Once all the CCDs were measured and their intended positions in the focal plane were known, the adjustment to the 3 mounting feet on each sub-package was computed in order to bring the surfaces of each CCD to a common plane. The CFH12K focal plane was assembled using this technique and the result was flat with a peak-to-peak deviation of only 20 μm.

In addition to flatness, the IMACS specifications require that the CCD rows and columns be aligned to better than 5 pixels (with a goal of 0.5 pixel). An alignment jig (currently still being designed) will allow the sub-package to be attached to each CCD package in such a

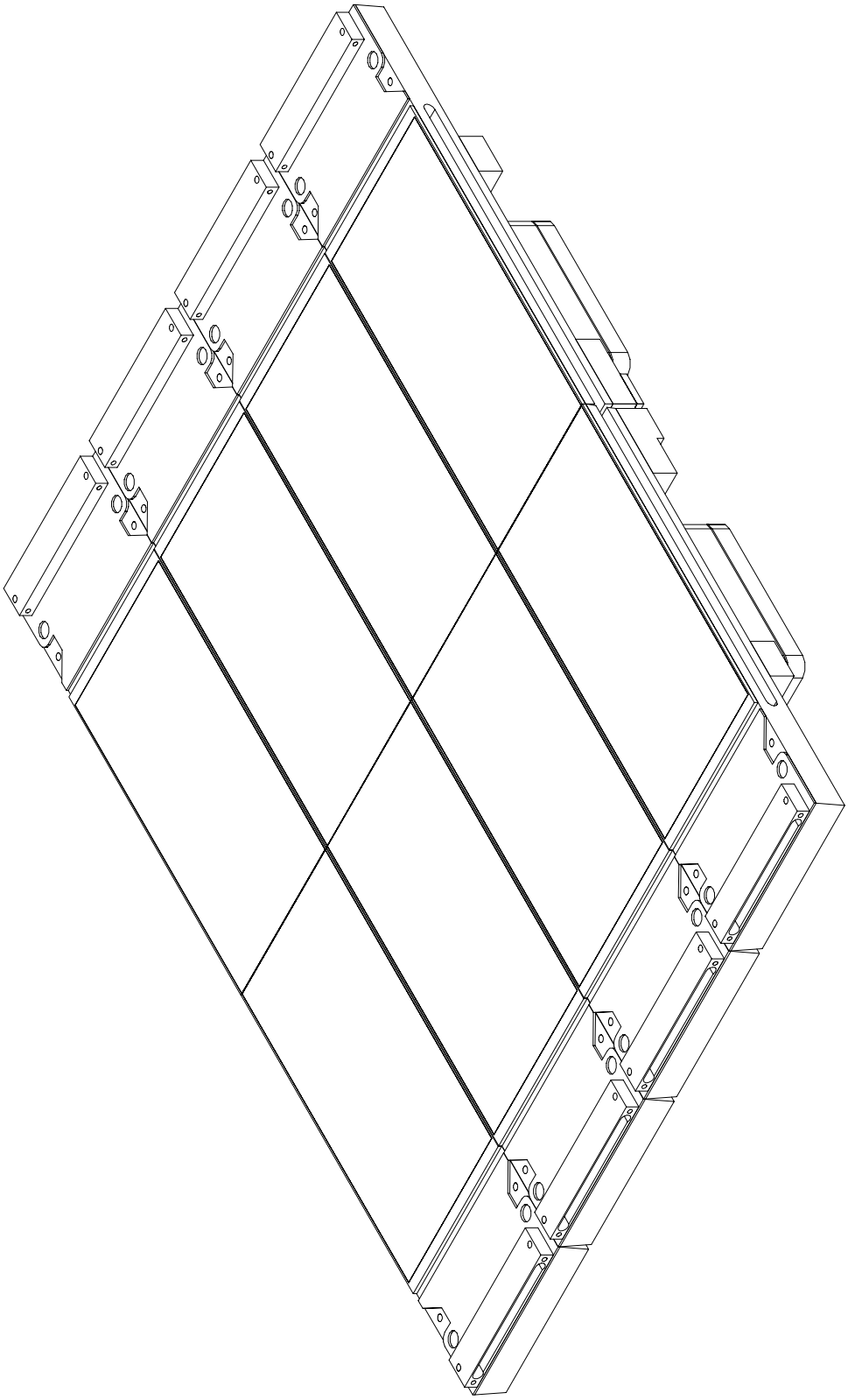

Figure 5.3: Isometric view of the focal plane.

way that the CCD is aligned to some fiducial and in turn to a hole and slot that are machined in the back of each sub-package. The alignment jig allows the CCD position to be adjusted with respect to the sub-package while looking at the surface of the CCD under a high powered microscope. Once aligned to a reference edge, the sub-package is locked onto the CCD package with its 4 screws. A hole and slot in the sub-package mate with a pair of pins located on the focal plane mounting plate thus aligning each CCD during installation. This pin/slot technique should achieve alignment accuracy and repeatability at the 1 pixel level (see Figure 5.4).

Another feature of this design is the way in which the thermal contact is made to the CCD packages. Rather than trying to cool the focal plane mounting plate to a uniform temperature and hoping that the CCDs are also isothermal, this design has the provision for attaching the copper cold-straps directly to each CCD sub-package. Each sub-package includes a thick rectangular section that extends through a hole in the focal plane mounting plate. The copper straps are clamped to this surface with an aluminum clamp (see Figures 5.5 and 5.6).

Heater resistors can also be attached to these aluminum clamps to apply heat locally to adjust the focal plane temperature. This may not prove to be necessary, but the option exists if needed. A similar copper strap design proved to be quite successful on the CFH12K focal plane. The LL CCID-20 packages included a temperature sensor, making it possible to measure the chip to chip temperature differences and the temperature difference between the CCDs and the focal plane mounting plate. The result was that the temperature gradient was less than 0.1 C between CCDs and between CCDs and focal plane.

The focal plane mounting plate is attached to, and thermally isolated from the XY stage through three G10 fiberglass tube stand-offs that are 12mm in diameter with 1mm thick walls. The stand-offs are approximately 45mm long. If necessary, the overall focal plane tilt with respect to the optical axis can be adjusted with these stand-offs (see Figures 5.5 and 5.6).

5.1.1.4 Array Cooling System

There are two design options for cooling the focal plane array to the desired 170 K temperature:

1. Dual APD Cryotiger closed-cycle coolers

2. Liquid nitrogen (LN2) dewar.

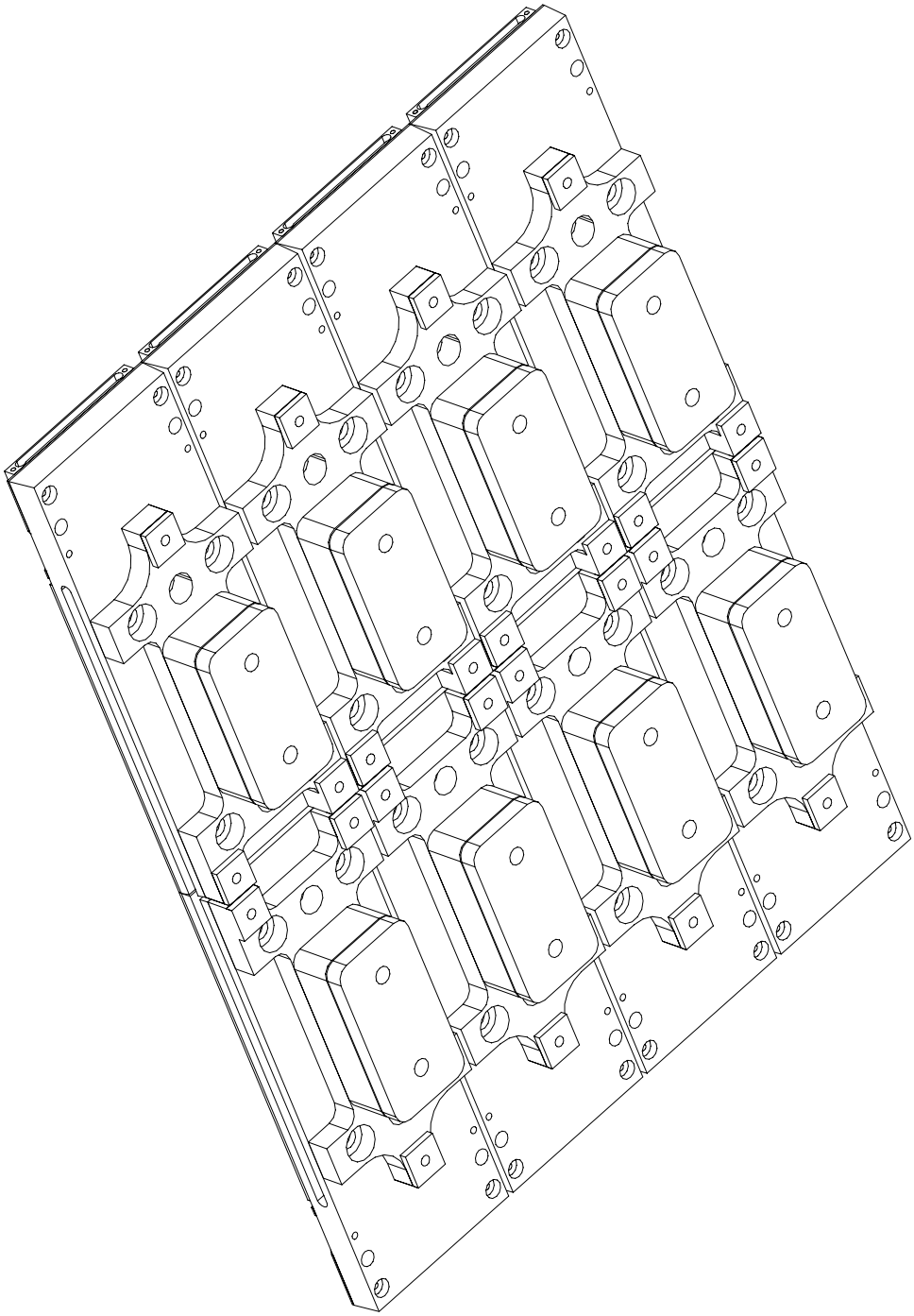

Figure 5.4: Isometric view of the focal plane.

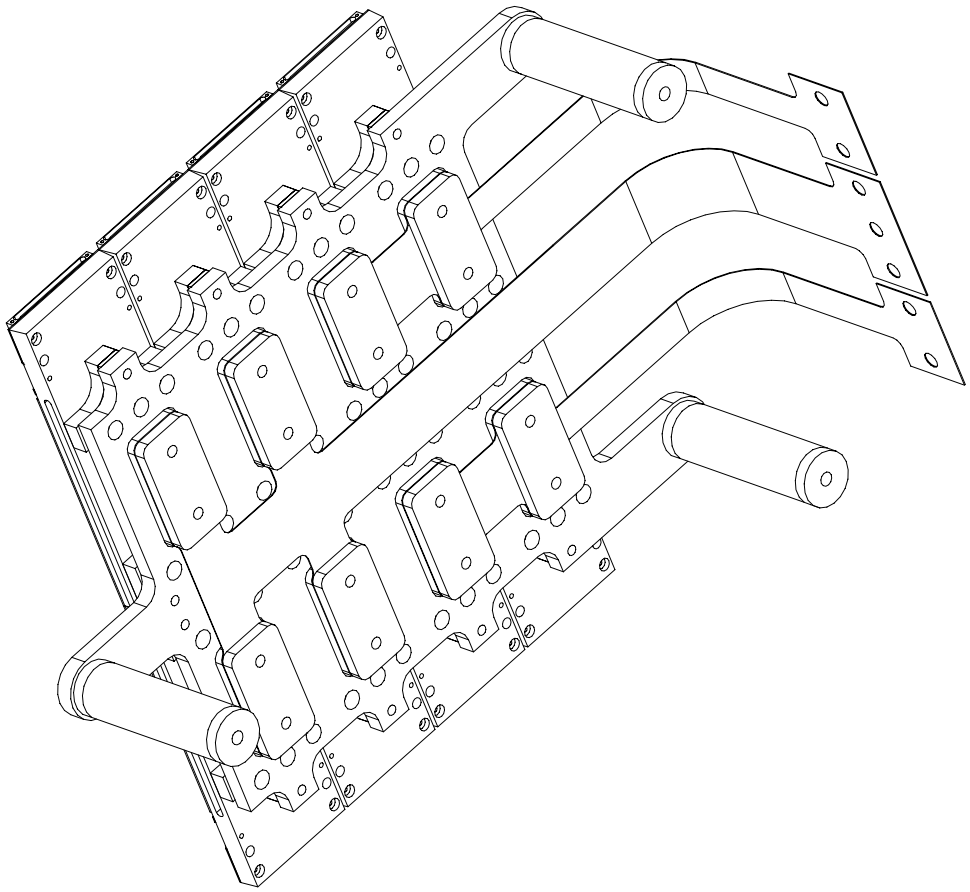

Figure 5.5: Isometric view of the focal plane mounting.

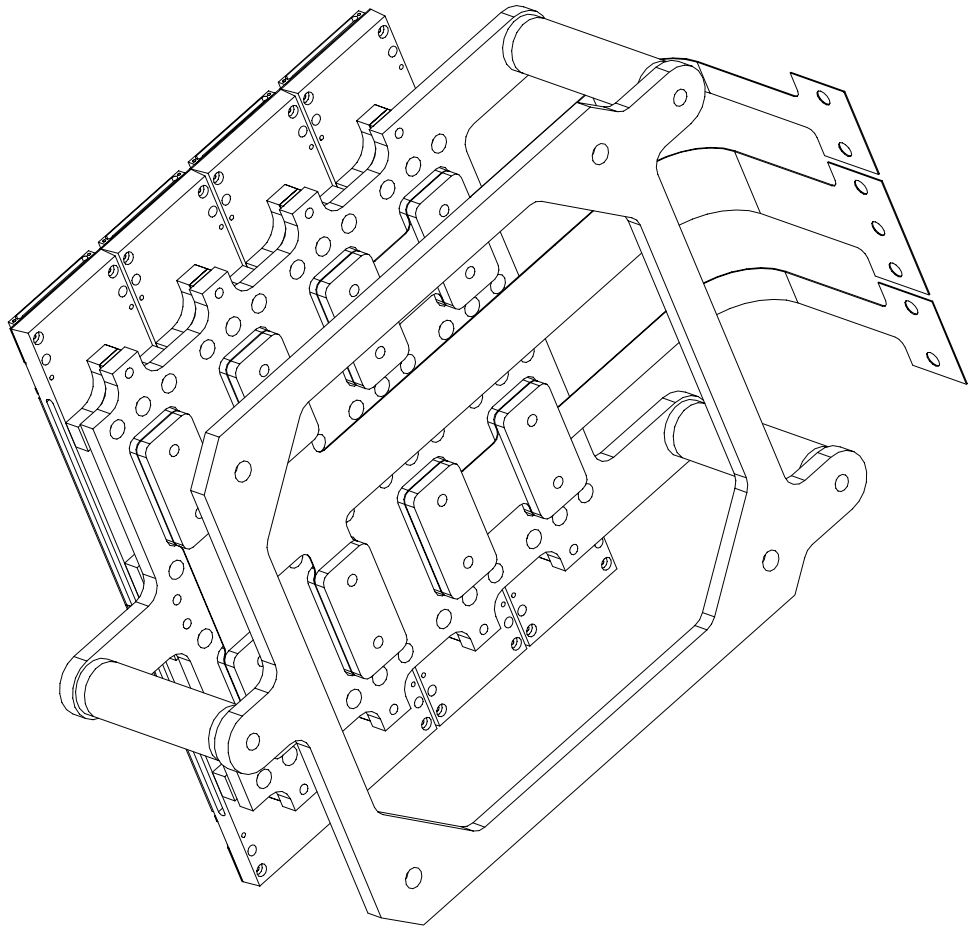

Figure 5.6: Isometric view of the focal plane mounting.

Each of these options is discussed below.

1. Dual APD Cryotigers

   The Cryotiger closed cycle coolers made by APD Cryogenics are ideal for this application. Their specifications claim they can cool a 10W load to approximately 100K depending on the gas mixture used. The coolers have no moving parts in the cold head, and so do not present serious problems with vibration. The compressors are compact, can be located 50 m away, and only dissipate 500 watts. MTBF is 100,000 hours.

   Calculating the heat load on a focal plane like this is difficult. If the proper flex cables and G10 stand-offs are used, the mechanical heat load can be limited to 1-2 watts. The remainder of the heat load is dominated by the thermal radiation on the focal plane, and depends on the various emissivity constants used and the details of the geometry. A straightforward way to estimate the load is to consider the actual performance of similar instruments. The total thermal load on the CFH12K is approximately 15 watts (based on the hold-time of the LN2 dewar used on this camera). The CFH12K focal plane is 50% larger than the IMACS focal plane, but is otherwise very similar in its thermal properties. Thus the IMACS camera should have a heat load of approximately 10 watts. Although according to the APD specs, it should be possible to achieve 170K with this load with a single Cryotiger cooler, the design has been developed to use two of these coolers to insure that performance is not marginal.

   The two coolers attach to a mounting plate that in turn bolts to one of the access ports on the side of the square camera body. There is a copper bar that attaches to the cold heads of the coolers. The copper straps from the focal plane are clamped to this copper bar. A temperature sensor will also be mounted to this bar to allow monitoring of the Cryotiger base temperature. The copper straps have their width and thickness adjusted (empirically) to bring the focal plane temperature to within 5-10 degrees of the desired operating temperature. Additional regulation is accomplished with the focal plane heater resistors. Various views and details of the coolers can be seen in Figures 5.1,5.2 and 5.7.

2. LN2 dewar

   The focal plane can also be cooled with a conventional LN2 dewar. The mechanical restrictions to the thickness of the camera, however, require that the LN2 dewar not

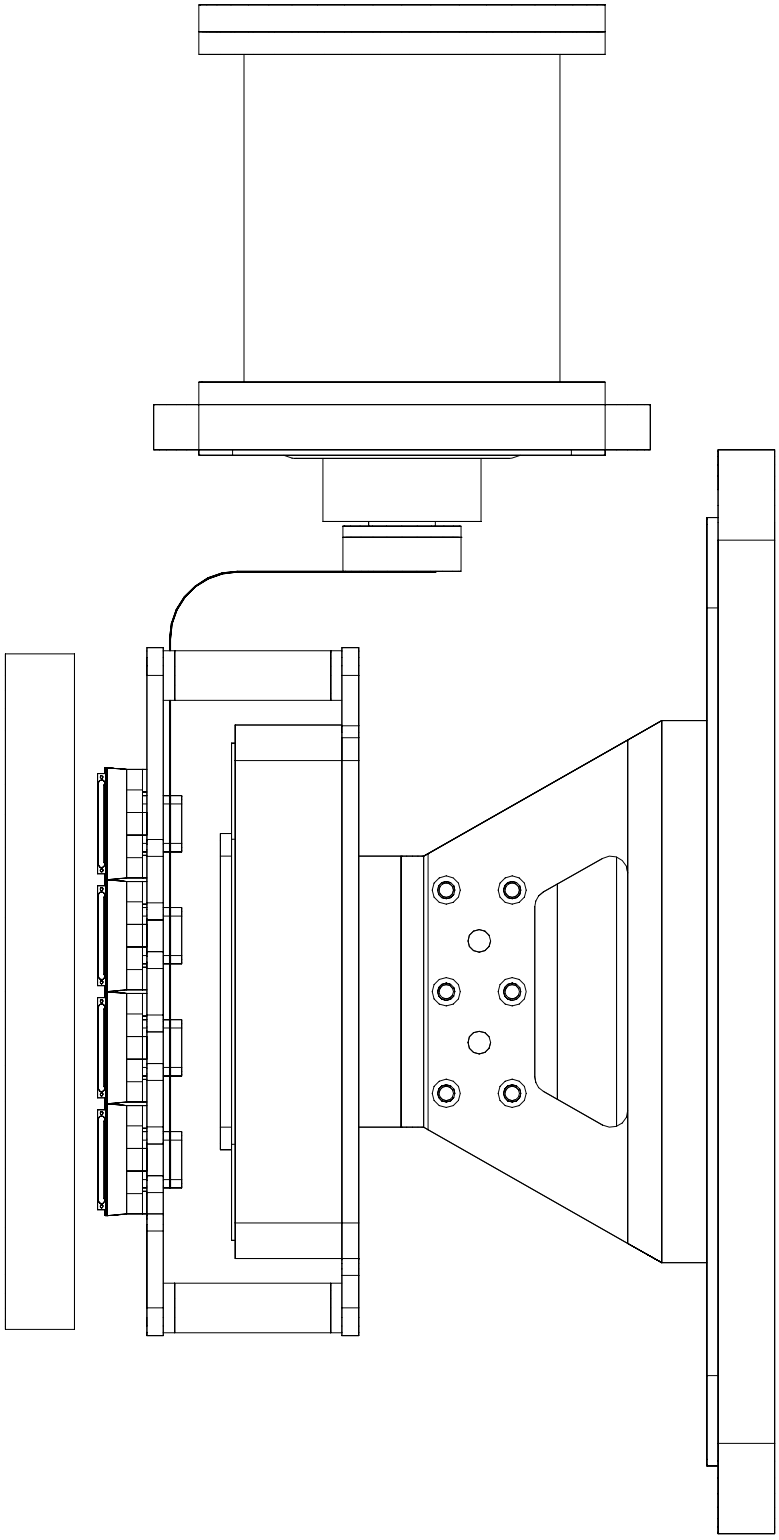

Figure 5.7: Side view of the dewar interior.

extend out the back of the camera, but rather to the side. This is, in fact, the preferred arrangement for this camera because of the XYZ stages which would make a back-mounted dewar problematic. The LN2 dewar is being designed so that it can be interchanged with the dual Cryotiger cooler by simply removing one mounting plate and attaching another. In order to achieve the desired hold time, the dewar will have to be substantial. LN2 has a heat capacity of 160 J/ml. A heat load of 10 watts requires 7.2 liters of LN2 to achieve the hold time goal of 30 hrs. Considering that this is the volume of the can when only *half* full, this leads to a fairly sizable dewar whose internal LN2 tank is a cylinder approximately 200mm diameter and 400mm long! The size and weight of this dewar may be objectionable.

5.1.2 Flexure Control

5.1.2.1 X–Y Translation Stage

The flexure compensation mechanism has been designed to use an off-the-shelf XY stage from Polytec PI (model P-517.2CL). This stage is a 2-axis piezo-driven unit with 200 μm travel in each direction and a resolution is 2 nm, well in excess of the requirement. The stage measures 150mm x 150mm and weighs 1.4 kg. It has a load capacity of 5 kg and can be provided suitably prepared for high vacuum operation. Polytec PI can also provide an electronics unit for closed loop control of the stage. This controller can be interfaced to a host computer through a serial port. The cost for the vacuum prepared stage and controller is approximately $30K.

The XY stage cannot be operated at cryogenic temperatures, so the focal plane needs to be thermally isolated from the stage. The current design has the focal plane mounting plate suspended above the stage via three G10 fiberglass stand-offs. The stand-offs attach to an adapter plate under the outer perimeter of the XY stage and every effort is made to get the center of gravity of the focal plane as close to the stage as possible. Counterweighting of this point is possible to bring the CG within the body of the stage (if this proves to be necessary). The focal plane components (sub-packages and mounting plate) have been designed so as to minimize the weight of this assembly. The present focal plane assembly (including CCDs) has a mass of approximately 2.5 kg. The XY stage attaches to the Z-axis focus stage (described

below) in the following manner. The XY stage has a square central hole that goes all the way through the stage. This hole slips over a mating boss that is part of the Z-axis flexure, and is is rigidly clamped from above (see Figure 5.8).

5.1.3 Array Z-axis Focus Stage

The array focus stage is based on a flexure design used in the Gemini Near Infrared Imager (NIRI) instrument. NIRI uses two similar flexures to move the wavefront sensor and the science detector array. The NIRI design must function at cryogenic temperatures, whereas in this design, the flexure is mounted to the camera back plate and is at ambient temperature. The flexure is quite substantial and has a high degree of stiffness in the X and Y directions (with Z defined as the direction along the optical axis). As designed, the stage has the desired ± 1mm range, and is wire-EDM machined out of a single block of titanium (see Figures 5.8 and 5.9).

The focus stage will be actuated by a 1mm pitch ball screw driven by a Phytron stepper motor operating inside the camera head. The ball screw is supplied with ceramic balls and is cleaned and prepared for vacuum use. Phytron can supply stepper motors qualified for very high vacuum (several orders of magnitude lower than is needed for this instrument) as well as for cryogenic operation. This approach has been used quite successfully in NIRI and other astronomical instruments, and is preferred over an arrangement where the motor resides outside of the cryostat and must be coupled to the internal mechanism through some rotary feed-through. The exact gearing for the focus assembly is still being worked out, but the motor will likely be coupled to the lead screw through a gear train with a reduction of at least 5:1. The stepper motor will be a conventional type with 200 steps per revolution, so a single step will correspond to a linear motion of 1 μm. If an absolute encoder is required, one can be attached as well.

Control of the motor is straightforward. Any stepper motor controller (with micro-stepping capability) can be employed.

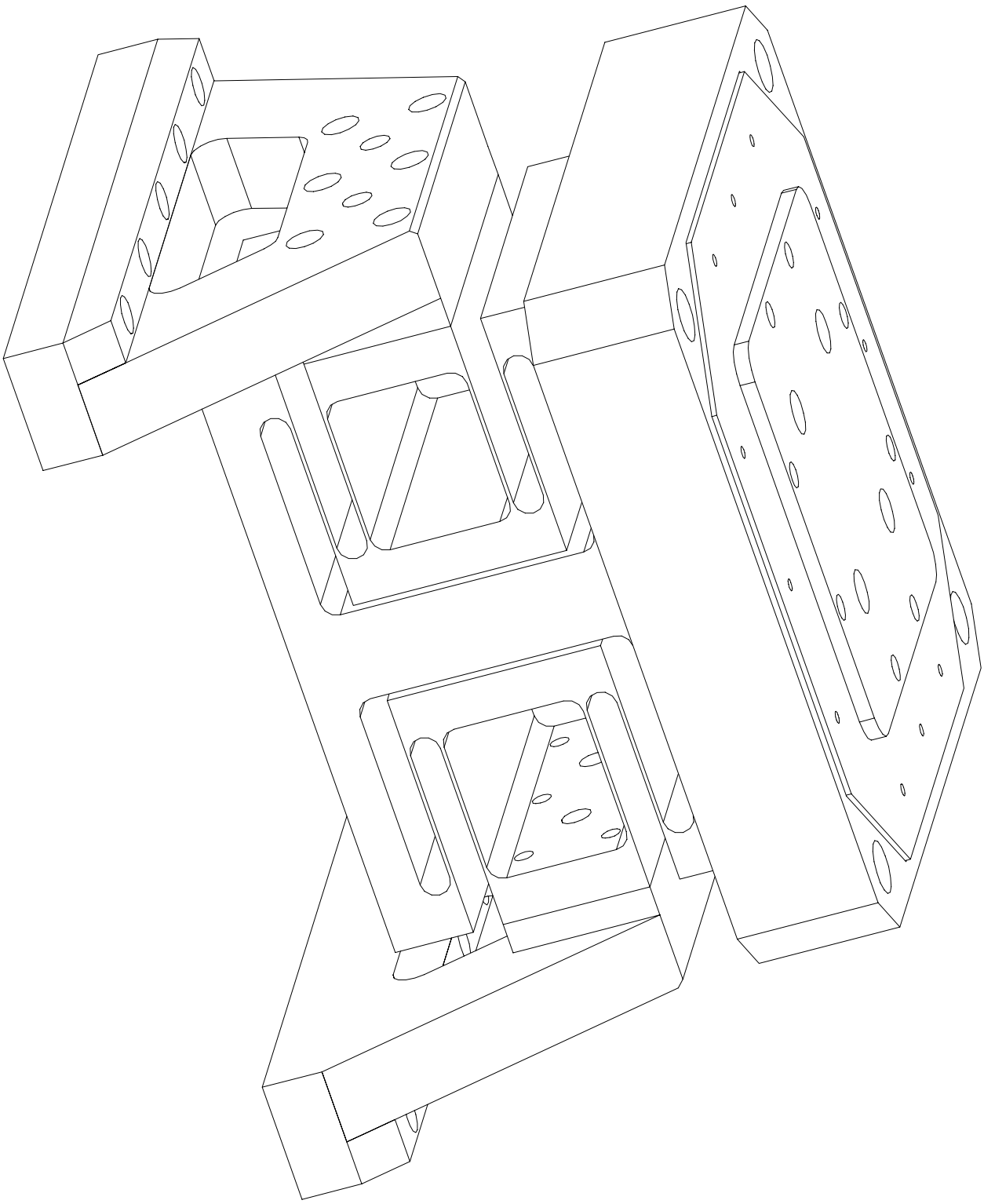

Figure 5.8: Isometric view of the flexure control and focus stages.

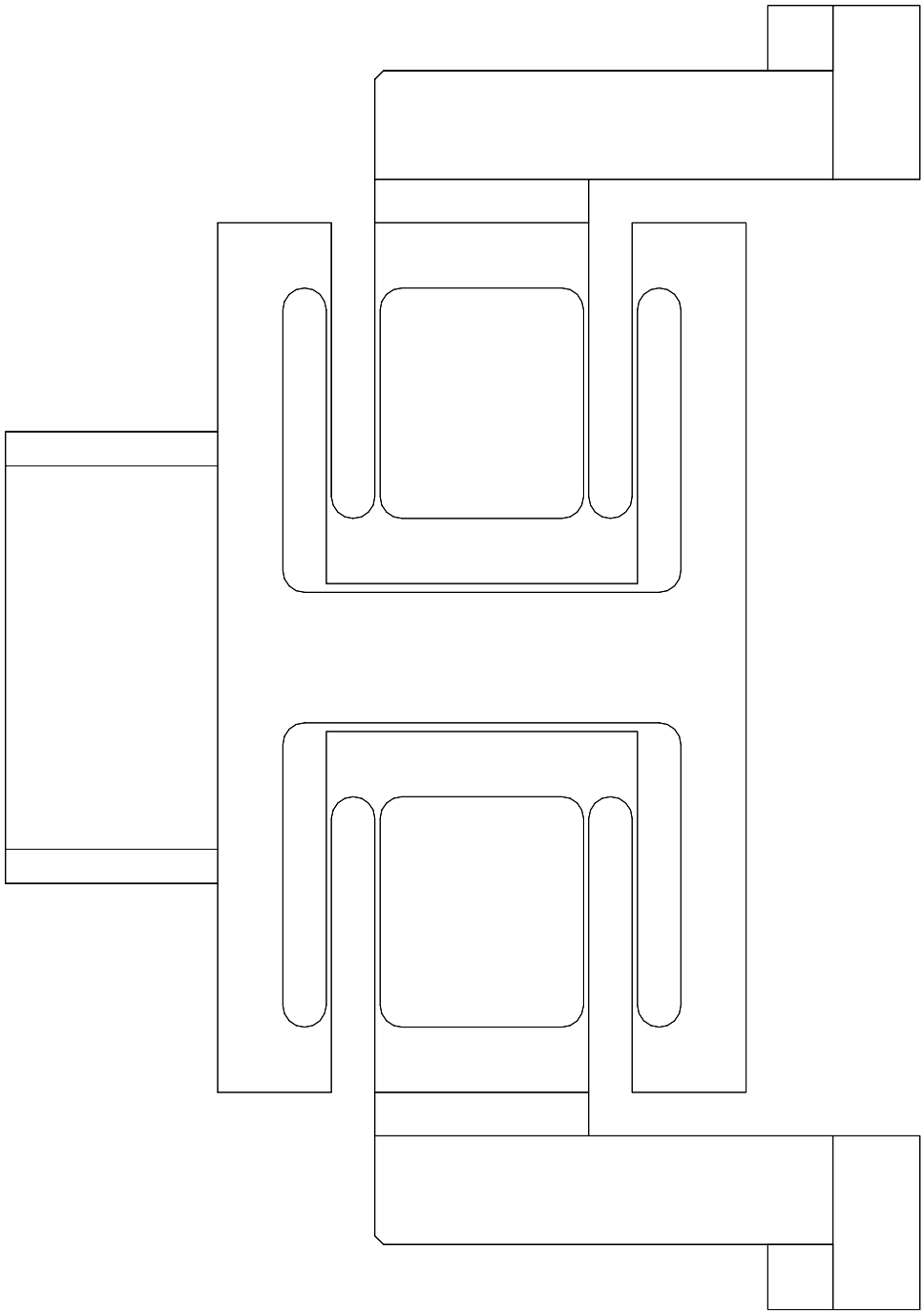

Figure 5.9: Side view of the Z-flexure stage.

5.2 CCD Mosaic Controller

The IMACS mosaic detector consists of an array of eight SITe CCD detectors, a CCD controller to operate the detectors and a host PC to interface with the controller.

Preliminary documentation is on-line at http://www.ociw.edu/~burley/ccd/base.html.

5.2.1 CCD Controller Mechanical Design

The CCD controller electronics consists of seven circuit boards

- 1 DSP timing generator board
- 2 Signal processing boards
- 2 Clock driver boards
- 1 Power supply board
- 1 Backplane board

in an enclosure with dimensions of 5.25″ x 8.0″ x 11.0″.

Each of the circuit boards is VME-sized. There is room in the enclosure for a fan, if necessary. The cables which connect to the dewar will come from the backplane, not from the individual circuit boards.

Inside the dewar there are two preamplifier boards. There may be a flex interconnect board in the dewar as well.

Figures 5.10, 5.11 and 5.12 show the arrangement of the detector system.

5.2.2 CCD Controller Electronics

The design of the CCD controller is based on a digital signal processor (DSP), providing software programmable timing, binning, clock voltages, and so on. The design is a super-set of the guider camera design, with the same basic architecture and many of the same circuit designs.

The CCD controller is ideal for an eight detector mosaic CCD array. The CCD clocking sequences are generated by the digital-signal processor. All of the detectors are clocked in lock-step. The controller provides independent, software programmable parallel and serial

clock voltages for each detector. Other programmable features include the exposure time, binning, clock timing, signal processing gain and offsets. The controller has eight 16-bit signal processing channels, each capable of 500 kpix/s conversion rates. Each chip has an individual temperature monitor, and programmable heater current. The digitized image data is transferred by an 80 Mbps optical link to a PCI interface in the host computer.

The controller provides a signal to trigger an external shutter. The standard readout time for the array is 50 seconds. The electronics dissipate 40 watts.

5.2.3 Computer interface

Operation of the IMACS detector and the display of the CCD images is split among two computers – a Linux-based PC, and a Sparc workstation running Solaris. The two computers are linked by a high speed ethernet connection.

The linux PC is dedicated to low-level functions of operating the controller. It sends commands and control codes to the controller DSP, and receives and formats the digitized image data. It is linked to the controller by an optical fiber interface.

The Sparc workstation is used to interact with the user (via a graphical interface), to display and manipulate the images, and to write them to disk.

The interconnect between the controller electronics, the dedicated PC, the Sparcstation, and the telescope system is shown in Figure 5.13.

5.2.4 Controller Software

The DSP software directly operates the CCD controller electronics. The DSP generates the parallel and serial clock waveforms. It writes to the digital-to-analog converters to set the voltages for the CCD clocks. It provides the sequencing for the signal processing to read out each pixel. And, it multiplexes the image data from the eight analog-to-digital converters onto the optical link.

The Linux PC software provides the low-level interface to the controller. The PC down-loads the program code into the DSP, at start-up. Additional data is loaded into the DSP to specify the size of the array, binning, clock voltages, and the sequence of operations. The DSP

sends the image data to the PC as it is read from the detectors via an optical fiber interface.

At the PC, the optical fiber link terminates on a PCI-bus peripheral card. There is a Linux device driver which operates the PCI card, and interfaces it to the operating system.

The controller PC software receives and buffers the digitized image data. If necessary, it can perform basic formatting, such as reversing the pixel ordering per line. The PC exports the images to the Sparcstation, where they are displayed and written to disk.

The user will select the operating mode of the controller from a graphical user interface. Besides the obvious parameters of exposure time and binning, the interface will permit the selection of a fast readout mode (2 μs/pixel), a standard mode (5 μs/pixel), and a slow, low-noise mode (10 μs/pixel), depending on acceptable read noise values. The controller software will then set the offset level automatically. Separate control of the signal processing gain (low or high) will also be possible.

A separate engineering graphics interface will control adjustment of clock voltages, timing of the clock waveforms, and analog-to-digital converter voltage offsets, for example.

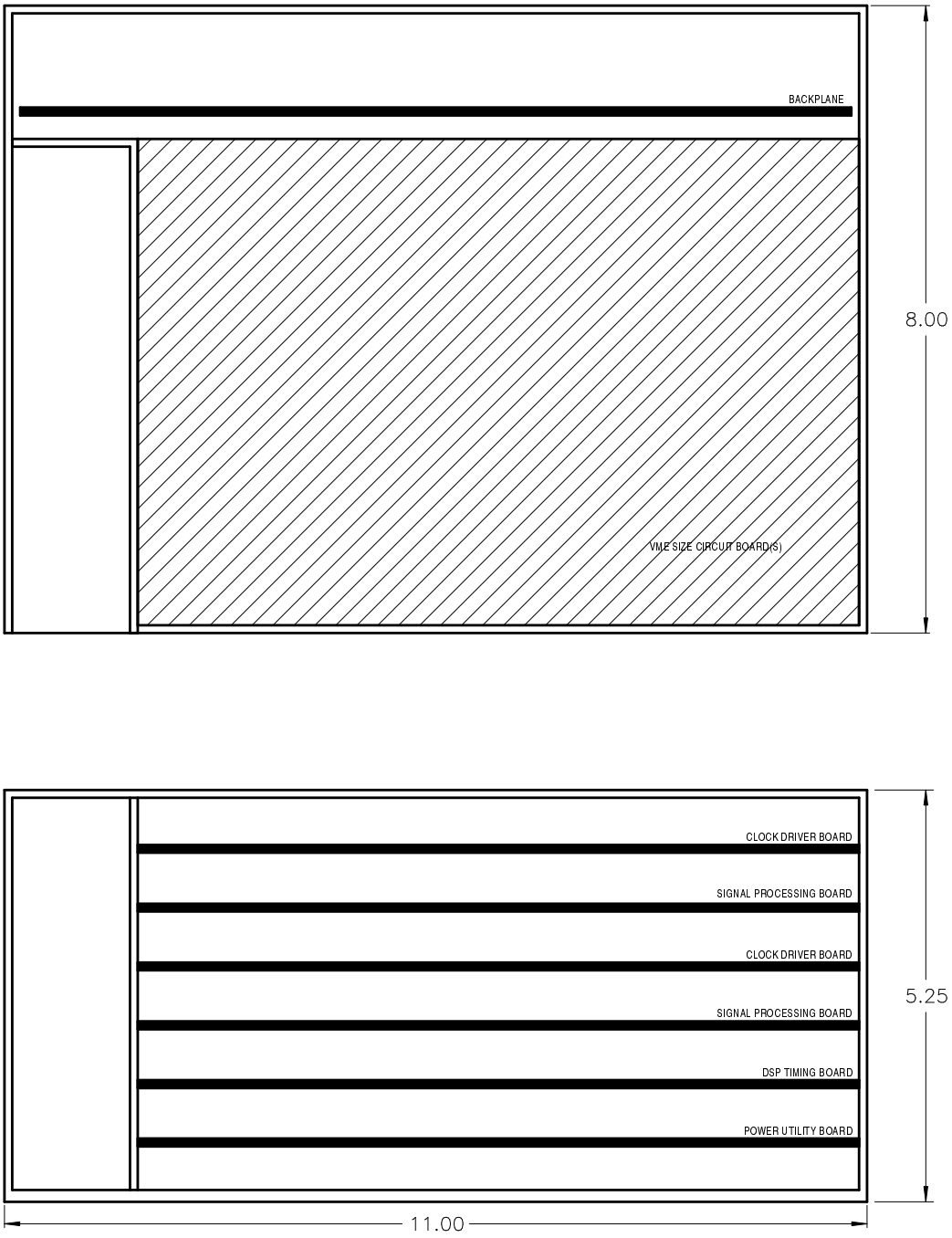

SKETCH OF CCD CONTROLLER ENCLOSURE

Figure 5.10: Sketch of CCD Controller Enclosure.

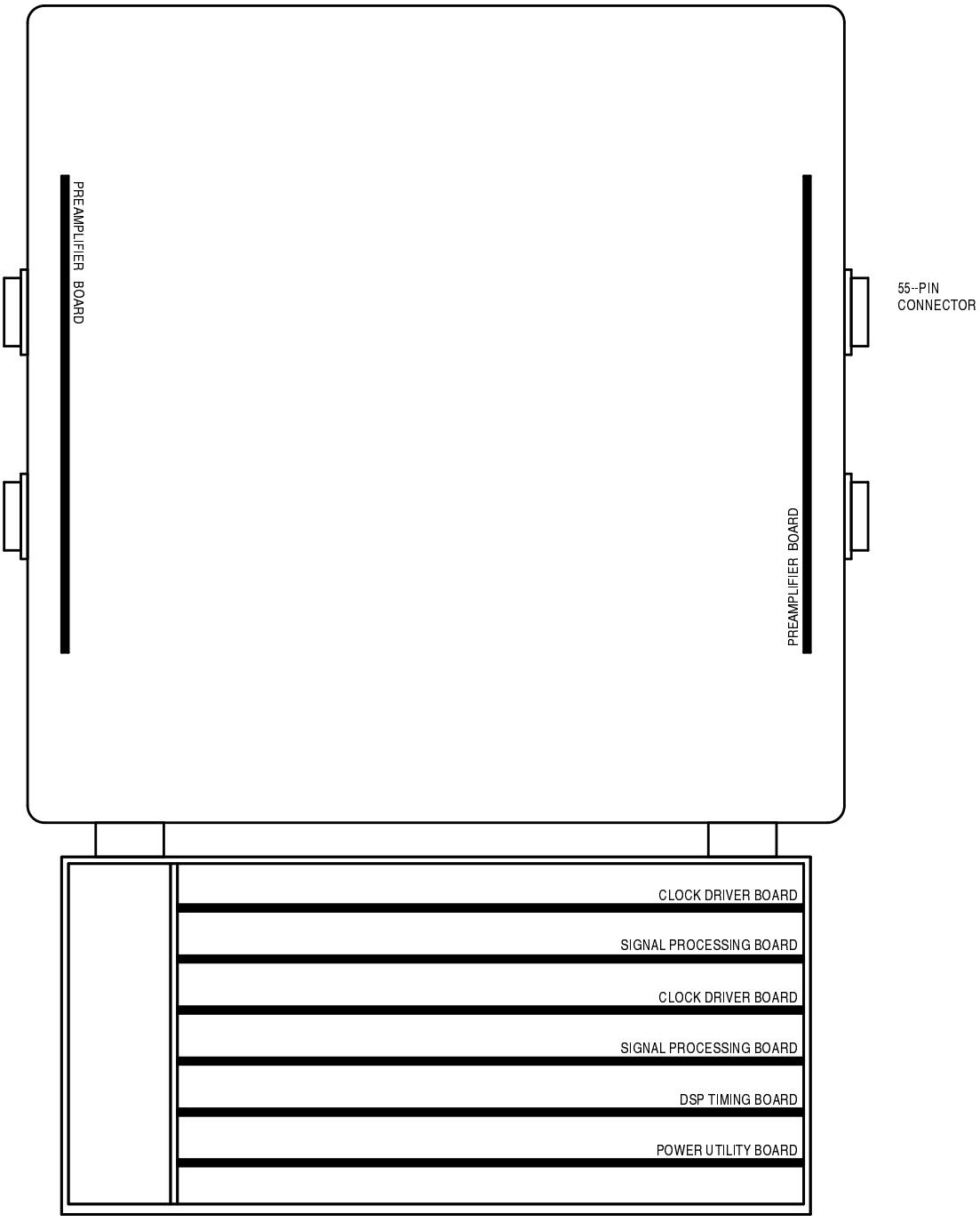

Figure 5.11: Sketch of Preamplifiers and Connectors – Option A.

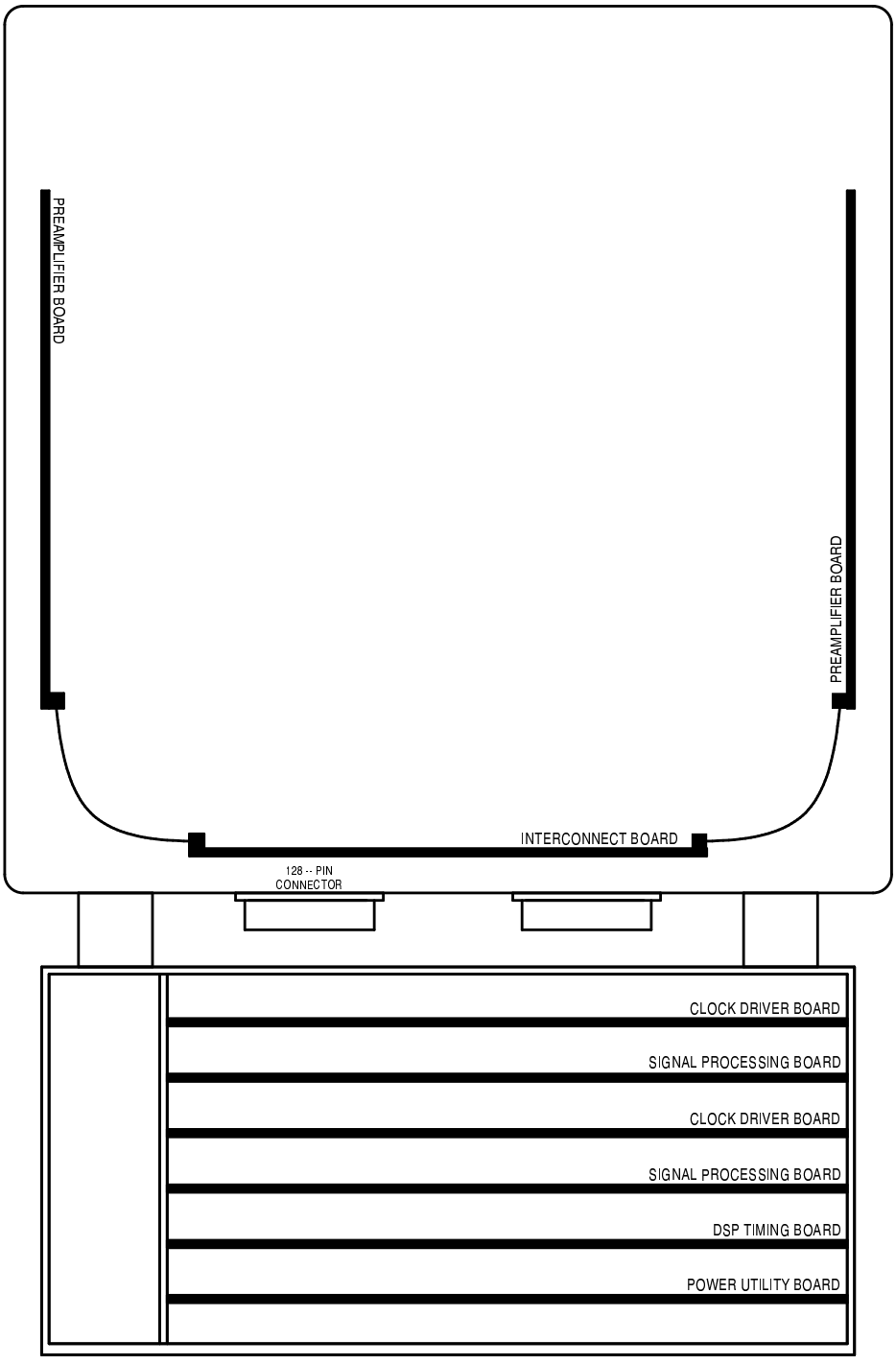

Figure 5.12: Sketch of Preamplifiers and Connectors – Option B.

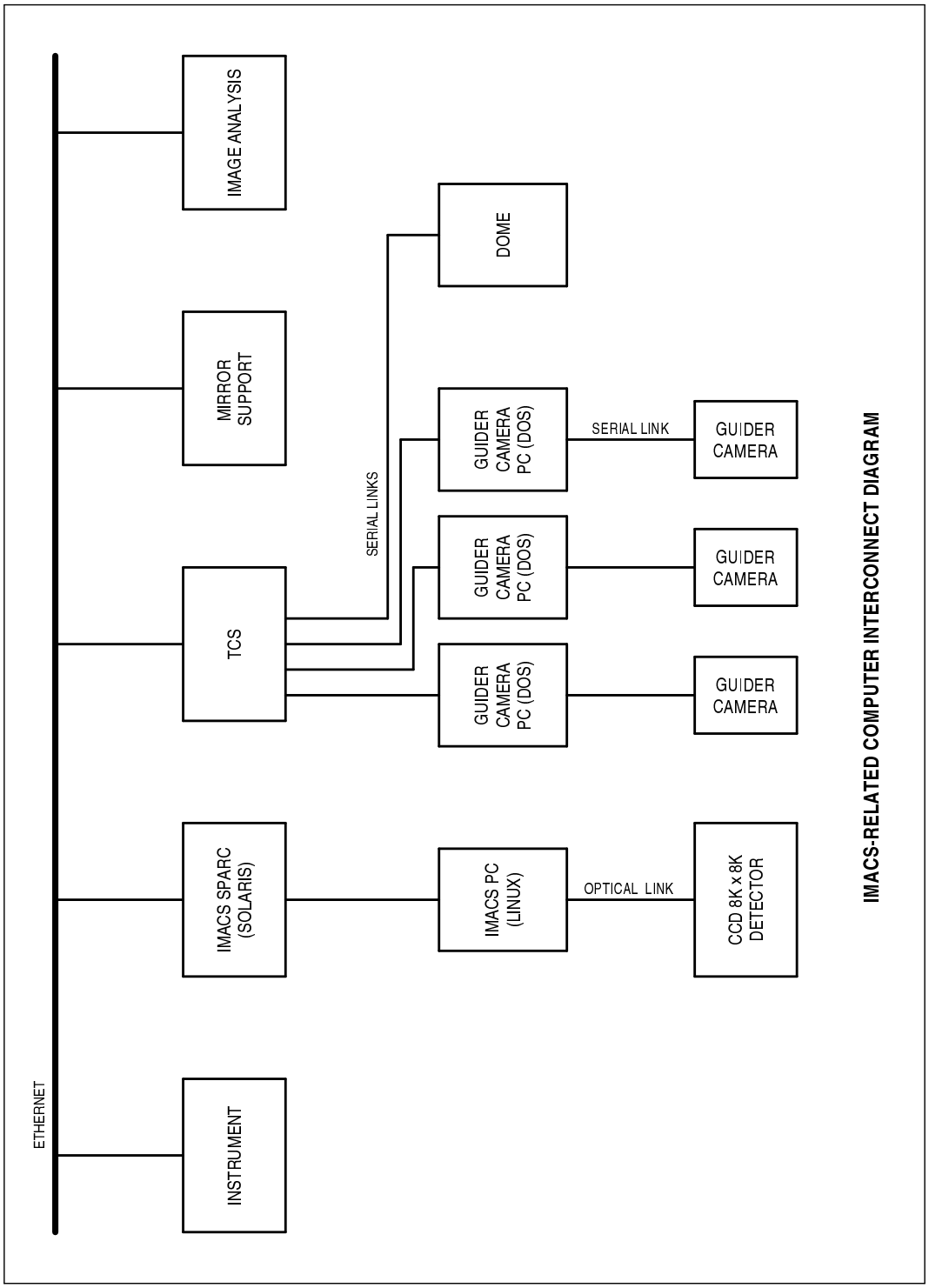

Figure 5.13: IMACS Mosaic Camera Interconnect diagram.

Chapter 6

Preliminary Motion Control Electronics Design

6.1 Introduction

It is the job of the Motion Control System (MCS) to do the positioning and maintain the status of the many motors and actuators incorporated in the IMACS instrument. The MCS is the interface between the instrument computer (SparcStation) and the hardware that moves the various elements in the instrument. It handles the low level tasks associated with running motors and monitoring sensors in the instrument and converts them to high level commands, easing the task of writing and maintaining the software for the instrument computer.

6.2 Design Philosophy

6.2.1 Maintenance

It is easy to put together a motion control system and make it function in the lab environment. One of the more challenging aspects of a system like this is to keep it operational at the telescope site, several thousand miles from the lab. The MCS is being designed to be quick and easy to maintain. For this reason, off-the-shelf hardware will be used whenever possible. It is also very desirable to use hardware that is of the same type as that used in the Magellan Control

System so that the spare parts inventory is minimized, and so the technicians responsible for maintaining the system have some familiarity with the hardware. To assist the technician in the event of a hardware failure, the system is being designed to be very modular and to include LED indicators showing bit level status of each module. It is hoped that a technician familiar with the system will be able to localize problems simply by observing the LED's and replace a module to quickly get the system up and running. It is possible that diagnostic software could be written to further aid the technician in maintaining the system.

6.2.2 Thermal Concerns

Do to the close proximity of the MCS to the instrument another design goal should be to keep power dissipation to a minimum. The control tasks for the instrument do not require high speed processing so a slower, low-power computer can be used to reduce heat. Because the motors and their drivers dissipate the greatest amount of power, they will be switched off whenever possible to further reduce heat near the instrument. Any remaining heat dissipated by the control electronics can be ducted away into the telescope plenum or removed with chilled liquid. Both are available close to the instrument.

6.2.3 Safety

The software and hardware should be designed to prevent the instrument from damage in the event of communication errors received from the instrument computer. The MCS software should also do "sanity checks" continuously and shut down the system if a malfunction is detected. For example if a motor does not get to a commanded position in a set length of time. A watch dog timer should be included in the MCS computer to detect hardware and software errors there. If any errors are detected, the motion power will be removed and the computer reset.

After rebooting, the computer will notify the instrument computer that a reset has occurred, and report the current state of the instrument. It will then wait for user input before resuming normal operation. It should take no more then 10-20 seconds for the system to become operational again after an error condition is detected. A reboot due to a hardware or software error should be a rare event and should NOT be a part of the normal operation of

the instrument. A self-reboot will be reported to the appropriate technical personnel.

Another safety concern is the potential danger to personal working near or inside the instrument. All motors and actuators will be powered from the telescopes "Direct power" and the controlling electronics will be wired to the "UPS power". There are emergency stop buttons located through out the dome, if one of them is pressed the direct power is cut off removing power to all motors and actuators, leaving the electronics powered. A local switch, possibly a key switch, will be available for personnel to disable all motors and actuator during maintenance operations.

6.3 System Architecture

6.3.1 Motion Control Interface

The MCS serial interface is the communication link to the instrument computer. This interface will consist of an RS485 serial link running from the MCS computer on the Nasmyth platform through the telescope cable wrap to the instrument computer in the control room. Under normal operating conditions all motion commands to the instrument will occur over this serial link. RS485 was chosen because it is relatively immune to electrical noise and because it is easily supported when writing software in the DOS environment. The serial command structure to the MCS will consist of ASCII characters that can easily be interpreted with any computer. An example of a typical command, in this case OPEN HATCH, might have a format something like this: (OH<cr>), the characters "OH" followed by a carriage return. The MCS would respond to the instrument computer that the command will be carried out, or with an error message, if the command can not be carried out. It will not be necessary for the users to know all the commands. The GUI will have a button or some other graphical icon that the user will press in order to open the hatch. All the ASCII commands to the MCS will be transparent to the user.

6.3.2 Software

The system software has two main components, the operating system and the motion control program. Unlike the operating systems in the other computers for the IMACS instrument, the

MCS operating system needs to hand complete control of the computer over to the control program. This is because the motion control computer must respond quickly to outside events such as a motor coming to a limit switch. For this reason the DOS operating system was chosen for the MCS computer. DOS has an advantage over more modern multi-tasking operating system in that a program can control every aspect of the computer at all times, giving the motion control program the ability to respond to outside events in a few milliseconds.

The actual control program for the MCS will be written in the C programming language. The program will be written to allow the safe motion of more than one actuator at a time and will display the system's current status on a local display at all times, including the state of all actuators, sensors and motions in progress. The program will also make this information available to the GUI computer. For trouble shooting purposes the program will also keep a log of any errors detected and of the last several hundred motions made by the system. The program will periodically (on the order of 100 ms) generate a signal to the watch dog timer. If the program fails to do this it is an indication the computer hardware or the software has encountered a problem, the watch dog timer will then reset the computer and disable the motion drivers until the computer is running properly again.

6.3.3 MCS Computer

The MCS computer will be a 50 to 100 MHz Intel 486 based system with at least 5 ISA type slots and 3 PCI slots. The computer will contain the following eight hardware elements.

1 Mother board described above.
1 Hard drive for system development.
1 VGA video card and monitor for system devel. and local system status display.
1 Floppy disk drive for system back up.
1 Serial IO card for communication to the GUI computer.
3 Indexer cards for stepper motor control.
1 Parallel IO card for Pneumatic control.
1 Watch dog timer card for system error detection.

Only the last four will be described in any detail because the others are fairly self-explanatory.

The computer will hold three stepper motor indexer cards; each card controls 4 stepper motors. These cards do a number of things that ease the programming task in the computer. They generate the ramp up and ramp down profiles for the stepper motors and output pulses

to the motor drivers to cause a motion in the system. These cards also monitor the limits and home positions of each motor.

For pneumatic control the system will use one 48 I/O line input/output card. This card will control the pneumatic control valves and monitor the state of the pneumatic actuator limit switches. This card can also be used to operate any other general on/off type of control functions in the future design.

The watch dog timer card monitors the system for error as described above in the Motion Control Software section of this document. If the watchdog does not get a pulse from the computer every 50-500 milliseconds then it removes power to motors and actuators then reboots the computer.

The RAMDISK card is a device that enables the computer to boot up and start running the control program very quickly. It will work by storing the operating system and control program in non-volatile memory. To the computer, the RAMDISK looks like a disk drive, so at boot-up, the computer loads it's systems from memory rather then the hard drive. Boot up time of order 10-20 seconds should be possible.

6.3.4 Input / Output Hardware

The I/O card described above inputs and outputs 5V logic level signals from the computer. Because the control signals to the actuator and from the sensor are generally of a higher voltage and current then the I/O card can deal with, some type of signal conditioning is necessary to protect the card and computer from damage. Opto 22 modules are a good solution to this problem for the following reasons. First, they optically isolate the logic in the computer from the high voltages and currents of the rest of the system. Second, each module has an LED indicator making system checking easier. And third, each output module has a replaceable fuse on its output, for protecting the hardware from overload conditions.

A similar situation is true for the stepper motor indexers in the computer. A stepper driver is needed to translate signals from the indexer to motors. To meet the special need of the five phase stepper motors that are being considered for IMACS, there are few driver manufactures to chose from. The Magellan telescope and the IR camera currently being built use MYCOM Corp. drivers. These drivers have opto isolation and power shut down capability,

making them a good solution to the IMACS motion control needs.

6.3.5 Motors and Sensors

The current design calls for 12 stepper motors in the instrument. To avoid some of the resonance problem associated with conventional 2-phase steppers, the IMACS project is considering 5-phase stepper motors. These come in a wide range of sizes and torques. If back-driving of actuators is a problem they can be ordered with brakes and/or zero back-lash gear reduction. Sensors being considered range from conventional mechanical limit switches to electronic proximity switches. More work will be needed to further refine the system requirements before this selection process can be completed.

6.3.6 Pneumatic Actuator Control

The 13 Pneumatic Actuators used in the current design require 13 control valves with 2 solenoids per valve. It makes sense to locate these valves as close to the actuators as possible to help reduce the amount of plumbing in the instrument. Skinner Valve sells a commercial toggling solenoid valve that has been used successfully and extensively for Keck instruments, and it will be used here as well.

6.3.7 Cabling, Connectors and Cable Wraps

Interconnecting cables should be Teflon insulated and large enough to avoid braking at terminal block and solder points. Typically the smallest wire to use in a terminal block is #16. Professional quality electrical wiring practices will be used throughout the instrument. The standard connectors used in Magellan have been the Bendix mil-spec SP series. These are recommended for most of the interconnections in the instrument. The cable wrap needs have not been identified at this time, but IGUS cable wraps are being used in Magellan and will be used here as well.

6.4 Preliminary Design Schematics

The following figures are included here for reference.

Fig. 1 System Architecture Block Diagram
Fig. 2 Rack Mount Layout
Fig. 3 Stepper Limit Chassis
Fig. 4 Stepper Driver Chassis
Fig. 5 Pneumatic Control Chassis
Fig. 6 Motion Control Computer Chassis
Fig. 7 Hatch Block Diagram
Fig. 8 Principal TV Scan Block Diagram
Fig. 9 Principal TV Filter Block Diagram
Fig. 10 Principal TV Insert Block Diagram
Fig. 11 SH TV Scan Block Diagram
Fig. 12 SH TV Insert Block Diagram
Fig. 13 CF TV Insert Block Diagram
Fig. 14 Mask Select Block Diagram
Fig. 15 Mask Insert Block Diagram
Fig. 16 Mask Lock Block Diagram
Fig. 17 Dewar Focus Block Diagram
Fig. 18 Flexure Control Block Diagram
Fig. 19 Disperser Select Block Diagram
Fig. 20 Grating Tilt (1) Block Diagram
Fig. 21 Grating Tilt (2) Block Diagram
Fig. 22 Grating Tilt (3) Block Diagram
Fig. 23 Filter Select (1) Block Diagram
Fig. 24 Filter Select (2) Block Diagram
Fig. 25 Filter Insert (1) Block Diagram
Fig. 26 Filter Insert (2) Block Diagram
Fig. 27 Shutter (1) Block Diagram
Fig. 28 Shutter (2) Block Diagram
Fig. 29 Parts List

Chapter 7

Instrument Control Preliminary Design

7.1 Introduction

The IMACS control system is responsible for controlling the IMACS instrument. It serves as the interface between observer and all IMACS related hardware (e.g., science array, motion controllers and guiders).

7.2 Control Functions

There are automated features in the instrument which are either motor-driven or toggled by air cylinders. Table 7.1 lists the automated functions and the numbers of motor/encoder units, high-resolution (HR) encoders, air solenoids, fiducials, limit switches, and the type of motion required to provide those functions. Figure 7.1 shows a schematic representation of the instrument control functions.

7.3 Design Philosophy

All code for the IMACS control system will be written in ANSI C and run under both Linux and Solaris. All graphical components will make use of the X11 libraries without any special extensions to ensure high flexibility and compatibility over all platforms.

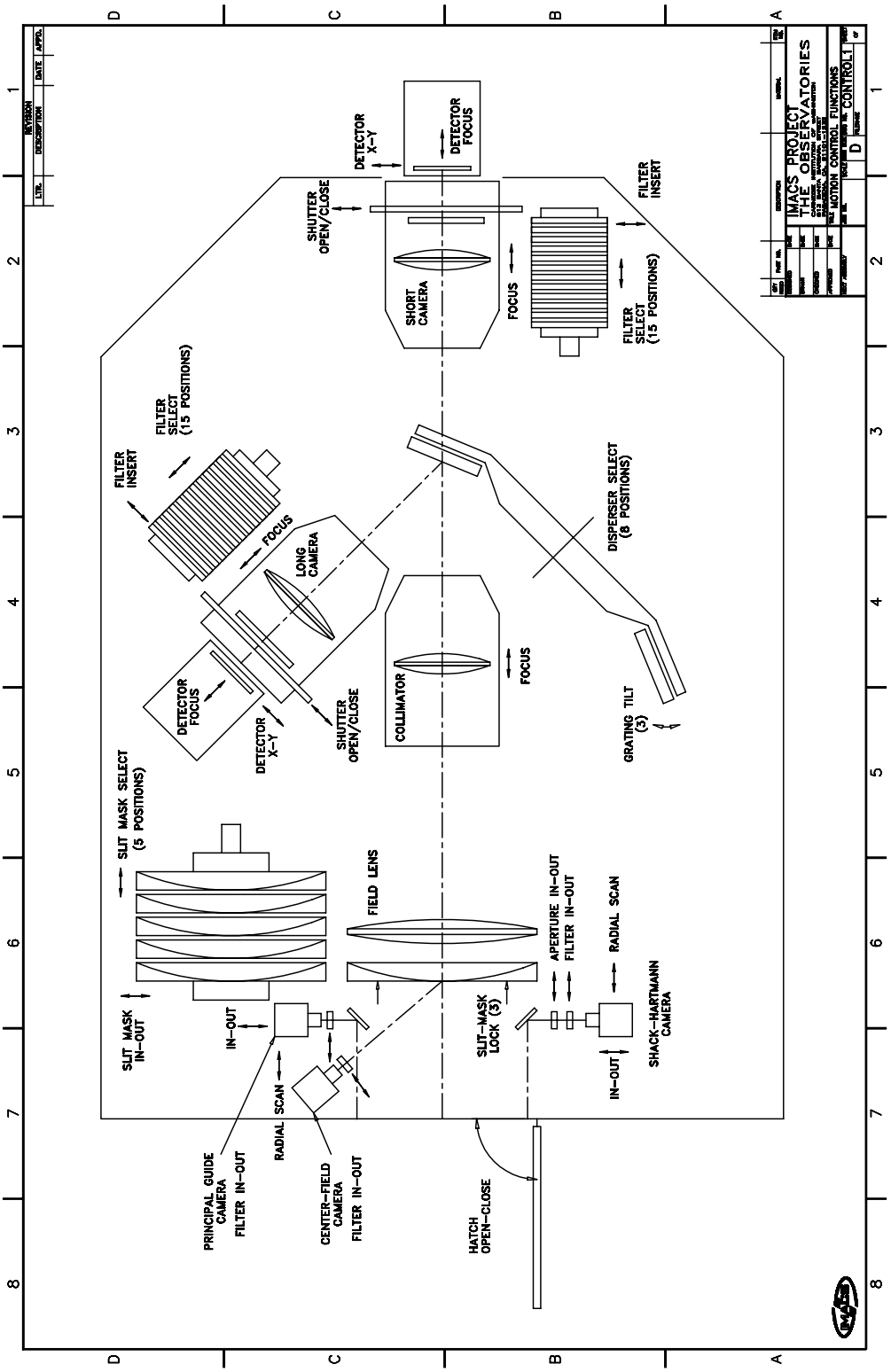

Figure 7.1: IMACS control functions schematic.

Stage	Mot/Enc	HR Enc	Air Sol	Fiducial	Limits	Motion
Hatch			1		2	op/cl
Pr. TV scan	1			1	2	cont.
Pr. TV filter			1		2	in/out
S-H TV scan	1			1	2	cont.
S-H TV insert	1			1	2	in/out
S-H TV filter			1		2	in/out
S-H Direct/S-H			1		2	in/out
C-F TV filter			1		2	in/out
Mask select	1			1	2	cont.
Mask insert			1	1	2	in/out
Mask lock			1		6	on/off
Dewar Focus	1			1	2	cont.
Flexure contr.	1 + 2 PZT			1	2	cont.
Disperser Sel.	1			1	2	cont.
Grating Tilt 1	1	1		1	2	cont.
Grating Tilt 2	1	1		1	2	cont.
Grating Tilt 3	1	1		1	2	cont.
Filt select (2)	2			2	4	cont.
Filt insert (2)			2		4	in/out
Shutters (2)			4		8	op/cl
Totals	13	3	13	14	52	

Table 7.1: Control Functions.

7.4 System Architecture

The IMACS control system consists of four largely independent modules. They are

- Science Array Control
- Guider Camera Control
- Instrument Motion Control
- Environmental Status

Each module stores its status in a common database. This database allows each module to retrieve status information about other modules while keeping interfaces between modules as simple as possible. Communication between all IMACS control system modules will be done over TCP/IP sockets. This allows for maximum flexibility and compatibility between operating systems, since the IMACS control system will be spread over a number of computers all connected by a local area network (LAN). See Figure 7.2 and Figure 7.3.

7.4.1 Science Array Control

The Science Array Control graphical user interface (GUI) will run on a Linux PC (see Figure 7.2) and display its window on a monitor (#1 in 7.2) connected to the SparcStation.

The GUI will provide the following functions: - set exposure time - set readout mode (e.g., subraster, binning, operating mode (see Controller Software Chapter 5) - set filename (FITS) - set object name (written into FITS header) - run command sequences (macros) - provide status information about data acquisition (e.g., time to finish exposure, free disk space) - TBD

The data files will be written in FITS format, one for each of the eight chips. The filename convention is

`PREFIX_####_C#.FITS`

where '`####`' is a running exposure number, automatically incremented by the control software and '`C#`' designates the corresponding chip.

Detailed information about the science camera system can be found in Chapter 5.

7.4.2 Guider Camera Control

The guider cameras will each be controlled by a PCs running DOS. These computers receive their commands from the Telescope Control System (TCS) over a fast serial line. The IMACS control system will not directly communicate with the guide camera computers but rather through a the TCS over TCP/IP. Limited access to the guider cameras / controllers is necessary to allow automated procedures.

The GUI will provide the following functions: - switch guiding on/off - control integration time, feedback gain, etc. - move cursor - display position, mode, status, etc. - TBD

Detailed information about the guide camera system can be found in Chapter 4.

7.4.3 Instrument Motion Control

The Instrument Motion Control software will run on the SparcStation (Figure 7.2) and display its GUI on monitor-1. The SparcStation will talk via a serial line (alternately, TCP/IP) to a PC

that holds a number of PCI-cards. All stepper-motors, encoders, air cylinders, limit-switches and fiducials will be controlled by this PC. All higher level commanding and safety checking will be done by the SparcStation GUI.

The Motion Control Software allows the user to set up the instrument (disperser, filter, grating angle, etc.) in parallel with safety checks and interlocks to avoid collisions where they may be possible.

Macros will allow the user to store instrument configurations for rapid, reliable changes between modes.

7.4.4 Environmental Control

The Environmental Control GUI will display information about external parameters, e.g., telescope position, dome position, temperatures, etc. These parameters will be stored in the common database and written into the FITS headers of the datafiles. There also will be logfile(s) with a time stamp for each value and graphical output capability.

This information will be used to control instrument settings, where appropriate, for example, to correct effects due to thermal variations.

7.4.5 System Diagnostics

- The IMACS control system will log changes in status of the instrument (see 7.6.2).
- The TCP/IP will allow the running of instrument control modules individually from any remote system, for aid in diagnosing fault conditions.
- A graphical display of the instrument configuration and light path will provide rapid access to deployment of IMACS controls and devices.

7.5 Control Functions

In addition to the functions called out explicitly below, an initialization routine will allow the user to reset all IMACS components into a predetermined "home" state.

7.5.1 Control of Guide Camera Stages

- Principal Guide Camera

  The Principal Guider can be moved over a range of (semi-continuous) angular positions. This movement is done by a stepper-motor and monitored by an encoder and limit switches. The encoder uses a fiducial to define a "home" position. The GUI will make available this motion as a position angle in an edit-box and include a "go to" feature.

  The Principal Guider has a filter that will be moved by an air cylinder. The IN- and OUT-position will each be defined by a limit switch. This function will be implemented in the GUI as a popup menu (in,out).

- Shack-Hartmann Guide Camera

  The Shack-Hartmann Guide Camera can be moved over a range of (semi-continuous) angular and radial positions. These movements are done by stepper-motors and monitored by encoders and limit switches. The encoders use fiducials to define a "home" positions. The GUI will make available these motion as a position angle and radial position in an edit-box.

  The Shack-Hartmann Guide Camera operates in two modes, direct imaging and lenslet array for Shack-Hartmann testing. An air cylinder is used to switch between the modes. The end positions are defined by limit switches.

  The Shack-Hartmann Guide Camera has a filter that will be moved by an air cylinder. The IN- and OUT-position will each be defined by a limit switch. This function will be implemented in the GUI as a popup menu (in,out).

- Center-Field Guide Camera

  The Center-Field Guider is fixed in position in front of the focal surface. It is addressed by a mirror and transfer optics that ride on a stage inserted by the slit mask assembly. The C-F Guider has a filter that will be moved by an air cylinder. The IN- and OUT-position will each be defined by a limit switch. This function will be implemented in the GUI as a popup menu (in,out).

7.5.2 Control of Instrument Hatch

The Instrument hatch in moved by an air cylinder and has 2 positions. Each end position is defined by a limit switch. The Motion-Control-GUI will allow the user to move the hatch but will make a safety check of TBD environmental parameters (e.g. telescope position) and issue a warning if any potential problems are found. This function will be implemented as a popup menu (open,closed).

7.5.3 Control of Slit-Mask Handler

The slit-mask mechanism allows to select, insert and lock an aperture mask. The selection is done by a moving tray (5 positions) driven by a motor/encoder pair. It has a fiducial to detect "home" and two limit switches at the end positions.

When the table has moved to its designated position a mask is moved from the tray into the field of view of the science camera. This function uses another motor/encoder/fiducial and limit switches at both ends.

After the mask is inserted it will be locked by 3 air cylinders controlled by a single air solenoid. The lock/unlock position of the three air cylinders are each defined by two limit switches.

The GUI implements these three functions as a single popup menu offering the following selection: (None, Mask-1, Mask-2, Mask-3, Mask-4, Mask-5)

7.5.4 Control of Disperser Server

The Disperser offers eight positions on a wheel. This wheel is driven by a stepper motor with encoder.

The GUI will implement the Disperser Server as a popup menu offering the following selection (mirror, grating-1, grating-2, grating-3, grism-1, grism-2, grism-3, open).

7.5.5 Control of Grating Tilt Stages

Three positions of the the Disperser Server are used by gratings. The tilt of each of these gratings can be adjusted with a stepper-motor/encoder/fiducial mechanism. There also will be two limit switches at each grating. The GUI will provide an edit-box for each of the grating tilts.

7.5.6 Control of Filter Changers

The Filter Changers are mounted on a moving tray with 15 positions. The tray is controlled by a stepper-motor/encoder/fiducial mechanism. Both ends of the movement range are secured by limit switches.

An air cylinder moves the selected filter into its designated position defined by a set of two limit switches (in/out).

The GUI will provide a popup menu with the following selection (none, filter-1, filter-2,...filter-15).

7.5.7 Control of Science Array Shutter

The control of the Science Array shutter will be done by the Science Array Control Computer (see Chapter 5).

7.5.8 Control of Camera Focus

Control of the camera focus can be implemented within the present design of the lens cell, but is not planned at this time.

7.5.9 Control of Collimator Focus

Control of the collimator focus can be implemented within the present design of the lens cell, but is not planned at this time.

7.5.10 Control of Flexure and Focus

Compensation of instrument flexure is done by two-axis (x-y) piezo control and one-axis (focus stage) stepper motor control of the Science Array mount within dewar (see Chapter 5). Flexure control can be enabled/disabled by the user with a popup menu.

7.6 Data Handling

7.6.1 Quick Look Display and Data Storage

The Linux-PC writes FITS files to a disk at the SparcStation, mounted on the PC via NFS. The FITS header will contain, besides mandatory keywords, a TBD set of environmental and status information from the entire IMACS Control System. This information can be gathered from the common database, where all modules keep their status data.

The Science Array Control GUI updates the database when new files are written to disk. "Quick-look" parameters set by the user will allow rapid assessment of part or all of the science frame, using monitor-2 of the SparcStation (see Figure 7.3).

7.6.2 Logging of Instrument Status

Each module keeps a logfile containing time stamps of all status changes and events and writes actual status information to a common database on the SparcStation.

From this information the complete system status can be reconstructed during an observation or any time later. This will be especially helpful during troubleshooting and test periods of IMACS.

7.6.3 Interface to Telescope

The interface to the telescope control system (TCS) will be done either over a TCP/IP socket or a serial line. Both ways are acceptable in regard to speed since no command (for example, *execute offset*) or status request (for example, *telescope position*) will require sub-second reaction time.

The IMACS Control System will require TBD status information from the TCS. It will also be necessary to command offsets of the telescope and guider cursor position to enable automated sequences.

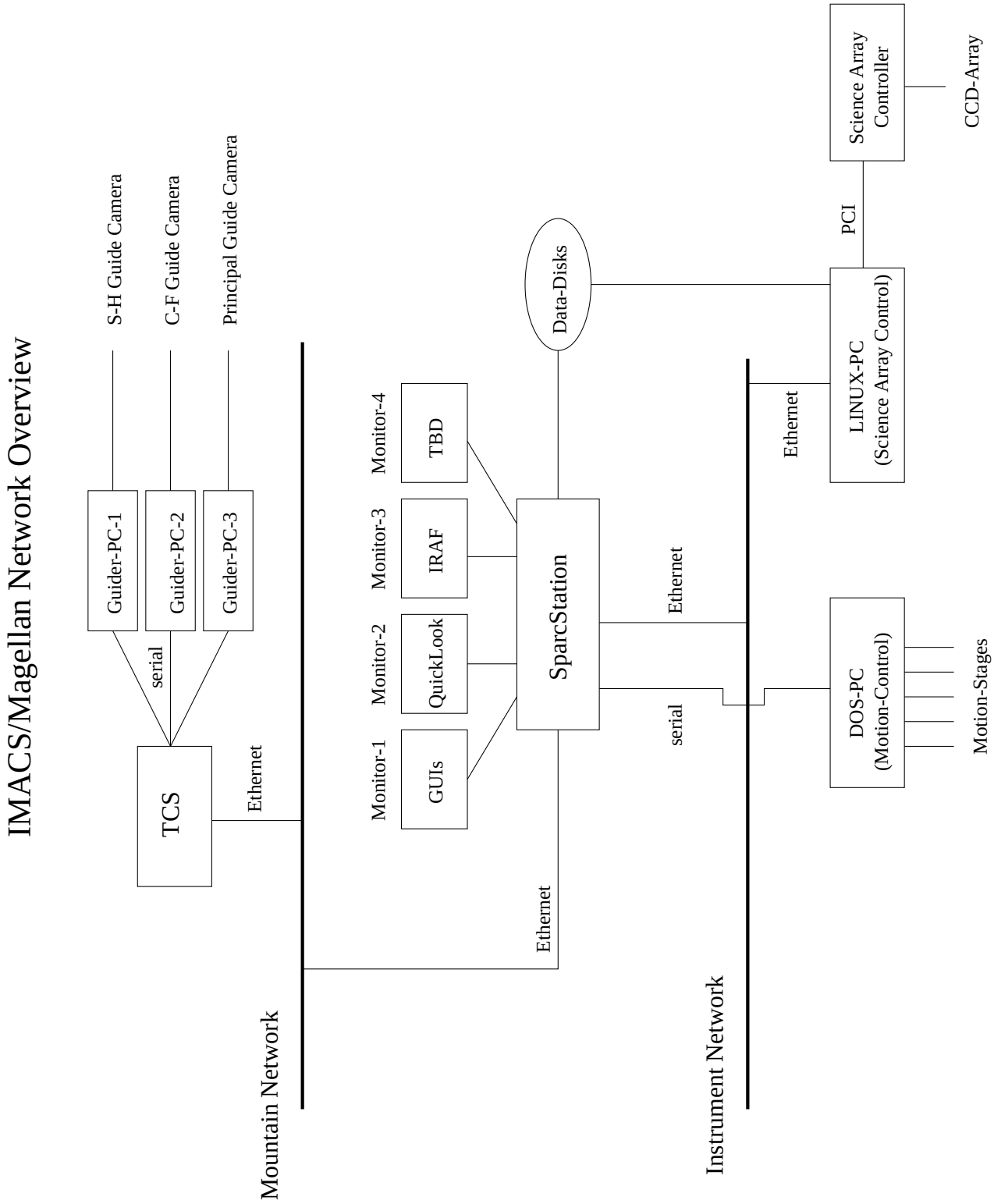

Figure 7.2: IMACS / Magellan network overview.

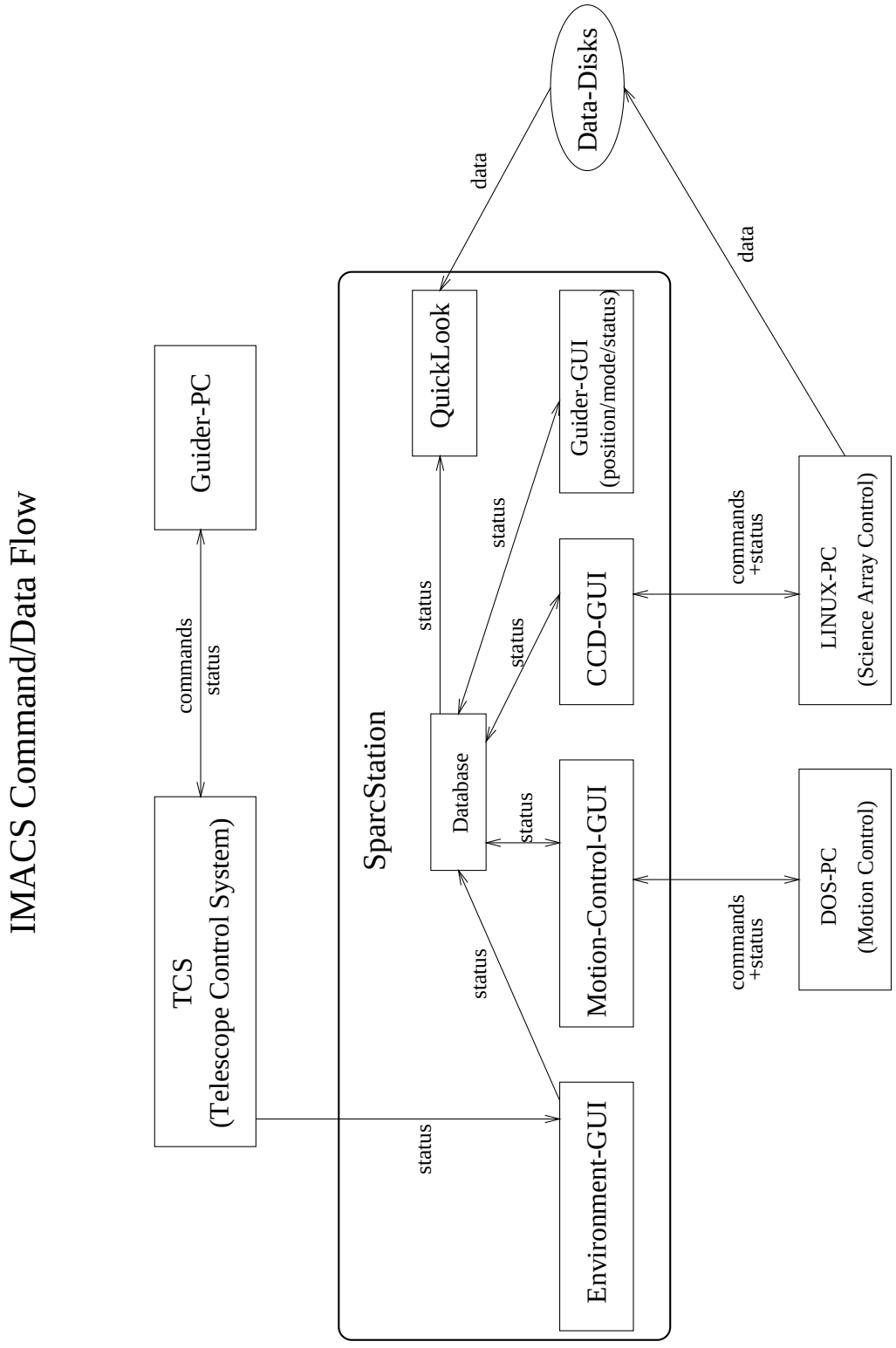

Figure 7.3: IMACS / Magellan dataflow overview.

Chapter 8

Project Management

8.1 Introduction

The IMACS project is a substantially more complicated instrument than has been attempted previously by OCIW. Project management techniques which have been appropriate for smaller, less technically challenging instruments are probably not sufficient for a project of this scope, budget, and schedule. Consequently, the following sections detail our plans for managing the IMACS project.

8.2 Tracking and Reporting

IMACS is being funded by OCIW through the Magellan instrumentation budget, and is being designed and fabricated at OCIW. In effect, the customer and supplier are the same entity, which both simplifies and complicates project tracking and reporting. In order to keep the OCIW community and outside contributers (consultants, contractors, crucial suppliers) informed about the state of the project, monthly progress reports are being produced and distributed, both via email and the IMACS website.

When the various technical areas of the project (optics, detector systems, mechanics, electronics, and software), reach a sufficient level of maturity, regular project meetings will be held to review current work and coordinate plans for the next reporting period. Minutes from the project meetings will become the primary source for information distributed in the progress

reports. The first two such meetings were held in February and March, in preparation for the PDR.

8.3 Design Reviews

Design reviews are typically required of projects by funding bodies, to insure that the scientific and technical requirements for the project are met. In the case of IMACS, we propose to hold a sequence of small, informal reviews, to provide the OCIW community an opportunity to verify that the project demonstrates a reasonable chance of meeting its technical, cost, and schedule objectives.

A preliminary design review (PDR) will be held to present the preliminary design of the instrument, including the optical design, CCD detector systems, image quality, and preliminary designs for all of the major mechanical, electronic, and software components.

Following the preliminary review, detailed design of the mechanical and opto-mechanical systems will begin with the intent of carrying the critical component design work to the pre-fabrication stage. During this period, the electrical and software design tasks can be started, based on designs from the PDR. Long lead-time tasks, including the optical and CCD systems, will begin fabrication during this period. Well defined, non-critical mechanical and electronic tasks can also begin fabrication. Following the detail design phase, a critical design review (CDR), focused on critical aspects of the detailed design work, may be held. The exact content and format of the CDR is not yet determined. The purpose of the CDR will be to establish that the selected design work, supported by appropriate analysis (thermal, optical, finite element, etc.), conforms to the requirements approved at the PDR.

A final, pre-shipment review (PSR) will be the last review held. The purpose of the PSR will be to demonstrate the assembled instrument meets the performance requirements, based on testing of the finished components and the instrument as a whole. Following the PSR, the instrument will be disassembled and shipped to Chile.

8.4 Staffing

The manpower requirements for the IMACS instrument currently exceed the available staffing at OCIW, if the project is to be completed on schedule. The current OCIW team dedicated and/or contributing to IMACS includes:

- A. Dressler - principal investigator, science requirements
- B. Bigelow - project management, mechanical engineering
- B. Sutin - optical design, analysis, procurement
- T. Bond - mechanical engineering
- I. Thomson - CCD detector systems (science and guider cameras)
- G. Burley - CCD detector systems (science and guider cameras)
- C. Birk - instrument control software
- D. Carr - motion control electronics system

We are also using consultants to minimize the time required to complete the instrument mechanical design. The currently active consultants are:

- G. Luppino - Dewar and flexure control mech. design
- A. Schier - Field lens, collimator, and long camera mech. design

8.5 Fabrication Strategies

8.5.1 Optical Fabrication

All of the optical fabrication work is being completed by outside sources. This work is described in the optics sections.

8.5.2 Mechanical Fabrication

Although no fabrication for IMACS is yet underway, the instrument fabrication facilities at OCIW are fully occupied with Magellan Project work, as well as on-going work in support of the telescopes and instruments at the Las Campanas Observatory (LCO). We anticipate adding an additional machinist and NC mill for fabrication of IMACS components. We also anticipate making use of commercial fabrication shops already qualified in the production of Magellan. Design work completed by consultants may be fabricated in-house, or may be contracted out as well.

8.5.3 Electronics Fabrication

Electrical fabrication will be less extensive than mechanical, and the IMACS electronics may be completed by existing staff. Electronics fab requirements will be established as Magellan and IMACS requirements become more clear.

8.5.4 Software

Software for IMACS is being modeled on existing work for Magellan and existing instruments at LCO. It is currently expected that existing staff will complete the software tasks for IMACS, although some work may be contracted out if required. No additional hires are anticipated at this time.

8.6 Assembly Strategies

IMACS will be completely assembled and tested in Pasadena. Both internally and externally fabricated sub-assemblies will be gathered and integrated on the instrument structure as the subsystems become available. No additional staffing or resources (space or equipment) are currently anticipated for expressly for assembly, but contracting electro-mechanical technicians could be used if necessary.

8.7 Testing Strategies

IMACS will be completely tested in Pasadena. Sub-assemblies will be wired and software-controlled as they become available. Completed assemblies will be integrated as they become available. Optical testing will be carried out on the individual subsystems, prior to end-to-end testing on the instrument.

8.8 Budget

A revised budget will be presented at the PDR meeting.

8.9 Schedule

A revised schedule will be presented at the PDR meeting.

Appendix A:

IMACS System Specification

Alan Dressler

Bruce Bigelow

V1.3, 20 March 1999

Appendix B:
Preconstruction Optical Designs I,
H.W. Epps, 5 September 1997

Appendix C:
Preconstruction Optical Design II,
H.W. Epps, 21 January 1998

Appendix D:
Preconstruction Optical Design III,
H.W. Epps, 4 May 1998

Appendix E:
Optical Modeling of IMACS,
B.M. Sutin, 21 November 1997